



Division of Intramural Research

Fifteenth Annual NHLBI DIR Research Festival



Photo courtesy of NIH Almanac

Friday, June 9, 2017
Natcher Conference Center
Bethesda, MD

2016 – 2017 NHLBI DIR Fellows Advisory Committee

Koyeli Banerjee
Biochemistry and Biophysics
Center

Emilia Barbu
Sickle Cell Branch

Steven Brooks
Sickle Cell Branch

Teegan Dellibovi-Ragheb
Cell Biology and Physiology
Center

Debbie Figueroa
Cardiovascular-Pulmonary
Branch

Jessica Flynn
Biochemistry and Biophysics
Center

Elizabeth Gordon
Cardiovascular and
Pulmonary Branch

Lo Lai
Biochemistry and Biophysics
Center

Ryan O'Neill
Cell Biology and Physiology
Center

Beverley Rabbitts
Systems Biology Center

Rajiv Ramasawmy
Cardiovascular and Pulmonary
Branch

Sreya Tarafdar
Biochemistry and Biophysics
Center

Heather Teague
Cardiovascular and
Pulmonary Branch

Laxminath Tumburu
Sickle Cell Branch

Ling Yang
Center of Molecular
Medicine

**Special thanks to the Foundation for Advanced Education in Sciences (FAES)
for providing lunch for the Research Festival.**

Visit their website at: www.faes.org



NHLBI DIR Office of Education

Herbert Geller, Director
Dami Kim, Program Coordinator
Jackie Lee, Program Coordinator

NHLBI Office of the Scientific Director

NHLBI Cores and Offices

Table of Contents

| | |
|---------------------------------------|----|
| Schedule | 4 |
| Keynote Speaker Introduction | 5 |
| Pitch Schedule | 6 |
| NHLBI Cores and Offices Summaries | 11 |
| Poster Location Map | 20 |
| Poster Titles and Session Assignments | 21 |
| Abstracts | 26 |
| Registered Attendants | 56 |

Fifteenth Annual NHLBI DIR Research Festival

Friday, June 9th, 2017

| | | |
|---------------|--|---------------------------------|
| 8:00 – 8:30 | Arrival, Registration, Check-In | <i>Lower Level Lobby</i> |
| 8:30 – 8:40 | Introduction and Welcome Debbie Figueroa, Ph.D., Chair Fellows Advisory Committee, NHLBI | <i>Auditorium</i> |
| 8:40 – 10:30 | Morning Pitch Session <i>Session Chairs: Jessica Flynn, Ph.D. and Elizabeth Gordon, Ph.D.</i> | <i>Auditorium</i> |
| 10:30 – 10:40 | BREAK | |
| 10:40 – 11:40 | Keynote Speaker Enrique De La Cruz, Ph.D. – <i>“Without each other, we are nothing”</i> | <i>Auditorium</i> |
| 11:40 – 11:45 | Introduction to FAES Christina Farias, M.B.A., Executive Director, FAES | <i>Auditorium</i> |
| 11:45 – 11:50 | Introduction to the Office of Education Herbert M. Geller, Ph.D., Director, Office of Education, NHLBI | <i>Auditorium</i> |
| 11:50 – 12:00 | Group Picture | <i>Auditorium</i> |
| 12:00 – 12:30 | Lunch | <i>Atrium & Conf. Rooms</i> |
| 12:30 – 1:45 | Poster Session I – #1-15, 17-70 | <i>Atrium</i> |
| 1:45 – 3:25 | Afternoon Pitch Session <i>Session Chairs: Koyeli Banerjee, Ph.D. and Beverley Rabbitts, Ph.D.</i> | <i>Auditorium</i> |
| 3:25 – 4:40 | Poster Session II – #7-16, 71-123 | <i>Atrium & Balcony</i> |
| 4:40 – 5:00 | Awards Ceremony & Closing Remarks Best Pitch Awards – Postbaccalaureate and Postdoctoral Fellows Best Poster Awards – Postbaccalaureate, Predoctoral, Postdoctoral Fellows, and Staff Scientist Outstanding Fellow Awards Outstanding Mentoring Awards – PI and Staff Scientist | <i>Auditorium</i> |
| 5:00 – | Networking Hour Rock Bottom Restaurant & Brewery – Bethesda, MD | |



Enrique M. De La Cruz, Ph.D.

Professor

**Department of Molecular Biophysics and Biochemistry
Yale University**

NHLBI Research Festival 2017 Keynote Speaker

“Without each other, we are nothing”

Enrique M. De La Cruz, Ph.D. is a Professor in the Department of Molecular Biophysics and Biochemistry (MB&B) at Yale University. He is a first-generation Cuban-American who was raised in Newark, NJ. Dr. De La Cruz received his undergraduate degree in Biology from Rutgers University where he was inducted into *Phi Beta Kappa* and *Beta Beta Beta* Honor Societies. He earned his Ph.D. degree in Biochemistry, Cell & Molecular Biology (BCMB) with Dr. Thomas D. Pollard at Johns Hopkins University School of Medicine and received postdoctoral training in the laboratories of Drs. H. Lee Sweeney and E. Michael Ostap at the University of Pennsylvania School of Medicine. He was a Visiting Scientist at Centre National de la Recherche Scientifique (CNRS), Commissariat à l'Énergie Atomique (CEA) & Université Joseph Fourier in Grenoble, France in 2009, a Mayent-Rothschild Senior Researcher Fellow at the Institut Curie, Paris in 2015, and an Invited Professor Fellow at ESPCI Paris Tech (école supérieure de physique et de chimie industrielles de la ville de Paris), Paris in 2016.

Dr. De La Cruz has published extensively in the areas of actin and myosin regulation, RNA helicases, and signaling enzymes, for which he has received a number of awards and honors. Among them are the American Heart Association Established Investigator Award, NSF CAREER award, Keith R. Porter Symposium Award from the Society for General Physiologists, and a Hellman Family Fellowship. He was the Abbott Distinguished Lecturer at Purdue University, Plenary Lecturer at the Ibero-American Congress of Biophysics Meeting held in Brazil, Plenary Lecturer of the 44th Annual Meeting of the Biophysical Society of Japan, and has delivered Keynote and named lectureships at Washington University in St. Louis, Johns Hopkins, University of Pennsylvania, Duke University, Notre Dame, University of North Carolina, Rutgers University, and the University of Illinois.

Dr. De La Cruz is actively involved with various scientific societies, journals and peer review committees, as well as numerous outreach activities to promote underrepresented minorities in the sciences. He has or currently serves on the Editorial Board of the *Journal of Biological Chemistry*, *Biophysical Journal* and *Biophysical Reviews*, the Publications Committee of the American Society for Biochemistry & Molecular Biology (ASBMB), and the Macromolecular Structure & Function C Study Section of the National Institutes of Health. He has organized annual national meetings for ASBMB and Biophysical Society, served on the Biophysical Society Council, chaired its Nominating Committee, and served on research panels for the NSF, American Heart Association, as well as funding agencies in England, Israel and France. He also serves on the Scientific Advisory Boards of Myokardia, Inc. in San Francisco, CA and Inozyme Pharma LLC in New Haven, CT.

Directions for Pitch Presenters

1. Two Session Chairs will help those who are giving pitches queue up and keep track of time.
2. The allowed pitch time per person is three minutes total. You will be escorted off the stage if you surpass three minutes.
3. Please introduce yourself and give your pitch number at the start of your pitch. You should be on the stage ready to talk as the person before you is still speaking in order to minimize delays.

Pitch Judging

We invite all audience members to judge the pitches for the “Best Pitch” Awards. Please rate each pitch on a scale of 1-10, where 1 is the lowest and 10 is the highest, based on how clear and effective each presenter was in convincing you to visit their poster later. There is a separate web page for each session as listed below.

Morning Pitch Session Schedule

Judging URL: <http://nhlbioe.poll daddy.com/s/morningpitch17>



| Order | Time | Poster # | Name | Title |
|-------|--------|----------|----------------------|--|
| 1 | 8:45AM | 17 | Jaffar Khan | Intentional Laceration of the Anterior Mitral Valve Leaflet to Prevent Left Ventricular Outflow Tract Obstruction (LAMPOON) During Transcatheter Mitral Valve Replacement: Pre-Clinical Findings |
| 2 | 8:48AM | 18 | Madeleine Strickland | A Novel HIV-1 Inhibitor Blocks Ubiquitin Recognition by Tsg101 |
| 3 | 8:51AM | 19 | Seyit Kale | Facilitator Models of Weak Binding in Protein-Protein Interactions |
| 4 | 8:54AM | 20 | Andrew Dittmore | Does Supercoiling Locate DNA Lesions? |
| 5 | 8:57AM | 21 | Todd Schoborg | Uncovering Molecular Mechanisms of Microcephaly |
| 6 | 9:00AM | 22 | Hong Yuen Wong | Personalized Deep Detection of Measurable Residual Disease in Acute Myeloid Leukemia |
| 7 | 9:03AM | 23 | Daniela Malide | Illuminating Mitophagy in Living mt-Keima Mouse Tissues via Super-Resolution Microscopy |
| 8 | 9:06AM | 24 | Komudi Singh | Parkin Targets NOD2 to Regulate Astrocyte ER Stress and Inflammation |
| 9 | 9:09AM | 25 | Florentina Tofoleanu | Differences in Protein Hydration in Cryo-EM and X-Ray Structural Models |

| Order | Time | Poster # | Name | Title |
|-------|--------|----------|--------------------|---|
| 10 | 9:12AM | 26 | Juan Pablo Ruiz | VEGFA Concentration In-Vitro Modulates Hemogenic Endothelium Differentiation and Downstream Hematopoietic Stem and Progenitor Cell Identity |
| 11 | 9:15AM | 28 | Emma O'Leary | Membrane Binding and Fluidity Sensing by α -, β -, and γ -Synuclein |
| 12 | 9:18AM | 29 | Hannah Robinson | A Novel CD19/CD3 Bispecific Antibody Induces Potent Response Against Chronic Lymphocytic Leukemia |
| 13 | 9:21AM | 32 | Kate Stringaris | In-vivo Trafficking of Adoptively Transferred NK Cells Using $^{89}\text{Zirconium}$ Cell Labelling and PET/CT |
| 14 | 9:24AM | 34 | Lynda Bradley | Expression and Purification of Human Bloom's Syndrome Helicase for Comparative Single-Molecule Studies of Post-Translational Modifications on Enzyme Activity |
| 15 | 9:27AM | 37 | Heather Teague | Low Density Granulocytes Associate with Non-Calcified Coronary Plaque and Endothelial Cell Damage in Psoriasis |
| 16 | 9:30AM | 38 | Purevdorj Olkhanud | Evaluation of Early Biomarkers Associated with Graft Rejection in Patients with Sickle Cell Disease |
| 17 | 9:33AM | 39 | Natasha Fillmore | A Role for PPAR α in Sex Differences in Cardiac Hypertrophy |
| 18 | 9:36AM | 40 | Rafique Islam | Structure-Function Studies of ApoA-I Mimetic Peptides for ABCA1-dependent Cholesterol Efflux and HDL Formation |
| 19 | 9:39AM | 41 | Beverley Rabbitts | Oxidative Phosphorylation Complex Interactions in Intact Mitochondria |
| 20 | 9:42AM | 42 | Chaarushi Ahuja | Unfavorable Perceptions of Neighborhood Environment are Associated with Greater Sedentary Time: Data from the Washington, D.C. Cardiovascular Health and Needs Assessment |
| 21 | 9:45AM | 45 | Rajiv Ramasawmy | Real-Time Flow MRI to Monitor Exercise Stress |
| 22 | 9:48AM | 46 | Debbie Figueroa | Apolipoprotein A-I and Apolipoprotein E Differentially Modulate the Expression of Extracellular Matrix Proteins by IPF Lung Fibroblasts |
| 23 | 9:51AM | 48 | Dai Nguyen | Altered Extracellular Matrix Metabolism as a Potential Link to the Pathophysiology of Vascular Abnormalities in Autosomal Dominant Hyper-IgE Syndrome |

| Order | Time | Poster # | Name | Title |
|-------|---------|----------|--------------------|--|
| 24 | 9:54AM | 49 | Kacey Guenther | Eltrombopag Promotes DNA Repair in Human Hematopoietic Stem and Progenitor Cells: Implications for the Treatment of Fanconi Anemia |
| 25 | 9:57AM | 50 | Xueting (Tina) Jin | Cholesterol-Enrichment of Cells Induces Unique Extracellular Cholesterol Microdomains |
| 26 | 10:00AM | 51 | Mona Mirzaeimoghri | Micro Fabrication of Hard X-Ray Compound Refractive Lens Using Nanoprinting Process |
| 27 | 10:03AM | 53 | Thaddeus Davenport | Examination of Induced Endocytic Structure Formation in B Lymphocytes |
| 28 | 10:06AM | 54 | Ryan O'Neill | A <i>Drosophila melanogaster</i> Screen Reveals Novel Functions For Microcephaly Genes |
| 29 | 10:09AM | 58 | Mohit Mathew | Multifaceted Role of Glycan Interactions on Clathrin-Independent Endocytosis of MHC1 and CD59 |
| 30 | 10:12AM | 60 | Craig Pearson | Modifying Chondroitin Sulfate Proteoglycans Enhances Retinal Ganglion Cell Axon Regeneration in the Mouse Optic Nerve |

Afternoon Pitch Session Schedule

Judging URL: <http://nhlbioe.poll daddy.com/s/afternoonpitch17>



| Order | Time | Poster # | Name | Title |
|-------|--------|----------|-----------------|--|
| 1 | 1:50PM | 71 | Zongheng Wang | Developmental Regulation of Mitochondrial Biogenesis During <i>Drosophila</i> Oogenesis |
| 2 | 1:53PM | 75 | Iris Garcia-Pak | A Long-Term Co-Culture with Supporting Cells of the Developing Heart Promotes Maturation of Induced Pluripotent Stem Cell-Derived Cardiomyocytes |
| 3 | 1:56PM | 79 | Julia Liu | Molecular and Physiological Impact of Regulated Mitochondrial Calcium Uptake |
| 4 | 1:59PM | 80 | Kaiyuan Wu | GCN5L1 Interacts with RanBP2 to Mediate Lysosome Positioning |

| Order | Time | Poster # | Name | Title |
|-------|--------|----------|------------------|---|
| 5 | 2:02PM | 73 | Jessica Flynn | Cellular Conformations of α -Synuclein Probed by Raman Spectroscopy |
| 6 | 2:05PM | 72 | Jonathan Chung | High Risk Features of Coronary Plaque Increase with Worsening Skin Disease in Psoriasis |
| 7 | 2:08PM | 74 | Elizabeth Gordon | House Dust Mite-Derived Proteases Induce Apolipoprotein E Secretion from Asthmatic Alveolar Macrophages via a ROS-dependent Pathway |
| 8 | 2:11PM | 76 | Javier Traba | Prolonged Fasting Suppresses Mitochondrial NLRP3 Inflammasome Assembly and Execution via SIRT3 Mediated Activation of Superoxide Dismutase 2 |
| 9 | 2:14PM | 77 | FNU Samarjeet | Equilibration of the Chemical Potential Between Lipid Leaflets During Molecular Dynamics Simulation |
| 10 | 2:17PM | 78 | George Amanakis | Cardioprotection in Mice with a Knock-In Mutation in Cyclophilin D (CyPD-C202S): A Site of S-nitrosylation |
| 11 | 2:20PM | 81 | Shannon Lacy | Effects of Alpha-synuclein Uptake on Cellular Viability, Morphology, and Localization |
| 12 | 2:23PM | 84 | Sharada Tilve | Peculiar Cell Phenotypes Caused by Plasticity Related Gene 3/5 Due to RhoA/Rac1 Imbalance |
| 13 | 2:26PM | 88 | Joshua Rivers | Association Between Neighborhood-level Socioeconomic Deprivation and Incident Hypertension: A Longitudinal Analysis of Data from the Dallas Heart Study |
| 14 | 2:29PM | 89 | Steven Brooks | Which Alpha Globin Gene Is Primarily Expressed in the Vascular Endothelium? |
| 15 | 2:32PM | 94 | Yvonne Baumer | Psoriasis Induced Chronic Inflammation Results in Pro-Atherosclerotic Changes in Macrophages Resulting in Enhanced Atherosclerosis Development |
| 16 | 2:35PM | 95 | Giacomo Waller | Development of an Optimized Toolkit for High-Efficiency Lentiviral Genetic Modification of Human Natural Killer Cells |
| 17 | 2:38PM | 96 | Yi Zhang | Selective Protein Synthesis on the Mitochondrial Surface Drives the mtDNA Selection |
| 18 | 2:41PM | 99 | Aparna Kishor | Sequence-Specific Protection of mRNAs from Nonsense-Mediated Decay |

| Order | Time | Poster # | Name | Title |
|-------|--------|----------|--------------------|--|
| 19 | 2:44PM | 103 | Alex Grubb | Macrophages from Patients with Arterial Calcification due to CD73 Deficiency Have Impaired Ability to Resolve an Inflammatory Response |
| 20 | 2:47PM | 104 | Huiqing Li | Novel Degenerative and Developmental Defects in a Zebrafish Model of Mucopolidiosis Type IV |
| 21 | 2:50PM | 105 | Naijil George | Arylsulfatase B Induce Increased Neurite Outgrowth in Hippocampal Neurons When Cocultured With Astrocytes |
| 22 | 2:53PM | 109 | Lo Lai | Generation of Methionine Sulfoxide Reductase Quadruple Knockout Mice |
| 23 | 2:56PM | 111 | Amit Dey | Improvement in Skin Inflammation is Associated with Improvement in Aortic Vascular Inflammation by 18-FDG PET/CT |
| 24 | 2:59PM | 112 | Zhanghan Wu | Distinct Focal Adhesion Morphologies Emerge from Interplay Between Retrograde Actin Flux and Stress Fiber |
| 25 | 3:02PM | 115 | Randi Parks | CypD-Mediated Regulation of the Permeability Transition Pore is Altered in Mice Lacking the Mitochondrial Calcium Uniporter |
| 26 | 3:05PM | 116 | Deepa Mokshagundam | Fetal Mouse Heart Imaging Using Echocardiography |
| 27 | 3:08PM | 119 | Karolyn Oetjen | Single-Cell RNA Sequencing Analysis of Bone Marrow Populations |
| 28 | 3:11PM | 122 | Fabrizio Marinelli | Molecular Breakdown of DEER Data from Self-Learning Atomistic Simulations |
| 29 | 3:14PM | 123 | Cydney Nichols | High Sensitivity Detection of Mutations Implicated in Chronic Lymphocytic Leukemia Drug Resistance |

NHLBI Cores and Offices

Animal MRI Core

Stasia A. Anderson, Ph.D., Director

Building 10, Room B1D49C; E-mail: andersos1@nhlbi.nih.gov

Phone: (301) 402-0908

Web: <https://www.nhlbi.nih.gov/research/intramural/researchers/core/animal-mri-core>

The AMRI Core performs magnetic resonance imaging of small animal models in the NHLBI. We perform and interpret magnetic resonance imaging studies and work with investigators on the best approaches for the research model and goals. Training in MRI and data analysis is available and interested fellows may learn to perform MRI studies. Examples of imaging studies in the AMRI Core are:

- Cardiac imaging for heart function and size
- High resolution imaging of myocardium for identification of infarct and scars
- Imaging blood vessels; angiography and vessel wall imaging
- Atherosclerotic plaque imaging
- Perfusion of skeletal muscle or tumors
- Whole body imaging for identification of non-cardiac defects in mouse models
- High resolution microimaging of embryos and fixed tissue

Core imaging studies are performed in the NIH Mouse Imaging Facility (MIF). Through the MIF, it is possible to incorporate additional imaging modalities such as computed tomography, ultrasound and bioluminescence as needed.

Animal Surgery & Resources (ASR) Core

James “Buster” Hawkins, DVM, MS, DACLAM

Animal Program Director

Building 14E, Room 105C; E-mail: hawkinsj@nih.gov

Phone: (301) 451-6743, Fax: (301) 480-7576

Randall R. Clevenger, B.S., LATG, 14E Surgical Facility Manager,

Building 14E, Room 106B; E-mail: rc85n@nih.gov

Phone: (301) 496-0405, Fax: (301) 402-0170

Joni Taylor, B.S., LATG, Large Animal Resources Manager

Building 10, Room B1D416; E-mail: jt100s@nih.gov

Phone: (301) 496-0823

Timothy Hunt, B.S., LATG, CRC Surgery Manager

Building 14E, Room 106B; Email: th118w@nih.gov

Phone: (301) 402-0913, Fax: (301) 402-0170

Main phone: 301-496-5927

Web: <https://www.nhlbi.nih.gov/research/intramural/researchers/core/animal-surgery-and-resources-core>

The Animal Surgery & Resources (ASR) Core provides veterinary medical care and technical services for NHLBI research animals used in both basic and preclinical research. These support services include: anesthesia, veterinary medical care, surgery, surgical support, training in surgical and microsurgical techniques, post-operative care, purchasing (large animals), and health monitoring. In addition, ASR provides technical services such as blood & tissue collection, and tail vein injections.

The ASR staff also provides NHLBI investigators with collaborative research support services such as developing animal models and new surgical procedures, assistance with research design, as well as animal protocol development and execution. Our surgical support equipment includes anesthesia machines with mechanical ventilation for species ranging from rodents to nonhuman primates, radiography, digital fluoroscopy, Faxitron, ultrasound, laser Doppler, and operating microscopes.

ASR supports a wide range of animal models for DIR investigators. Some of the animal models we provide surgical support for include xenotransplantation (involving baboons and genetically engineered pigs), stem cell models (rats, mice and pigs) myocardial infarction with and without reperfusion (rats, mice, rabbits, dogs, and nonhuman primates), hind limb ischemia (rats, mice, rabbits), gene vector delivery to liver (mice, rabbits), plethysmography (mice) and support for MRI and other imaging procedures. We can also perform cardiac function testing on rats and mice including invasive blood pressure, left ventricular pressure, and pressure-volume loops. Surgical and perioperative support services are provided in the Building 14E Surgical Facility, the B-2 level of the CRC and the NMR Center. We provide support services to all NHLBI animals housed in NIH facilities.

Our goal is to facilitate getting the research accomplished expeditiously using the best, most humane methods. We will work with each investigator in developing their respective animal model and then either train them in all procedures to enable them to work independently, perform the procedures for them, or work in concert to expedite the animal data generated.

Biochemistry Facility

Duck-Yeon Lee, Ph.D., Director

Building 50, Room 3120 & 3121; E-mail: leedy@nhlbi.nih.gov

Phone: (301) 435-8369, Fax: (301) 451-5459

Web: <http://www.nhlbi.nih.gov/research/intramural/researchers/core/biochemistry-facility>

The mission of the Biochemistry Facility is to provide services and consultation with expertise in biochemical enzyme/protein purification and assay to NHLBI researchers. The Facility currently features 1) ESI-LC/MS spectrometers to measure accurate mass of intact protein and small organic compounds, 2) HPLCs equipped with radiochemical and fluorescence detector that allow a purification of protein labeled with radioisotope or fluorescence probe, 3) atomic absorption spectrometer to measure metal content, and 4) amino acid analysis.

Bioinformatics and Computational Biology Core

Mehdi Pirooznia, M.D., M.Sc., Ph.D., Director

Building 10, Room 7N218A; E-mail: mehdi.pirooznia@nih.gov

Phone: (301) 451-2772

Web: <https://www.nhlbi.nih.gov/research/intramural/researchers/core/bioinformatics-and-computational-biology>

The Bioinformatics and Computational Biology Core facilitates, amplifies, and accelerates biological and medical research and discovery through the application of the latest bioinformatics methods and technologies. This mission is achieved by delivering high quality and comprehensive support for experimental design, analysis and visualization in a timely fashion. The core is responsive to research scientists' needs and effectively evolve with advances in the field.

The core services include but are not limited to the following:

- Statistical analysis including basic statistical analysis, advanced statistical analysis (e.g., linear and generalized mixed model analysis, longitudinal modeling), and custom statistical methods (e.g., tailored to specific research projects)

- Omics Analysis including: Transcriptomics (Microarray and RNA-seq), Genomics (Genome, exome and targeted DNA-seq), Epigenomics (Methyl-seq, ChIP-seq, etc.), Proteomics, and Metabolomics
- Gene/Target/Disease Analysis: Functional annotation at variant, gene, and geneset level, Interaction analysis, and Pathway enrichment analysis
- Ad-hoc consultation: Advise on experimental designs, data management and analysis
- Computing resource development and maintenance, including Bioinformatics Software Development, Systems Toolkits Development, customized biological databases and Web Services development
- Training: Personalized training to match user's specific requirements and group training and workshops

Biophysics Core Facility

Grzegorz (Greg) Piszczek, Ph.D., Director

Building 50, Room 3124; E-mail: piszczeg@nhlbi.nih.gov

Phone: (301) 435 8082; Fax: (301) 496-0599

Web: <http://www.nhlbi.nih.gov/research/intramural/researchers/core/biophysics-core>

The Biophysics Core provides support in the study of macromolecular interactions, dynamics, and stability by offering consultations, training, professional collaborations, and instrument access. The Facility assists researchers with comprehensive biophysical characterization of biomolecules, including proteins, DNA, RNA, nanoparticles, and their cognate ligands.

Services/Instruments:

- Isothermal Titration Calorimetry, ITC (iTC200 and VP-ITC)
- Differential Scanning Calorimetry, DSC (VP-DSC)
- Surface Plasmon Resonance, SPR (Biacore 3000)
- Bio-Layer Interferometer, BLI (Octet RED96)
- MicroScale Thermophoresis, MST (Monolith NT.115)
- Analytical Ultracentrifugation, AUC (XLI and XLA)
- Dynamic Light Scattering, DLS (DynaPro Nanostar)
- Multi Angle Light Scattering, SEC-MALS (Dawn-HELEOS II)
- Circular Dichroism, CD (Jaso J715)
- Fluorescence (PFI)

DNA Sequencing and Genomics Core Facility

Yuesheng Li, Ph.D., Director

Building 10, Room 5N107; E-mail: yuesheng.li@nih.gov

Phone: (301) 594-8346

Web: <https://www.nhlbi.nih.gov/research/intramural/researchers/core/dna-sequencing-and-genomics-core>

The DNA Sequencing Core and Genomics Core (DSGC) strives to provide the state-of-art next generation sequencing (NGS) services to NHLBI investigators in a cost-effective manner. Equipped with Illumina sequencers (Miseq and Hiseq), the core supports diverse NGS applications, including not but limited to genome/exome sequencing, RNAseq, ChIP-seq, and small RNA sequencing.

Our integrated services consist of experimental design and consultation, library QA/QC and preparation, data acquisition, and preliminary data analysis. In addition, the DSGC also offers trainings on library preparation for a wide range of NGS applications. Additional assistance will also be provided in a collaborative manner for projects that require extensive protocol optimization and software development.

Echocardiography Laboratory

Vandana Sachdev, M.D., Director

Building 10-CRC, Room 5-1436, E-mail: vs74y@nih.gov

Phone: (301) 496-3015; Fax: (301) 435-8886

Cynthia L. Brenneman, R.N., R.C.S., Lab Manager

Building 10-CRC, Room 5-1436, E-mail: cb179i@nih.gov

Phone: (301) 451-3799; Fax: (301) 435-8886

Web: <http://www.nhlbi.nih.gov/research/intramural/researchers/core/echocardiography-laboratory>

The Echocardiography Laboratory performs comprehensive cardiac imaging for NHLBI and all institutes at the Clinical Research Center. They collaborate in prospective and retrospective cardiovascular phenotyping studies and implement new technologies as necessary for detailed assessment of ventricular systolic and diastolic function, valvular abnormalities, and structural heart disease.

Representative research applications include:

- 3D imaging for structural cardiac defects
- Strain imaging for ventricular function
- Contrast imaging for left ventricular size, function, and evaluation of intracardiac abnormalities
- Contrast perfusion imaging of myocardium and skeletal muscle for the evaluation of microvascular flow
- Protocol-specific imaging of patients with mitral regurgitation to evaluate newer methods for quantitation of regurgitation severity

Electron Microscopy Core Facility

Christopher Bleck, Ph.D., Director

Building 14E, Room 111B

Phone: (301) 496-4711, E-mail: christopher.bleck@nih.gov

Erin Stempinski, Scientific Support Staff

Building 14E, Room 104A, E-mail: erin.stempinski@nih.gov

Phone: (301) 496-6448

Camron Keshavarz

Building 14E, Room 104

Phone: (301) 402-1229, Email: camron.keshavarz@nih.gov

Web: <http://www.nhlbi.nih.gov/research/intramural/researchers/core/electron-microscopy-core>

The NHLBI Electron Microscopy (EM) Core staff works with investigators and fellows to provide high-resolution transmission and scanning electron microscopy images of a variety of their samples including tissue, cell pellets, tissue culture, and inorganic material. In addition to conventional processing techniques for electron microscopy, we also provide microwave processing, negative staining, on-section gold immunolabeling, freeze fracture, platinum replicas, correlative light and electron microscopy, and other project-specific techniques. Potential clients can contact us to set up an initial consultation so that we can better understand the needs of your project. We will work with you when you submit a sample request to establish a projected cost and date when the EM Core will receive and process the samples. We encourage fellows to get training on any part of the sample processing and imaging to streamline future projects.

Flow Cytometry Core Facility

J. Philip McCoy, Jr., Ph.D., Director

Building 10, Room 8C104, E-mail: mccoyjp@mail.nih.gov

Phone: (301) 451-8824, Fax: (301) 480-4774

Web: <http://www.nhlbi.nih.gov/research/intramural/researchers/core/flow-cytometry-core>

The mission of the NHLBI Flow Cytometry Core Facility is to provide investigators at the NHLBI access to state-of-the-art flow cytometry, including cell sorting, high dimensional cell analysis, cytokine quantification, and imaging flow cytometry. This is done by having cytometers and software available in the core facility and by providing consultation to investigators. Investigators are responsible for specimen preparation and staining. The staff of the flow cytometry laboratory will gladly assist you in designing your experiments and in developing optimal preparation and staining procedures. For analytical experiments, data will be provided as either hard copies or on appropriate media as listmode files. Software and computer workstations are available for "offline" analysis of these files. For sorting experiments, each investigator is responsible for bringing appropriate media and test tubes. In addition to cell sorting and analytical cytometry, the core facility also provides multiplex bead array expertise for analysis of extracellular cytokines, and imaging flow cytometry where the staining patterns of fluorochromes can be visualized.

iPSC Core

Jizhong Zou, Ph.D., Director

Building 10, Room 6N317

Phone: (301) 827-7510; E-mail: zouj2@nhlbi.nih.gov

Web: <https://www.nhlbi.nih.gov/research/intramural/researchers/core/ipsc-core>

The mission of induced Pluripotent Stem Cells (iPSC) Core is to accelerate stem cell research in the NHLBI by providing investigators consultation, technical services and training in human pluripotent stem cell technology. The major services that iPSC Core currently provides include (1) generation of human iPSCs from fibroblast cells, CD34+ hematopoietic stem/progenitor cells, and peripheral blood mononuclear cells (PBMCs) using non-integration methods; (2) CRISPR/Cas9 mediated human iPSC gene knockout, gene correction, and AAVS1 safe harbor transgene knockin; (3) human iPSC-cardiomyocyte (CM) differentiation. The Core also provides control iPSC lines and validated iPSC culture reagents. In addition to providing services and consultations to NIH researchers, the Core staff collaborates with investigators to work on custom and exploratory projects. Research conducted by the Core seeks to better understand the mechanisms underlying pluripotent stem cell self-renewal and differentiation to optimize culture conditions and operating procedures.

Imaging Probe Development Center

Rolf Swenson, Ph.D., Director

9800 Medical Center Dr, Building B, Room 3042

E-mail: rolf.swenson@nih.gov; Phone: (301) 217-7626

Web: <http://www.nhlbi.nih.gov/research/intramural/researchers/programs/imaging-probe-development-center/>

The Imaging Probe Development Center (IPDC) was founded with the goal of providing the fundamental synthetic chemistry support needed to advance molecular imaging technologies for the interdisciplinary NIH research community. The IPDC laboratories are located in Rockville, Maryland, with state-of-the-art equipment and the new PET facility at the NIH main campus. The IPDC has a rolling solicitation system, and NIH scientists are welcome to contact us and submit a proposal requesting synthesis of a particular probe in which they are interested. Probes can be intended for all types of imaging modalities, such as optical fluorescence, PET/SPECT, and MRI. IPDC scientists can synthesize requested probes that are completely novel or that are published in literature but commercially unavailable. We look for automation solutions to improve capabilities and throughput. We have produced molecular imaging probes ranging from low-molecular-weight entities to high-molecular-weight conjugates, including fluorescent dyes and their analogs, lanthanide complexes, fluorogenic enzyme substrates, caged dyes that become

fluorescent upon irradiation, radio- and fluorescent-labeled peptides, proteins and antibodies, gold and iron oxide nanoparticles, dendrimers, and liposomes. Recent efforts have included hyperpolarized MRI probes, tools for super-resolution spectroscopy, and PET probes derived from tyrosine kinase inhibitors. Examples of some of our recent projects will be provided.

Light Microscopy Core Facility

Christian A. Combs, Ph.D., Director

Building 10, Room 6N-309; E-mail: combsc@nhlbi.nih.gov

Phone: (301) 496-3236; Mobile: 301-768-2568

Daniela A. Malide, M.D., Ph.D., Facility Manager

Building 10, Room 6N-309; E-mail: dmalide@nhlbi.nih.gov

Phone: (301) 402-4719, Fax: (301) 480-1477

Xufeng Wu, Ph.D., Deputy Director

Building 50, Room 2318; E-mail: wux@nhlbi.nih.gov

Phone: (301) 402-4187, Fax: (301) 402-1519

Web: <http://www.nhlbi.nih.gov/research/intramural/researchers/core/light-microscopy-core/>

We are a state-of-the-art microscopy facility that has served the needs of the NHLBI DIR since 2000. We have helped to publish more than 250 papers in this period and have helped researchers from all of the NHLBI Centers and Branches. The mission of this facility is to provide state of the art equipment, training, experimental design, and image processing capabilities to assist researchers in experiments involving light microscopy. We have twenty-two microscopes in six locations in Bldgs. 10 and 50. These microscopes provide a wide array of techniques including wide-field fluorescence and transmitted light imaging, confocal, two-photon, total internal reflection fluorescence microscopy (TIRF), and super-resolution microscopy (STED/SIM/STORM). While we primarily serve the needs of NHLBI DIR researchers, a few of our microscopes are available to other NIH researchers. In addition to the microscopes, we also have a broad array of image processing software for quantification of image intensities, morphological analysis, co-localization analysis, particle tracking, 3D volume reconstruction, etc. Our poster will highlight in a general way the various capabilities, techniques, microscopes available in the facility.

Murine Phenotyping Core

Danielle Springer, V.M.D., D.A.C.L.A.M., Director

Building 14E, Room 107A; E-mail: springerd@nhlbi.nih.gov

Phone: (301) 594-6171; Fax: (301) 480-7576

Web: <http://www.nhlbi.nih.gov/research/intramural/researchers/core/murine-phenotyping-core>

The Murine Phenotyping Core's central mission is development of a comprehensive in-depth knowledge of murine phenotyping methodologies in order to assist investigators with design, research applications, experimental methodologies, data acquisition and interpretation of murine cardiovascular, metabolic, neuromuscular and pulmonary platforms. We seek to provide investigators with high quality scientific and technical support as well as centralized access to state of the art murine phenotyping equipment for the characterization of genetically engineered mouse models. We are currently developing Standard Operating Procedures for our specialized equipment in order to provide high quality, reproducible and reliable data.

We provide consultation on appropriate methodologies to acquire cardiovascular, metabolic, neuromuscular, or pulmonary data from your mouse model. The lab assists with experimental design, data collection and acquisition, and data analysis. As most platforms require technical expertise, well developed standard operating procedures, and consistent and refined technique we recommend using our laboratory to collect your data for you. We also are happy

to train any interested NHLBI scientist on any SOP, technical skill, equipment operation, etc. that you would like to acquire knowledge on.

NHLBI Safety Committee

Ilsa I. Rovira, M.S., Co-Chair

Building 10-CRC, Room 5-3288; E-mail: rovirai@nih.gov

Phone: (301) 594-2466

Laurel Mendelsohn, Co-Chair

Building 10 Room 6S245; E-mail: mendelsohnl@mail.nih.gov

Phone: (301) 451-0208

Véronique A. Bonhomme, Health Sciences Safety Specialist

Building 13, Room 3K03; Email: veronique.bonhomme@nih.gov

Phone: (301) 496-2346

The NHLBI Safety Committee was formed to promote a safer working environment by encouraging more staff involvement, improved communication of common safety hazards and a more proactive attitude to safety issues. The members were chosen from laboratory areas to benefit from their collective experience. We intend to gather more practical input of common safety problems. We strive to become a resource for all staff regarding safety questions that come up regularly in laboratories and welcome input from the community to improve safety practices in the Institute.

Office of Biostatistics Research (OBR)

Nancy L. Geller, Ph.D., Director

Rockledge 2, Room 9202; E-mail: gellern@nhlbi.nih.gov

Phone: (301) 435-0434

The OBR collaborates in the planning, design, implementation, monitoring and analyses of studies funded by NHLBI. OBR also provides statistical consultation to any NHLBI investigator who requests advice. OBR has expertise in study design and collaborates in data management and analysis of many studies sponsored by the NHLBI DIR. OBR's primary responsibility is to provide objective, statistically sound, and medically relevant solutions to problems that are presented. When a question raised requires new methodology, the OBR is expected to obtain a new and valid statistical solution. OBR has a broad research mission and the professional staff is often asked to serve on in-house administrative committees as well as advisory committees for other Institutes within NIH and other agencies within DHHS.

Office of Technology Transfer and Development (OTTAD)

Alan H. Deutch, Ph.D., Director

Building 31, Room 4A29F; E-mail: deutch@nhlbi.nih.gov

Phone: (301) 402-5579; Fax: (301) 594-3080

Michael Davis, Ph.D., J.D., Technology Development Specialist

Building 31, Room 4A29; E-mail: michael.davis4@nih.gov

Phone: (301) 451-9032; Fax: (301) 594-3080

Web: <https://www.nhlbi.nih.gov/research/tt>

The primary mission of the National Institutes of Health (NIH) is to improve national and global public health. In support of this mission, the **National Heart, Lung, and Blood Institute's Office of Technology Transfer and Development (NHLBI OTTAD)** engages in array of transactional and technology development activities and

services that support NHLBI's robust biomedical and clinical research activity. In particular, NHLBI OTTAD oversees the day-to-day negotiation of agreements that facilitate: (i) the exchange of research materials [**M**aterial **T**ransfer **A**greements]; (ii) the exchange of confidential information [**C**onfidential **D**isclosure **A**greements]; (iii) clinical studies for evaluating the safety and efficacy of new pharmaceuticals [**C**linical **T**rial **A**greements & **C**linical **M**aterial **S**upply **A**greements]; and (iv) research collaboration, that provide an opportunity for NHLBI and outside parties, typically pharmaceutical and biotechnology companies, to work together to enhance and advance pre-existing technologies and/or develop and characterize new technologies [**C**ooperative **R**esearch and **D**evelopment **A**greements]. Unlike most of the agreements identified above, the Cooperative Research and Development Agreement, or CRADA, is unique, in that it is the only agreement mechanism that allows NIH Institutes and Centers, such as NHLBI, to accept financial resources that support the CRADA's research aims, while providing the CRADA partner an exclusive option to license NIH-only and joint inventions developed during the term of the CRADA. These features make CRADAs one of NIH's most scrutinized agreements. Whether you have or haven't participated in a CRADA, the information disclosed here will provide valuable insight into one of the most complex agreements used by NIH.

Pathology Core Facility

Zu-Xi Yu, M.D., Ph.D., Core Director

Building 10, Room 5N315; E-mail: yuz@mail.nih.gov

Phone: (301) 496-5035, Fax: (301) 480-6560

Web: <http://www.nhlbi.nih.gov/research/intramural/researchers/core/pathology-core>

The Pathology Core provides morphologic services for the studies of experimental pathology (animal models) and optimizes the uses of supplies and equipment for histology to all NHLBI DIR scientists. Services include standard histological and tissue preparation, embedding, sectioning and routine histology staining; frozen tissue section, immunohistochemistry and diagnostic pathology. Ongoing interaction of Pathology Core personnel with each investigator facilitates communication regarding histology products, morphologic findings, histopathological interpretation, and new technical developments, thus increasing the efficiency of the research projects. Staff members are well-trained, extremely experienced technicians, and the laboratory has a wide repertoire of specialized techniques. The research pathology and immunohistochemistry are subsequently operating using standard operating procedures based on good lab practice guidelines.

Proteomics Core Facility

Marjan Gucek, Ph.D., Director

Building 10, Room 8C103C; E-mail: marjan.gucek@nih.gov

Phone: (301) 594-1060, Fax: (301) 402-2113

Web: <http://www.nhlbi.nih.gov/research/intramural/researchers/core/proteomics-core>

We provide investigators at the NHLBI access to mass spectrometry and gel based proteomics for identification and quantitation of proteins and their posttranslational modifications (PTM). We have state-of-the-art equipment, including an Orbitrap Fusion instrument.

Our workflows for relative protein quantitation are based on DIGE, label-free, SILAC and TMT approaches. We can also help investigators identify and quantify protein posttranslational modifications, including phosphorylation, nitrosylation, acetylation, ubiquitination, succinylation, etc. We provide training in proper sample preparation and lead the researchers through mass spectrometric analysis to data searching and interpretation. Users have access to a variety of proteomics software platforms (Mascot, Proteome Discoverer, Sequest, Scaffold) for re-searching the data or viewing the results.

In addition to helping the NHLBI investigators, we develop new approaches for PTM characterization and absolute protein quantitation.

Transgenic Core

Chengyu Liu, Ph.D., Director

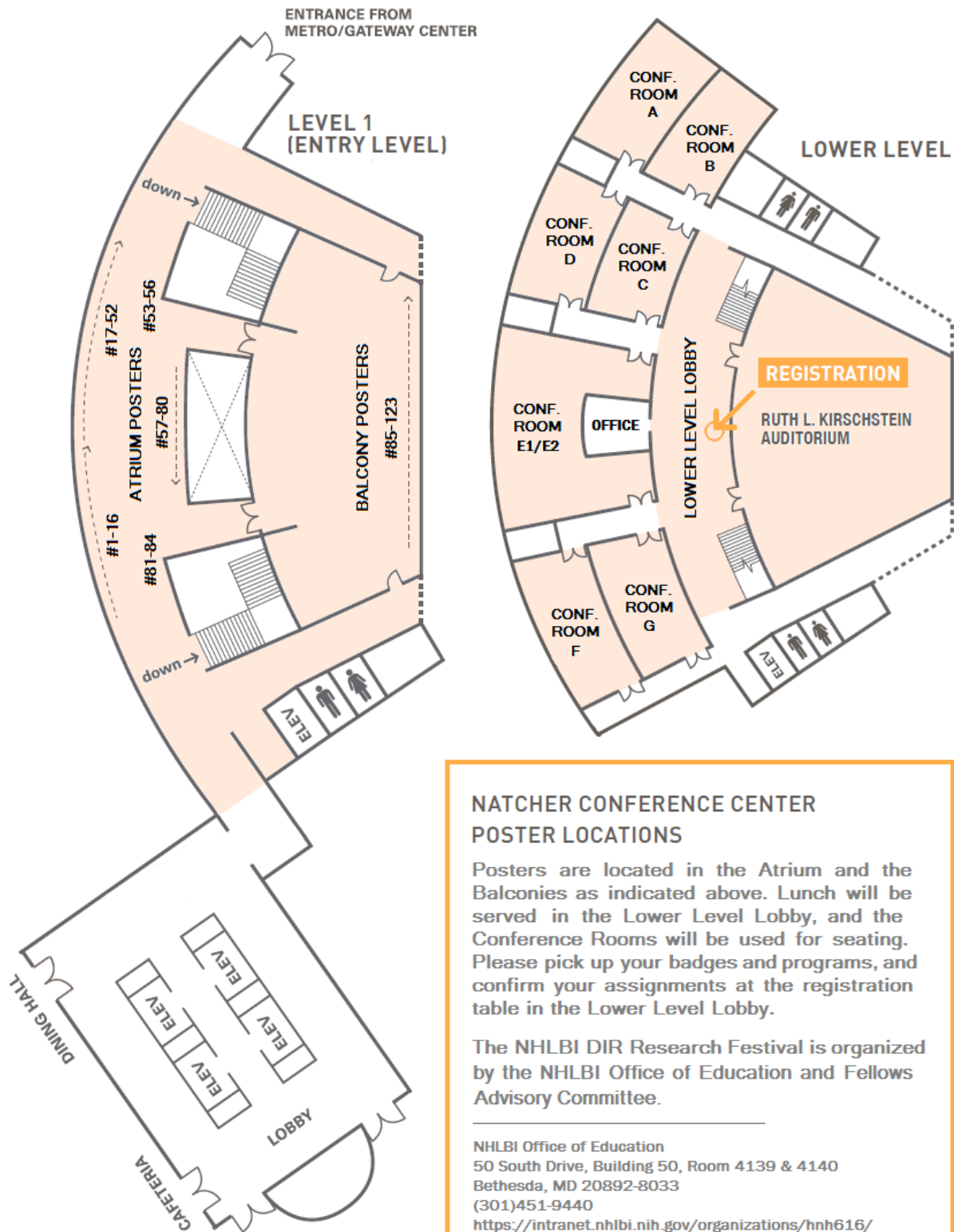
Building 10, Room 6D18; E-mail: liuc2@mail.nih.gov

Phone: (301) 435-5034; Fax: (301) 435-4819

Web: <https://www.nhlbi.nih.gov/research/intramural/researchers/core/transgenic-core>

The Transgenic Core's main mission is to keep up with the latest advancements in genome engineering technologies and to provide state-of-the-art services to assist NIH scientists in generating genetically engineered animal models. In the past several years, the Core has successfully used the ZFN, TALEN, and CRISPR methods to generate gene-targeted mouse lines. The revolutionary CRISPR technology has enabled the Core to simultaneously target multiple genomic loci and achieve gene knockout in difficult mouse strains, such as immunocompromised mice. Besides developing these new technologies, the Core is continuing to provide a variety of services using the classical mouse genetic and reproductive methodologies, such as producing transgenic lines using the pronuclear microinjection method, generating knockout mice using ES cell-mediated homologous recombination and blastocyst microinjection, cryopreserving and resurrecting mouse lines. The Core has imported the TARGATT mouse line, which enables the insertion of a single copy transgene into a predefined genomic locus. In addition, the core also offers services for injecting stem cells or differentiated cells into immunocompromised mice for testing their ability to form teratomas or evaluating their differentiation capabilities.

NATCHER CONFERENCE CENTER



NATCHER CONFERENCE CENTER POSTER LOCATIONS

Posters are located in the Atrium and the Balconies as indicated above. Lunch will be served in the Lower Level Lobby, and the Conference Rooms will be used for seating. Please pick up your badges and programs, and confirm your assignments at the registration table in the Lower Level Lobby.

The NHLBI DIR Research Festival is organized by the NHLBI Office of Education and Fellows Advisory Committee.

NHLBI Office of Education
50 South Drive, Building 50, Room 4139 & 4140
Bethesda, MD 20892-8033
(301)451-9440
<https://intranet.nhlbi.nih.gov/organizations/hnh616/office-of-education>

Poster Titles and Session Assignments

Please mount your poster upon arrival so it may be viewed for the entire Festival.

Poster Session I (12:30-1:45PM): #1-15, 17-70

Poster Session II (3:35-4:50PM): #7-16, 71-123

Core and Office Posters

1. **Animal Surgery & Resources (ASR) Core.** R.R. Clevenger, J. Taylor, T. Hunt, J. Hawkins.
2. **Biochemistry Facility.** D.Y. Lee.
3. **Electron Microscopy Core Facility.** E. Stempinski, C. Keshavarz, C. Bleck.
4. **NHLBI Safety Committee.** I. Rovira, L. Mendelsohn, V. Bonhomme.
5. **Office of Technology Transfer and Development.** M. Davis, A. Deutch.
6. **Transgenic Core.** Y. Du, W. Xie, F. Zhang, C. Liu.
7. **Animal MRI Core.** S. Anderson.
8. **Bioinformatics and Computational Biology Core.** F. Seifuddin, M. Pirooznia.
9. **DNA Sequencing and Genomics Core Facility.** Y. Li.
10. **Imaging Probe Development Center.** O. Vasalatiy, R. Swenson.
11. **Light Microscopy Core.** D. Malide, X. Wu, C.A. Combs.
12. **Murine Phenotyping Core.** M. Allen, A. Noguchi, D. Springer.
13. **Office of Biostatistics Research.** N. Geller.
14. **Pathology Core.** D. Tang, X. Qu, Z.X. Yu.
15. **NHLBI Internal Communications Team.** L. Gibson, C. Sangalang.
16. **Biophysics Core Facility.** G. Piszczek.

Research Posters

17. **Intentional Laceration of the Anterior Mitral Valve Leaflet to Prevent Left Ventricular Outflow Tract Obstruction (LAMPOON) during Transcatheter Mitral Valve Replacement: Pre-Clinical Findings.** J.M. Khan, T. Rogers, W.H. Schenke, J.R. Mazal, M.Y. Chen, R.J. Lederman; Cardiovascular Intervention Program.
18. **A Novel HIV-1 Inhibitor Blocks Ubiquitin Recognition by Tsg101.** M. Strickland, L. S. Ehrlich, S. Watanabe, M. Khan, M-P. Strub, M. D. Powell, J. Leis, C. Carter, N. Tjandra; Laboratory of Molecular Biophysics.
19. **Facilitator Models of Weak Binding in Protein-Protein Interactions.** S. Kale, M. Strickland, A. Peterkofsky, N. Tjandra, J. Liu; Theoretical Cellular Physics.
20. **Does Supercoiling Locate DNA Lesions?** A. Dittmore, K.C. Neuman; Laboratory of Single Molecule Biophysics.
21. **Uncovering Molecular Mechanisms of Microcephaly.** T. Schoborg, L. Smith, C. Fagerstrom, N.M. Rusan; Laboratory of Molecular Machines & Tissue Architecture.
22. **Personalized Deep Detection of Measurable Residual Disease in Acute Myeloid Leukemia.** H.Y. Wong, M.P. Mulé, Q.G. Liu, C.S. Hourigan; Myeloid Malignancies Section.
23. **Illuminating Mitophagy in Living mt-Keima Mouse Tissues via Super-Resolution Microscopy.** D. Malide, N. Sun, T. Finkel; Light Microscopy Core.
24. **Parkin Targets NOD2 to Regulate Astrocyte ER Stress and Inflammation.** K. Singh, M.N. Sack; Laboratory of Mitochondrial Biology in Cardiometabolic Syndromes.
25. **Differences in Protein Hydration Dynamics in Cryo-EM and X-Ray Structural Models.** F. Tofoleanu¹, F. C. Pickard¹, L. Earl², S. Subramaniam², B. R. Brooks¹; ¹Laboratory of Computational Biology, NHLBI, ²Laboratory of Cell Biology, NCI.
26. **VEGFA Concentration *In-Vitro* Modulates Hemogenic Endothelium Differentiation and Downstream Hematopoietic Stem and Progenitor Cell Identity.** J.P. Ruiz, C. Porcher, A. Larochele; Laboratory of Regenerative Therapies for Inherited Blood Disorders.
27. **ZFR Coordinates Crosstalk Between RNA Decay and Transcription in Innate Immunity.** N. Haque¹, R. Ouda², K. Ozato², J.R. Hogg¹; ¹Laboratory of Biochemistry, NHLBI, ²Division of Developmental Biology, NICHD.
28. **Membrane Binding and Fluidity Sensing by α -, β -, and γ -Synuclein.** E.I. O'Leary, Z. Jiang, J.C. Lee; Laboratory of Protein Conformation and Dynamics.
29. **A Novel CD19/CD3 Bispecific Antibody Induces Potent Response Against Chronic Lymphocytic Leukemia.** H. Robinson¹, J. Qi², S. Baskar¹, C. Rader², A. Wiestner¹; ¹Hematology Branch, NHLBI; ²The Scripps Research Institute, Jupiter, FL.
30. **Non-Nuclear Estrogen Receptor Alpha Activation in Endothelium Reduces Cardiac Ischemia-Reperfusion Injury in Mice.** J. Sun, S. Menazza, E. Murphy; Cardiac Physiology Section.
31. **Mitochondria Maintain Intestinal Stem Cell Homeostasis via ROS and FOXO Pathways.** F. Zhang, H. Xu; Laboratory of Molecular Genetics.

32. **In-vivo Trafficking of Adoptively Transferred NK Cells Using ⁸⁹Zirconium Cell Labelling and PET/CT.** K. Stringaris¹, J.K. Davidson-Moncada¹, N. Sato², R. Reger¹, C. Dunbar¹, P. Choyke², R.W. Childs¹; ¹Laboratory of Transplantation Immunotherapy, NHLBI, ²Molecular Imaging Clinic, NCI.
33. **Local Hypoxia Controls Nerve-Mediated Arterial Branching via HIF-Independent Pathways in Developing Skin.** W. Li¹, K. Nakayama², Y.S. Mukoyama¹; ¹Laboratory of Stem Cell and Neuro-Vascular Biology, NHLBI, ²Oxygen Biology Laboratory, Medical Research Institute, Tokyo Medical and Dental University.
34. **Expression and Purification of Human Bloom's Syndrome Helicase for Comparative Single-Molecule Studies of Post-Translational Modifications on Enzyme Activity.** L. Bradley, K.C. Neuman; Laboratory of Single Molecule Biophysics.
37. **Low Density Granulocytes Associate with Non-Calcified Coronary Plaque and Endothelial Cell Damage in Psoriasis.** H.L. Teague, J.I. Silverman, A. Dey, A. Joshi, E. Stansky, M.M. Purmalek, Y. Baumer, P.K. Dagur, C.L. Harrington, T. Aridi, G. Sanda, A.V. Sorokin, D.A. Bluemke, M. Chen, M.P. Playford, J.P. McCoy Jr, M.J. Kaplan, N.N. Mehta; Section of Inflammation and Cardiometabolic Diseases.
38. **Evaluation of Early Biomarkers Associated with Graft Rejection in Patients with Sickle Cell Disease.** P. Olkhanud¹, F. Seifuddin², M. Pirooznia², C. Pittman¹, A. Biancotto³, R. Pfeiffer⁴, C. Fitzhugh¹; ¹Laboratory of Early Sickle Mortality Prevention, NHLBI, ²Bioinformatics and Computational Biology Core Facility, NHLBI, ³Center for Human Immunology, Autoimmunity, and Inflammation, NHLBI, ⁴Biostatistics Branch, NCI.
39. **A Role for PPAR α in Sex Differences in Cardiac Hypertrophy.** N. Fillmore, J. Harrington, S. Gao, Y. Yang, X. Zhang, P. Liu, A. Stoehr, D. Springer, J. Zhu, X. Wang, E. Murphy; Laboratory of Cardiac Physiology.
40. **Structure-Function Studies of ApoA-I Mimetic Peptides for ABCA1-dependent Cholesterol Efflux and HDL Formation.** R.M. Islam, M. Pourmousa, S. Gordon, D. Sviridov, R.W. Pastor, A.T. Remaley; Lipoprotein Metabolism Section.
41. **Oxidative Phosphorylation Complex Interactions in Intact Mitochondria.** B.M. Rabbitts, F. Liu, P. Lössl, A.J. Heck, R.S. Balaban; Laboratory of Cardiac Energetics, NHLBI and Bijvoet Center for Biomolecular Research, University of Utrecht, The Netherlands.
42. **Unfavorable Perceptions of Neighborhood Environment are Associated with Greater Sedentary Time: Data from the Washington, D.C. Cardiovascular Health and Needs Assessment.** C. Ahuja, C. Ayers, J. Hartz, J. Adu-Brimpong, V. Mitchell, M. Peters-Lawrence, D. Sampson, A. Brooks, G. Wallen, A. Johnson, L. Graham, A. Graham, F. Grant, J. Rivers, S. Thomas, L. Yngling, T. Powell-Wiley; Social Determinants of Cardiovascular Risk and Obesity.
43. **Structural Characterization of Very Low Density Lipoprotein Receptor and Insight into Interaction with Fibrin β N.** K. Banerjee¹, S. Yakovlev², L. Medved², N. Tjandra¹; ¹Laboratory of Structural Biophysics, NHLBI, ²University of Maryland School of Medicine, Baltimore, MD.
44. **LDL-Receptor Related Protein-1 Attenuates House Dust Mite-Induced Airway Inflammation by Suppressing Dendritic Cell-Mediated Adaptive Immune Responses.** A. Mishra¹, A. Saxena², E.M. Gordon¹, X. Yao¹, M. Kaler¹, R.A. Cuento¹, A.V. Barochia¹, P.K. Dagur², J.P. McCoy², K.J. Keeran³, K.R. Jeffries³, X. Qu⁴, Z. Yu⁴, S.J. Levine¹; ¹Laboratory of Asthma and Lung Inflammation, ²Flow Cytometry Core Facility, ³Animal Surgery and Resources Core Facility, ⁴Pathology Core Facility.
45. **Real-Time Flow MRI to Monitor Exercise Stress.** R. Ramasawmy¹, D. Herzka, J.M. Khan¹, T. Rogers¹, R.J. Lederman¹, M.S. Hansen², A.E. Campbell-Washburn²; ¹Cardiovascular Intervention Program, ²Laboratory of Imaging Technologies.
46. **Apolipoprotein A-I and Apolipoprotein E Differentially Modulate the Expression of Extracellular Matrix Proteins by IPF Lung Fibroblasts.** D.M. Figueroa¹, S. Bui², L. Rodriguez², G.M. Grant², S.D. Nathan³, S.J. Levine¹; ¹Laboratory of Asthma and Lung Inflammation, NHLBI, ²Department of Biology, George Mason University, ³Advanced Lung Disease and Lung Transplant Clinic, Inova Fairfax Hospital.
47. **The Role of Non-Muscle Myosin 2A and 2B in Contact Guidance.** A. Zhovmer¹, E. Tabdanov², H. Miao³, H. Wen³, L. Kam⁴, P. P. Provenanzo², X. Ma¹, R. S. Adelstein¹; ¹Laboratory of Molecular Cardiology, NHLBI, ²Laboratory for Engineering in Oncology, University of Minnesota, ³Imaging Physics Laboratory, NHLBI, ⁴Microscale Biocomplexity Laboratory, Columbia University.
48. **Altered Extracellular Matrix Metabolism as a Potential Link to the Pathophysiology of Vascular Abnormalities in Autosomal Dominant Hyper-IgE Syndrome.** D. Nguyen¹, N.I. Dmitrieva¹, B.A. Kozel², A.F. Freeman³, M. Boehm¹; ¹Laboratory of Cardiovascular Regenerative Medicine, NHLBI, ²Laboratory of Vascular and Matrix Genetics, NHLBI, ³Laboratory of Clinical Infectious Diseases, NIAID.
49. **Eltrombopag Promotes DNA Repair in Human Hematopoietic Stem and Progenitor Cells: Implications for the Treatment of Fanconi Anemia.** K.L. Guenther, R. Smith, A. Larochelle; Regenerative Therapies for Inherited Blood Disorders.
50. **Cholesterol-Enrichment of Cells Induces Unique Extracellular Cholesterol Microdomains.** X. Jin¹, Y. Liu², L. Addadi³, H.S. Kruth¹; ¹Laboratory of Experimental Atherosclerosis, NHLBI, ²NICHD, ³Weizmann Inst of Science, Rehovot, Israel.
51. **Micro Fabrication of Hard X-ray Compound Refractive Lens Using Nanoprinting Process.** M. Mirzaeimoghri, A. Morales, C. McCue, D. DeVoe, H. Wen; Imaging Physics Laboratory.
52. **Mutations in Non-Muscle Myosin 2A Causing MYH9-Related Disease Disrupt Sertoli Cell Junctions and Germ Cell Polarity Resulting in Infertility.** D.C. Sung, B.D. MacTaggart, C. Lerma, Y. Zhang, S. Kawamoto, M.A. Conti, X. Ma, R.S. Adelstein; Laboratory of Molecular Cardiology.

53. **Examination of Induced Endocytic Structure Formation in B Lymphocytes.** T.M. Davenport, K. Sochacki, A. Dickey, J. Taraska; Laboratory of Molecular and Cellular Imaging.
54. **A *Drosophila melanogaster* Screen Reveals Novel Functions For Microcephaly Genes.** R.S. O'Neill, N.M. Rusan; Laboratory of Molecular Machines and Tissue Architecture.
55. **alpha-Synuclein Crosslinked by Pyrrole Linkages Derived from Dopamine.** S. Monti, J.W. Werner-Allen, A. Bax, R.L. Levine; Protein Function in Disease.
56. **Soluble APP Functions as a Vascular Niche Signal That Controls Adult Neural Stem Cell Number.** Y. Sato, Y. Uchida, Y. Mukoyama; Laboratory of Stem Cell and Neuro-Vascular Biology.
57. **Identification of Novel Members of the Nonsense-mediated mRNA Decay Pathway.** T.D. Baird, J.R. Hogg; Laboratory of Ribonucleoprotein Biochemistry.
58. **Multifaceted Role of Glycan Interactions on Clathrin-Independent Endocytosis of MHC1 and CD59.** M.P. Mathew, J.G. Donaldson; Membrane Biology Section.
59. **Reconstitution of Mammalian *In Vitro* Translation Using Endogenously Assembled mRNPs.** S. Fritz, J.R. Hogg; Laboratory of Ribonucleoprotein Biochemistry.
60. **Modifying Chondroitin Sulfate Proteoglycans Enhances Retinal Ganglion Cell Axon Regeneration in the Mouse Optic Nerve.** C.S. Pearson, K.R. Martin, H.M. Geller; Developmental Neurobiology Section.
62. **Role of Ca²⁺/Calmodulin-Dependent Protein Kinase II (CaMKII) in Modulating Calcium Uptake in Mitochondria.** M. Oldham, G. Amanakis, R. Parks, E. Murphy; Laboratory of Cardiac Physiology.
63. **Passive Spiritual Health Locus of Control is Associated with Lower Physical Activity Levels in an Urban, Faith-based Community.** S. Thomas, A.T. Brooks, G.R. Wallen, C. Ayers, V. Mitchell, T. Powell-Wiley; Social Determinants of Cardiovascular Risk and Obesity.
64. **Generation of a Mouse with a Methionine Sulfoxide Mimic in Place of Met77 in Calmodulin.** M.C. Marimoutou, R.L. Levine, G. Kim; Laboratory of Biochemistry.
65. **Origin of Pericytes in Developing Skin and Brain Vasculature.** T. Yamazaki¹, A. Nalbandian¹, Y. Uchida¹, W. Li¹, T.D. Arnold², Y. Mukoyama¹; ¹Laboratory of Stem Cell and Neuro-Vascular Biology, NHLBI, ²Department of Pediatrics, Physiology, and Program in Neuroscience, University of California, San Francisco.
66. **Origin, Distribution and Functions of Neural Tube Microglia in the Immunoprivileged Central Nervous System.** C. Liu, Y. Mukoyama; Laboratory of Stem Cell and Neuro-Vascular Biology.
67. **Ibrutinib Acts as a Dual B-cell Receptor and Toll-like Receptor Inhibitor in Chronic Lymphocytic Leukemia.** E. Dashedian, S. Herman, E. McAuley, D. Wong, C. Sun, D. Liu, A. Wiestner; Laboratory of Lymphoid Malignancies.
68. **Consequences of Xyloside Treatment on Neuronal Cytoskeleton Assembly and Function.** C. Mencia, S. Tilve, C. Agbaegbu, H. Katagiri, H. Geller; Developmental Neurobiology Section.
69. **The Effects of Fasting and Refeeding on Regulating NLRP3 Inflammasome Activation in Asthmatic Subjects.** A. Nguyen, K. Han, J. Li, M. Kwarteng-Siaw, J. Traba, M. Sack; Laboratory of Mitochondrial Biology and Metabolism.
70. **iPS-Cardiomyocytes Transfer to Treat Heart Failure from Ischemic Cardiomyopathy – Non-Human Primate Model.** K. Navarengom, E.A. Ferrante, G. Chen, J. Hawkins, S. Hong, J. Chan, Y. Lin, J. Zou, C. Dunbar, M. Boehm; Laboratory of Cardiovascular Regenerative Medicine.
71. **Developmental Regulation of Mitochondrial Biogenesis During *Drosophila* Oogenesis.** Z.H. Wang, H. Xu; Laboratory of Molecular Genetics.
72. **High Risk Features of Coronary Plaque Increase with Worsening Skin Disease in Psoriasis.** J.H. Chung^{1,2}, A.K. Dey^{1,2}, J.B. Lerman^{1,2}, A.A. Joshi^{1,2}, J.P. Rivers^{1,2}, A. Rana^{1,2}, J.A. Rodante^{1,2}, M.P. Playford^{1,2}, M.Y. Chen², D.A. Bluemke², N.N. Mehta^{1,2}; ¹Section of Inflammation and Cardiometabolic Diseases, ²NHLBI.
73. **Cellular Conformations of α -Synuclein Probed by Raman Spectroscopy.** J.D. Flynn, S.M. Lacy, J.C. Lee; Laboratory of Protein Conformation and Dynamics.
74. **House Dust Mite-Derived Proteases Induce Apolipoprotein E Secretion from Asthmatic Alveolar Macrophages via a ROS-dependent Pathway.** E.M. Gordon, H. Xu, X. Yao, A.V. Barochia, M. Kaler, R. Cuento, S.J. Levine; Asthma and Lung Inflammation Section.
75. **A Long-Term Co-Culture with Supporting Cells of the Developing Heart Promotes Maturation of Induced Pluripotent Stem Cell-Derived Cardiomyocytes.** I.H. Garcia-Pak¹, W. Li¹, H. Uosaki², E. Tampakakis², J. Zou³, Y. Lin³, C. Kwon², Y. Mukoyama¹; ¹Laboratory of Stem Cell and Neuro-Vascular Biology, NHLBI, ²Division of Cardiology, The Johns Hopkins University School of Medicine, ³iPSC Core Facility, NHLBI.
76. **Prolonged Fasting Suppresses Mitochondrial NLRP3 Inflammasome Assembly and Execution via SIRT3 Mediated Activation of Superoxide Dismutase 2.** J. Traba, S.S. Geiger, M. Kwarteng-Siaw, K. Han, O.H. Ra, R.M. Siegel, D. Gius, M.N. Sack; Laboratory of Mitochondrial Biology in Cardiometabolic Syndromes.
77. **Equilibration of the Chemical Potential Between Lipid Leaflets During Molecular Dynamics Simulation.** F. Samarjeet, T. Woolf, B.R. Brooks; Laboratory of Computational Biology.

78. **Cardioprotection in Mice with a Knock-In Mutation in Cyclophilin D (CyPD-C202S): A Site of S-nitrosylation.** G. Amanakis, J. Sun, J. Boylston, E. Murphy; Laboratory of Cardiac Physiology.
79. **Molecular and Physiological Impact of Regulated Mitochondrial Calcium Uptake.** J.C. Liu, J. Liu, R.J. Parks, C. Liu, E. Murphy, T. Finkel; Laboratory of Molecular Biology.
80. **GCN5L1 Interacts with RanBP2 to Mediate Lysosome Positioning.** K. Wu, L. Wang, M.N. Sack; Laboratory of Mitochondrial Biology and Metabolism.
81. **Effects of alpha-Synuclein Uptake on Cellular Viability, Morphology, and Localization.** S. Lacy, J. Flynn, J.C. Lee; Laboratory of Protein Conformation and Dynamics.
82. **Biochemical Characterization of the *Drosophila* Methionine Sulfoxide Reductase A.** S. Tarafdar, G. Kim, N.M. Rusan, R.L. Levine; Laboratory of Biochemistry.
84. **Peculiar Cell Phenotypes Caused by Plasticity Related Gene 3/5 Due to RhoA/Rac1 Imbalance.** S. Tilve, C. Mencio, N. George, C. Agbaegbu Iweka, C. Pearson, Y. Katagiri, H.M. Geller; Developmental Neurobiology Section.
85. **The Plasma Protein Profiling of Sickle Cell Diseases Patients by Tandem Mass Spectrometry Based Proteomic Analysis.** D. Ma, A. Ikeda, Y. Yang, H. Ackerman; Sickle Cell Branch.
86. **Brownian Ratchet Mechanism for Faithful Segregation of Low-Copy-Number Plasmids.** L. Hu¹, A. G. Vecchiarelli³, K. Mizuuchi², K. C. Neuman¹, J. Liu¹; ¹Laboratory of Molecular Biophysics, NHLBI, ²Laboratory of Molecular Biology, NIDDK, ³Department of Molecular, Cellular, and Developmental Biology, University of Michigan.
87. **GCN5L1 Modulates Cross-Talk Between Mitochondria and Cell Signaling to Regulate FoxO1 Stability and Gluconeogenesis.** L. Wang, I. Scott, L. Zhu, K. Wu, K. Han, Y. Chen, M. Gucek, M.N. Sack; Laboratory of Mitochondrial Biology and Metabolism.
88. **Association Between Neighborhood-Level Socioeconomic Deprivation and Incident Hypertension: A Longitudinal Analysis of Data from the Dallas Heart Study.** J. Adu-Brimpong, A. Banks, C. Ayers, C. Ahuja, T.A. Kassim, J. Rivers, J. de Lemos, M.A. Albert, T.M. Powell-Wiley; Social Determinants of Cardiovascular Risk and Obesity.
89. **Which Alpha Globin Gene is Primarily Expressed in the Vascular Endothelium?** S.D. Brooks, Y. Yang, H.C. Ackerman; Physiology Section.
90. **Linking Lysosomal Activity to Parkinson's Disease.** R.P. McGlinchey, N. Tayebi, E. Sidransky, J.C. Lee; Laboratory of Protein Conformation and Dynamics.
91. **Development of a Targeted RNA-seq Assay for the Detection of Minimal Residual Disease in Acute Myeloid Leukemia.** G.W. Roloff, L.W. Dillon, H.Y. Wong, C.S. Hourigan; Myeloid Malignancies Section.
92. **A Membrane Trafficking Screen to Identify Clathrin-Independent Endocytosis Machinery.** J. Wayt, D. Dutta, J.G. Donaldson; Membrane Biology Section.
93. **Development Of "Ultra-High Speed" Western Blot Without Sacrifice of Sensitivity.** S. Higashi, Y. Katagiri, H.M. Geller; Developmental Neurobiology Section.
94. **Psoriasis Induced Chronic Inflammation Results in Pro-Atherosclerotic Changes in Macrophages Resulting in Enhanced Atherosclerosis Development.** Y. Baumer, Q. Ng, G.E. Sanda, A.K. Dey, A.V. Sorokin, H.L. Teague, P.K. Dakur, J.I. Silverman, C.L. Harrington, A. Chaturvedi, J.A. Rodante, D.A. Springer, M.C. Winge, M.P. Marinkovich, M.P. Playford, N.N. Mehta; Section of Inflammation and Cardiometabolic Diseases.
95. **Development of an Optimized Toolkit for High-Efficiency Lentiviral Genetic Modification of Human Natural Killer Cells.** G. Waller, D. Allan, D. Chinnasamy, M. Chakraborty, M. Hochman, R. Reger, R. Childs; Laboratory of Transplantation Immunotherapy.
96. **Selective Protein Synthesis on the Mitochondrial Surface Drives the mtDNA Selection.** Y. Zhang, H. Xu; Laboratory of Molecular Genetics.
97. **High-Dimensional Immunophenotyping of the NK Cell Compartment in Acute Myeloid Leukemia.** K. Lindblad, M. Goswami, K. Oetjen, C. Hourigan; Myeloid Malignancies Section.
99. **Sequence-Specific Protection of mRNAs from Nonsense-Mediated Decay.** A. Kishor, Z. Ge, J.R. Hogg; Laboratory of Ribonucleoprotein Biochemistry.
100. **Repeat-Swap Homology Modeling of the Anion Exchanger (AE1) Reveals an Elevator-Like Antiport Mechanism.** E. Ficici, J.D. Faraldo-Gómez, L.R. Forrest, M.L. Jennings; Theoretical and Molecular Biophysics Section.
101. **Functional Study of CCR5 in Human Macrophages using iPSC-Derived Myeloid *in vitro* Disease Model.** Y. Ma, Y. Huang, F. Calcaterra, D. Mavilio, L.G. Biesecker, G. Chen, D. Yang, M. Boehm; Laboratory of Cardiovascular Regenerative Medicine.
103. **Macrophages from Patients with Arterial Calcification Due to CD73 Deficiency Have Impaired Ability to Resolve an Inflammatory Response.** A. Grubb, Y. Ma, D. Yang, G. Chen, N. Dmitrieva, E. Ferrante, M. Boehm; Laboratory of Cardiovascular and Regenerative Medicine.
104. **Novel Degenerative and Developmental Defects in a Zebrafish Model of Mucopolysaccharidosis Type IV.** H. Li¹, W. Pei², S. Vergarajauregui^{1,3}, P.M. Zervas⁴, N. Raben⁵, S.M. Burgess², R. Puertollano^{1*}; ¹Protein Trafficking and Organelle Biology, NHLBI, ²Translational and Functional Genomics Branch, NHGRI, ³Experimental Renal and Cardiovascular Research, Department of

- Nephropathology, Institute of Pathology, Friedrich-Alexander-Universität Erlangen-Nürnberg, Erlangen, Germany, ⁴Office of Research Services, Division of Veterinary Resources, NIH, ⁵Laboratory of Muscle Stem Cells and Gene Regulation, NIAMS.
105. **Arylsulfatase B Induce Increased Neurite Outgrowth in Hippocampal Neurons When Cocultured With Astrocytes.** N. George, C. Mencio, P. Yu, Y. Katagiri, H.M. Geller; Developmental Neurobiology Section.
 106. **PRG-3 Modulates CSPG and LPA Inhibition of Neurite Outgrowth through the RHOA- ROCK Pathway.** C. Agbaegbu Iweka^{1,2}, N. George¹, C. Mencio¹, S. Tilve¹, C. Pearson¹, S. Higashi¹, P. Yu³, Y. Katagiri¹; H.M. Geller¹; ¹Developmental Neurobiology Section, NHLBI, ²Interdisciplinary Program in Neuroscience, Georgetown University, ³Guangdong-Hong Kong-Macau Institute of CNS Regeneration (GHMICR), Jinan University, Guangzhou, China.
 107. **Functional Implications of the RecQ Helicase - Topoisomerase III – SSB Complex: Insights from Single Molecule Measurements.** M. Mills, Y. Seol, K.C. Neuman; Laboratory of Single Molecule Biophysics.
 108. **The Adaptive Immune Microenvironment in the Bone Marrow of Healthy Adults and Relapsed/Refractory Acute Myeloid Leukemia Patients.** M. Goswami, K. Lindblad, K. Oetjen, C. Hourigan; Myeloid Malignancies Section.
 109. **Generation of Methionine Sulfoxide Reductase Quadruple Knockout Mice.** L. Lai, C. Liu, R. Levine; Protein Function in Disease Section.
 110. **Dynamic Epigenetic Status and Plasticity During CD4+T Cell Differentiation.** Y. Ding, J. Song, K. Zhao; Laboratory of Epigenome Biology.
 111. **Improvement in Skin Inflammation is Associated with Improvement in Aortic Vascular Inflammation by 18-FDG PET/CT.** A.K. Dey^{1,2}, A.A. Joshi^{1,2}, A. Chaturvedi^{1,2}, J.B. Lerman^{1,2}, T.M. Aberra^{1,2}, J.A. Rodante^{1,2}, H.L. Teague^{1,2}, C.L. Harrington^{1,2}, J.P. Rivers^{1,2}, J.H. Chung¹, M.T. Kabbany^{1,2}, B. Natarajan¹, J.I. Silverman^{1,2}, Q. Ng^{1,2}, G.E. Sanda^{1,2}, A.V. Sorokin^{1,2}, Y. Baumer^{1,2}, B.N. Lockshin³, M.A. Ahlman¹, M.P. Playford^{1,2}, J.M. Gelfand⁴, N.N. Mehta^{1,2}; ¹Section of Inflammation and Cardiometabolic Diseases, ²NHLBI, ³DermAssociates, Silver Spring, MD. ⁴Department of Dermatology, University of Pennsylvania.
 112. **Distinct Focal Adhesion Morphologies Emerge from Interplay Between Retrograde Actin Flux and Stress Fiber.** Z. Wu, J. Liu; Laboratory of Molecular Biophysics.
 113. **CRISPR/Cas9-Mediated Dissection of Functional Domains of the Transcription Factor c-MYB.** N. Angelis, X. Wang, I. Tunc, Y. Li, G. Bogoda, A. Esquinca, M. Pirooznia, S.L. Thein; Sickle Cell Branch.
 114. **Smooth Muscle Cell Proliferation in Fetal ELN Heterozygous Versus Control Mice, Suggests Mechanism Underlying William Syndrome Cardiac Disease.** A. Watson, M. Levin, B. Kozel; Laboratory of Cardiac Physiology.
 115. **CypD-Mediated Regulation of the Permeability Transition Pore is Altered in Mice Lacking the Mitochondrial Calcium Uniporter.** R.J. Parks¹, S. Menazza¹, A.M. Aponte², T. Finkel³, E. Murphy¹; ¹Systems Biology Center, ²Proteomic Core Facility, ³Center for Molecular Medicine.
 116. **Fetal Mouse Heart Imaging Using Echocardiography.** D. Mokshagundam^{1,2}; D. Donahue³; I. Garcia-Pak¹; B. Klaunberg³; Y. Mukouyama¹; L. Leatherbury^{1,2}; ¹Laboratory of Stem Cell and Neuro-Vascular Biology, NHLBI, ²Children's National Heart Institute, Children's National Health System, ³NIH Mouse Imaging Facility.
 117. **Determinants of Vascular Inflammation by 18-Fluorodeoxyglucose PET/MRI: Findings from the Psoriasis, Atherosclerosis and Cardiometabolic Disease Initiative.** M.T. Kabbany, A.K. Dey, A. Chaturvedi, J.P. Rivers, J.H. Chung, P. Shukla, A. Rana, J.A. Rodante, A.A. Joshi, J.B. Lerman, T.M. Aberra, J.I. Silverman, Q. Ng, H.L. Teague, A. Dahiya, M.A. Ahlman, D.A. Bluemke, N.N. Mehta; Section of Inflammation and Cardiometabolic Diseases.
 118. **Cell-Free DNA as a Biomarker in Sickle Cell Disease: Method Optimization and Analysis.** L. Tumburu, S. Yang, Y. Wakabayashi, N. Igbineweka, M. Pirooznia, I. Tunc, Y. Li, J. Zhu, S.L. Thein; Sickle Cell Branch.
 119. **Single-Cell RNA Sequencing Analysis of Bone Marrow Populations.** K.A. Oetjen, C.S. Hourigan; Myeloid Malignancy Section.
 120. **Genetic Modifiers of Cardiovascular Phenotype in Elastin-Mediated Disease.** P. Parrish, M. Lugo, B. Kozel; Laboratory of Vascular and Matrix Genetics.
 121. **NCF1 Mutation Improves Vascular Stiffness in Elastin Haploinsufficiency Through its Effect on Blood Pressure.** A. Troia, R. Knutsen, J. Danback, B. Kozel; Laboratory of Vascular and Matrix Genetics.
 122. **Molecular Breakdown of DEER Data from Self-Learning Atomistic Simulations.** F. Marinelli, G. Fiorin, J. Faraldo-Gómez; Theoretical Molecular Biophysics Section.
 123. **High Sensitivity Detection of Mutations Implicated in Chronic Lymphocytic Leukemia Drug Resistance.** C. Nichols, C. Underbayev, S. Herman, A. Wiestner; Hematology Branch.

Abstracts in Order of First Author

Association Between Neighborhood-level Socioeconomic Deprivation and Incident Hypertension: A Longitudinal Analysis of Data from the Dallas Heart Study. J. Adu-Brimpong, A. Banks, C. Ayers, C. Ahuja, T.A. Kassim, J. Rivers, J. de Lemos, M.A. Albert, T.M. Powell-Wiley; Social Determinants of Cardiovascular Risk and Obesity.

Hypertension (HTN), a major contributor to leading causes of morbidity and mortality, is significantly associated with neighborhood socioeconomic environment. However, existing studies have been largely cross-sectional (thus focusing on HTN prevalence), have taken place outside of the U.S. and/or employed limited definitions of neighborhood deprivation. In this study, we examine longitudinal associations between neighborhood deprivation and incident HTN. Movers and non-movers aged 18-65 (N=1989) in the Dallas Heart Study (DHS), a multi-ethnic, population-based cohort in Dallas County, Texas (N=6101), underwent blood pressure (BP) measurements between 2000 and 2009 (median 7-year follow up). HTN was defined by either: self-report, systolic BP \geq 140 mmHg, diastolic BP \geq 90 mmHg, or use of anti-HTN medication. Geocoded address data from DHS participants established block groups; a neighborhood deprivation (NDI) was created (higher NDI=greater deprivation). NDI was divided into tertiles: low, medium and high deprivation. Multi-level modeling determined incident HTN relative to NDI, adjusting for covariates including years spent in and movement between neighborhoods. NDI distribution ranged from -1.08 (minimum) to 5.83 (maximum). Systolic (beta=1.63, p-value=.0002) and diastolic BP (beta=.82, p-value=.0004) increased with increasing NDI. Significant association remained between NDI and incident HTN for those living in high deprivation areas [odds ratio 1.62 (95% CI = 1.09, 2.60)] compared to those in low deprivation areas following adjustment for covariates. Living in more socioeconomically deprived neighborhoods, irrespective of movement and length of time spent in neighborhood, was associated with incident HTN in a multiethnic, population-based cohort in Dallas, Texas.

PRG-3 Modulates CSPG and LPA Inhibition of Neurite Outgrowth through the RHOA-ROCK Pathway. C. Agbaegbu Iweka^{1,2}, N. George¹, C. Mencio¹, S. Tilve¹, C. Pearson¹, S. Higashi¹, P. Yu³, Y. Katagiri¹; H.M. Geller¹; ¹Developmental Neurobiology Section, NHLBI, ²Interdisciplinary Program in Neuroscience, Georgetown University, ³Guangdong-Hong Kong-Macau Institute of CNS Regeneration (GHMICR), Jinan University, Guangzhou, China.

Plasticity-related gene (PRGs) proteins, are integral membrane proteins characterized by six transmembrane domains and are a subclass of the lipid phosphate phosphatase (LPP) superfamily. A quantitative phosphoproteomic screen designed to determine global phosphorylation changes in neurons in response to chondroitin sulfate proteoglycans (CSPGs), revealed PRG-3 as a protein whose phosphorylation state was most altered by exogenous CSPG treatment. Here, we report that PRG3 expression in primary neurons overcomes neurite

outgrowth inhibition mediated by CSPGs. Furthermore, PRG-3 attenuates lysophosphatidic acid (LPA) induced neurite retraction in neuronal cell line by decreased phosphorylation of myosin light chain II. In summary, our data indicates that PRG-3 protein modulates neuronal response to CSPGs and LPA, both inhibitory molecules to axonal outgrowth, and therefore may mediate neuronal plasticity. These studies will contribute to a more comprehensive understanding of how neuronal plasticity is modulated and provide an avenue of investigation to improve therapeutic strategies after injury to the CNS.

Unfavorable Perceptions of Neighborhood Environment are Associated with Greater Sedentary Time: Data from the Washington, D.C. Cardiovascular Health and Needs Assessment. C. Ahuja, C. Ayers, J. Hartz, J. Adu-Brimpong, V. Mitchell, M. Peters-Lawrence, D. Sampson, A. Brooks, G. Wallen, A. Johnson, L. Graham, A. Graham, F. Grant, J. Rivers, S. Thomas, L. Yingling, T. Powell-Wiley; Social Determinants of Cardiovascular Risk and Obesity.

Sedentary time (ST) and unfavorable perceptions of neighborhood environment (NE) are independently associated with poor cardiovascular (CV) health. However, little is known about ST's relationship to NE perceptions. We examined associations between ST and NE perception in the Washington, D.C. CV Health and Needs Assessment. Participants underwent a CV health evaluation designed using community-based participatory research principles in lower socioeconomic (SES) areas in D.C. Participants responded, on a 5-point scale, to questions about NE perceptions (e.g. recreational areas, crime). Factor analysis was conducted to explore associations with overall NE perception. The factor sums were combined as Total Perception Score (TPS). For ST, participants reported hours "spent sitting or reclining on a typical day". Linear regression analyses were performed to determine the relationship between TPS (range 15-75, higher score=more favorable perception) and ST for 1) overall population, 2) D.C. Wards 5, 7, and 8 and 3) other DC/Maryland (MD) areas. In the sample (N=99, 99% African-American, 78% female), DC Wards 5, 7, and 8 had a higher percentage of households with yearly income of <\$60,000 (p<0.05) and lower mean TPS (p < 0.001). Three factors (neighborhood violence, physical and social environment, and social cohesion) were associated with overall NE perception. In lower SES wards, there was a negative association between TPS and ST that remained significant after adjusting for covariates. This relationship was not observed in higher SES areas. Targeted interventions to improve perceptions of physical and social environment in lower SES areas of D.C. may decrease ST and improve CV health.

Cardioprotection in Mice with a Knock-In Mutation in Cyclophilin D (CyPD-C202S): A Site of S-nitrosylation. G. Amanakis, J. Sun, J. Boylston, E. Murphy; Laboratory of Cardiac Physiology.

Our previous study in mouse embryonic fibroblasts showed that cysteine 202 of cyclophilin D (CyPD) is necessary

for redox stress-induced activation of the mitochondrial permeability transition pore (mPTP). To further investigate the essential function of this cysteine residue *in situ*, we used CRISPR to develop a knock-in mouse model (C57BL/6N strain), where CyPD cysteine 202 was mutated to a serine (C202S-KI). The amount of total CyPD expressed in the CyPD C202S-KI did not differ compared to the wild-type (WT). However, the CyPD C202S-KI mouse hearts elicit a significant cardioprotective effect against ischemia-reperfusion (I/R) injury in the Langendorff perfused heart model. After 20 min of global ischemia followed by 90 min of reperfusion, the post-ischemic recovery of rate pressure product (RPP= heart rate x LVDP) was $45.0 \pm 4.2\%$ in CyPD WT and $59.6 \pm 4.0\%$ in CyPD C202S-KI mice ($p=0.0455$). Myocardial infarct size was decreased in CyPD C202S-KI mouse hearts versus CyPD WT mice ($24.5 \pm 4.7\%$ vs $49.8 \pm 2.7\%$, $p=0.0095$). Isolated heart mitochondria from CyPD C202S-KI mice had a higher calcium retention capacity compared to CyPD WT mice (213.3 ± 16.67 vs 140.0 ± 20.82 $\mu\text{mol Ca}^{+2}/\text{g protein}$, $p=0.0371$). However, in contrast to CyPD knockout mice which exhibit more pronounced cardiac hypertrophy in response to pressure overload stimulation than control mice, CyPD C202S-KI mice developed a comparable level of hypertrophy to their WT littermate in an angiotensin II-induced hypertrophy model delivered by implanted osmotic minipumps. In conclusion, these results show that mutated CyPD C202S affords cardioprotection against I/R injury, suggesting that the redox-modification of cysteine 202 might play an important role in the regulation of CyPD and its downstream targets such as mPTP.

CRISPR/Cas9-Mediated Dissection of Functional Domains of the Transcription Factor c-MYB. N. Angelis, X. Wang, I. Tunc, Y. Li, G. Bogoda, A. Esquinca, M. Pirooznia, S.L. Thein; Sick Cell Branch.

De-repression of fetal hemoglobin (HbF), that is developmentally silenced in adults, has immense clinical benefits in patients with Sickle Cell Disease (SCD). c-MYB is a sequence-specific transcription factor that is encoded by the proto-oncogene *MYB*; it has an important role in hematopoiesis and erythropoiesis and has also been involved in regulation of HbF. We used the CRISPR/Cas9 gene editing system to dissect the various functional domains of the protein and to investigate if there are domain(s) specifically related to HbF regulation, using both the human erythroleukemia K562 and the Human Umbilical cord blood-Derived Erythroid Progenitor-2 (HUDEP-2) cell line. Several single-cell clones for each edited domain have been established and confirmed by DNA Sanger sequence analysis. These clones will be fully characterized to confirm the expression of MYB by total RNA sequencing and by Western blot analyses. RNA sequencing will provide the expression profile of other genes known to play an important role in regulation of HbF. HbF levels will be assessed by measuring F cells using FACS and the protein quantitated using HPLC, after induction of erythroid differentiation. Preliminary analyses suggested that clones which caused a reduction of c-MYB protein appears to be correlated with increased F cells, but other clones which affect the C-terminus domains of the

protein that minimally affects c-MYB quantitatively, is also correlated with increased F-cells. FACS analysis for CD235+ cells showed that deletions of these domains do not affect the erythroid maturation of HUDEP-2 cells, suggesting that the alteration in F-cells is directly mediated.

Identification of Novel Members of the Nonsense-Mediated mRNA Decay Pathway. T.D. Baird, J.R. Hogg; Laboratory of Ribonucleoprotein Biochemistry.

Eukaryotic mRNA decay is a highly dynamic process central to the regulation of gene expression and maintenance of cellular homeostasis. A major contributor to this regulation is the nonsense-mediated mRNA decay (NMD) pathway, which degrades diverse mRNAs in all eukaryotes. In addition to serving as a surveillance monitor for aberrant transcripts containing premature termination codons (PTCs) resulting from genetic mutations or errors during mRNA biogenesis, the NMD pathway degrades 5-10% of non-aberrant human mRNAs. To better understand the activities and regulation of the human NMD pathway, our collaborators (Inglese, Buehler, and Martin groups, NCATS) conducted a genome-wide screen in a human cell line using a siRNA library targeting over 21,000 genes. From this screen, we identified ICE1 and USPL1 as two novel members of the NMD pathway that, when depleted, lead to increased abundance of canonical NMD targets. Biochemical and RNAseq analyses indicate that these factors are required for proper recognition of NMD substrates harboring an exon junction complex (EJC) downstream of an open reading frame, a strong enhancer of NMD. Furthermore, we demonstrate that a predicted MIF4G domain in the C-terminus of ICE1 is sufficient to *co*-immunoprecipitate the core EJC *in vivo* and that disruption of this interaction precludes the formation of an EJC-NMD factor complex required for target recognition and decay.

Structural Characterization of Very Low Density Lipoprotein Receptor and Insight into Interaction with Fibrin β N. K. Banerjee¹, S. Yakovlev², L. Medved², N. Tjandra¹; ¹Laboratory of Structural Biophysics, NHLBI, ²University of Maryland School of Medicine, Baltimore, MD.

Very Low Density Lipoprotein Receptor (VLDLR) is a member of the low-density lipoprotein receptor family expressed in various tissues and more importantly in vascular endothelium. VLDLR influences transendothelial migration of leukocytes through its interaction with fibrin and thus leading to inflammation. Fibrin, which is formed by thrombin-mediated cleavage of fibrinogen, is abundantly present in blood. Interestingly, the β N domain of fibrinogen upon interaction with VLDLR reduces inflammation related atherosclerosis. We are interested in understanding the VLDLR-fibrin β N interaction and its role in inflammation related atherosclerosis. However, so far there is no structural information of VLDLR and neither of fibrin β N. Binding assays have shown that the highest affinity of the VLDLR and fibrin β N is when three-domain repeats from N-terminus of VLDLR are present. Solution NMR studies have been performed to attain the structural details of VLDLR, fibrin β N, and VLDLR-fibrin β N complex. Based on

backbone relaxation dynamics study, it has been observed that the two N-terminal domains of VLDLR seem to diffuse together, while the third domain diffuses independently. Combination of complete structural information and dynamics of all the domains of VLDLR only and upon binding with fibrin β N would provide better understanding of the biological significance of VLDLR-fibrin interaction and provide a step forward for designing better inhibitor of this interaction that can reduce inflammation.

Psoriasis Induced Chronic Inflammation Results in Pro-Atherosclerotic Changes in Macrophages Resulting in Enhanced Atherosclerosis Development. Y. Baumer, Q. Ng, G.E. Sanda, A.K. Dey, A.V. Sorokin, H.L. Teague, P.K. Dakur, J.I. Silverman, C.L. Harrington, A. Chaturvedi, J.A. Rodante, D.A. Springer, M.C. Winge, M.P. Marinkovich, M.P. Playford, N.N. Mehta; Section of Inflammation and Cardiometabolic Diseases.

Psoriasis is a chronic inflammatory skin disease with accelerated atherosclerosis, however mechanistic data linking these two disease states is lacking. We present a mouse model (K14-RacV12^{+/+}) with psoriatic skin and joint disease along with increased systemic inflammation, dyslipidemia (defects in HDL efflux capacity, pro-atherosclerotic macrophage phenotype) and cardiometabolic dysfunction, thus mimicking the human disease state. Furthermore, macrophages derived from psoriatic mice also displayed a pro-atherosclerotic gene profile (e.g. upregulation of *CD38*, *Fpr2*, *Arg1* and *iNOS*), with increased lipid uptake (1.4-fold), foam cell formation (1.3-fold), and early apoptotic events (1.5-fold) compared to littermate controls. Psoriatic macrophages also show a 6-fold increase in cholesterol crystal formation. We have also generated a triple genetic K14-RacV12^{+/+}/SRB^{-/-}/ApoER61^{H/H} mouse to characterize the effects of the psoriasis phenotype on atherogenesis. When placed on a high calorie diet, a 5-fold increase in atherosclerotic plaque development was observed when compared to SRB^{-/-}/ApoER61^{H/H} control. Messenger RNA analysis of psoriatic macrophages revealed a 60% reduction in Superoxide Dismutase 2 (SOD2) expression prompting suggestions that SOD2 may be a key regulator of atherogenesis. Treatment and differentiation of K14-RacV12^{+/+} macrophages with the SOD2 activator MnCl₂ or mimetic MnTBAP decreased lipid uptake and inhibited cholesterol crystal formation. In conclusion, we demonstrate that the K14-RacV12^{+/+} psoriasis mouse model captures important cardiometabolic features of psoriasis, notably a pro-atherogenic macrophage profile that when crossed with the SRB^{-/-}/ApoER61^{H/H} rapidly increased atherogenesis. These findings provide a platform on which to perform future studies of intervention on psoriasis to which lead to potential modulation of atherosclerotic pathways.

Expression and Purification of Human Bloom's Syndrome Helicase for Comparative Single-Molecule Studies of Post-Translational Modifications on Enzyme Activity. L. Bradley, K.C. Neuman; Laboratory of Single Molecule Biophysics.

As *in vitro* single-molecule techniques continue to deepen the understanding of mammalian enzymes' mechanistic details, it becomes imperative for such studies to produce proteins that most accurately reflect the protein's natural structure. Post-translational modifications, which vary significantly among common bacteria, yeast, and mammalian sources, can have profound effects on protein activity and interactions. Therefore, the host choice for protein production can impact protein function in a way that single-molecule techniques are particularly adept at detecting. This research aims to determine the nature and degree of any differences in activity of a mammalian enzyme depending on its expression host. We are focused on possible differences in the activity of Bloom's helicase (BLM), a human RecQ helicase that is integral to DNA repair and has many binding partners *in vivo* that may require specific features determined by post-translational modifications. This enzyme is particularly well behaved in single-molecule measurements of activity, exhibiting very robust, reproducible, and homogeneous behavior that enables fine-scale differences to be detected. Additionally, if differences are found, this presents new opportunities to measure the effects of post-translational modifications on many enzymes' activities using single-molecule techniques. Progress of protocol development of protein purification from human cells and current comparative enzyme results on single-molecule magnetic tweezers will be presented.

Which Alpha Globin Gene is Primarily Expressed in the Vascular Endothelium? S.D. Brooks, Y. Yang, H.C. Ackerman; Physiology Section.

Alpha globin was recently discovered in the endothelium of resistance arteries, where it interacts with endothelial nitric oxide synthase (*NOS3*) to regulate the diffusion of nitric oxide. In humans, alpha globin locus *HBA2* contributes 65% of total alpha globin in red blood cells, with *HBA1* contributing 35%. However, expression of each locus in the vasculature is currently unknown. Determining total and relative locus-specific expression of alpha globin in resistance arteries is critical to understand the consequences of *HBA1* or *HBA2* locus deletion.

Perfused vessels and whole blood were collected from C57Bl/6J mice. Middle cerebral arteries, skeletal muscle arterioles, mesenteric arteries, and renal arterioles were dissected and placed in RNAlater. Total mRNA was isolated from homogenized vessels and converted to cDNA.

Absolute gene expression of *Hba-a1* (mouse homolog of *HBA2*), *Hba-a2* (mouse homolog of *HBA1*), *Nos3*, and *Ae1* was quantified by digital droplet PCR. Abundant expression of *Hba-a1* and *Hba-a2* was observed in whole blood, as well as in all four vascular tissues. In whole blood, the *Hba-a1/Hba-a2* ratio was (2.55:1), consistent with expression reported in human blood. However, in all four groups of arteries the *Hba-a1/Hba-a2* ratio was inverted (0.60:1).

We report robust, locus-specific expression of alpha globin in four anatomically distinct arteries. The expression ratio of *Hba-a1* and *Hba-a2* is inverted between vascular tissue and whole blood in mice, suggesting differential regulation of alpha globin transcription.

High Risk Features of Coronary Plaque Increase with Worsening Skin Disease in Psoriasis. J.H. Chung^{1,2}, A.K. Dey^{1,2}, J.B. Lerman^{1,2}, A.A. Joshi^{1,2}, J.P. Rivers^{1,2}, A. Rana^{1,2}, J.A. Rodante^{1,2}, M.P. Playford^{1,2}, M.Y. Chen², D.A. Bluemke², N.N. Mehta^{1,2}; ¹Section of Inflammation and Cardiometabolic Diseases, ²NHLBI.

Psoriasis (PSO) is a chronic inflammatory disease and provides a reliable human model to study inflammatory atherogenesis. PSO is associated with the presence of high risk coronary plaque (HRP), a feature prone to rupture leading to myocardial infarction. Whether HRP characteristics modulate with worsening psoriasis skin disease is unknown. We hypothesized that HRP characteristics associate with psoriasis area severity index (PASI) score at baseline and would worsen in those who had increased skin disease severity at one-year. We looked at a subset of PSO patients (N=40) who had an increase in PASI score at one-year. Coronary HRP characterization was done by coronary computed tomography angiography (Toshiba) using QAngio CT (Medis). HRP identification was defined as positive remodeling (index ≥ 1.1), low attenuation (< 30 HU), or spotty calcification and tallied into a score. The cohort was middle-aged, predominantly male, were at low risk by Framingham risk score with mild to moderate psoriasis. At baseline, PASI score associated with HRP characteristics in unadjusted ($\beta=0.47$; $P=0.02$) and adjusted analyses ($\beta=0.69$; $P=0.01$). At one-year follow-up, the group had a median increase in PASI score of 22% ($p<0.001$) which was accompanied with a 36% increase in total HRP characteristics at one-year ($p=0.03$). HRP were associated with psoriasis skin disease severity at baseline and increased as psoriasis skin disease severity worsened at one-year. These findings underscore the importance of treatment of psoriasis skin disease severity to prevent development of early rupture prone, coronary plaques in PSO. However, larger studies are needed to confirm these findings.

Ibrutinib Acts as a Dual B-cell Receptor and Toll-like Receptor Inhibitor in Chronic Lymphocytic Leukemia. E. Dadashian, S. Herman, E. McAuley, D. Wong, C. Sun, D. Liu, A. Wiestner; Laboratory of Lymphoid Malignancies.

The Bruton's tyrosine kinase (BTK) inhibitor ibrutinib is clinically active in lymphoproliferative diseases driven by B-cell receptor (BCR) and Toll-like receptor (TLR) signaling. We previously identified gene signatures indicative of active BCR and TLR signaling in chronic lymphocytic leukemia (CLL) cells residing in lymphoid tissues. Further, TLR9 activating CpG oligonucleotides extend CLL cell survival *in vitro*, suggesting BCR and TLR signaling may cooperate to activate CLL cells in the tissue microenvironment. Here, we tested the hypothesis that targeting both BCR and TLR signaling could improve therapy for CLL. CLL PBMCs were treated with ibrutinib and/or an IRAK1/4 inhibitor for 1hr and then stimulated with soluble α IgM, CpG, or both. As expected, ibrutinib inhibited phosphorylation of BTK, PLC γ 2 and ERK (BCR pathway), and decreased the survival of CLL cells stimulated with α IgM. The IRAK1/4 inhibitor inhibited TLR signaling resulting in stabilization of IRAK1, decreased phosphorylation of STAT1/3,

and decreased viability compared to CpG stimulated cells. Ibrutinib had a reduced effect on CpG-induced IRAK1 degradation, but was comparable to IRAK1/4 inhibition in reducing STAT phosphorylation, suggesting inhibition of BTK can antagonize downstream effects of TLR activation, but not upstream IRAK dependent steps. In contrast, IRAK1/4 inhibition had no effect on α IgM-induced BCR activation. Next we modeled co-operative activation of both BCR and TLR pathways in the tumor microenvironment. Under these *in vitro* conditions, ibrutinib prevented BCR and TLR activation, while the IRAK1/4 inhibitor affected only the TLR pathway. Thus, dual BCR and TLR inhibition for the treatment of lymphoproliferative diseases warrants further investigation.

Examination of Induced Endocytic Structure Formation in B Lymphocytes. T.M. Davenport, K. Sochacki, A. Dickey, J. Taraska; Laboratory of Molecular and Cellular Imaging.

B lymphocytes are an essential component of the adaptive immune response. The ability of a B cell lineage to adapt to better recognize a given antigen depends critically upon the ability of each B cell to bind and internalize antigens through their B cell receptors (BCR). The mechanism of antigen internalization by B cells appears to require cooperation between BCR signaling, the actomyosin network and clathrin-mediated endocytic processes. However, it remains unclear how these actors are coordinated to achieve efficient and controlled uptake of structurally heterogeneous antigens. To better understand this process, we set out to directly observe antigen-induced endocytic structures in the human DG-75 B cell line using a combination of conventional and super-resolution microscopy techniques including confocal laser scanning microscopy (CLSM), total-internal reflected fluorescence microscopy (TIRF-M), and correlative super-resolution light and electron microscopy (CLEM). Cells were stimulated with anti-human IgM Fab² to model antigen-induced BCR clustering and internalization. We observed recruitment of early adaptors of clathrin mediated endocytosis to Fab²-induced BCR clusters by TIRF-M and CLSM. CLEM revealed that BCR clusters are heterogeneous in size and frequently partition with clathrin on larger membrane invaginations. This work reveals novel structural features of antigen-induced endocytic structures and expands our understanding of the mechanism by which B cells may accommodate antigen of varying size during internalization.

Improvement in Skin Inflammation is Associated with Improvement in Aortic Vascular Inflammation by 18-FDG PET/CT. A.K. Dey^{1,2}, A.A. Joshi^{1,2}, A. Chaturvedi^{1,2}, J.B. Lerman^{1,2}, T.M. Aberra^{1,2}, J.A. Rodante^{1,2}, H.L. Teague^{1,2}, C.L. Harrington^{1,2}, J.P. Rivers^{1,2}, J.H. Chung¹, M.T. Kabbany^{1,2}, B. Natarajan¹, J.I. Silverman^{1,2}, Q. Ng^{1,2}, G.E. Sanda^{1,2}, A.V. Sorokin^{1,2}, Y. Baumer^{1,2}, B.N. Lockshin³, M.A. Ahlman¹, M.P. Playford^{1,2}, J.M. Gelfand⁴, N.N. Mehta^{1,2}; ¹Section of Inflammation and Cardiometabolic Diseases, ²NHLBI, ³DermAssociates, Silver Spring, MD, ⁴Department of Dermatology, University of Pennsylvania.

Psoriasis is a chronic inflammatory skin disease which is associated with increased vascular inflammation (VI) by 18-fluorodeoxyglucose positron emission tomography computed tomography (18-FDG PET/CT) in vivo and future cardiovascular events. Psoriasis provides a human model to understand the effect of treating inflammation in the skin on vascular diseases. However, the longitudinal impact of changes in psoriasis severity on vascular disease is unknown. We hypothesized that, change in psoriasis severity would associate with change in vascular inflammation at one-year. Consecutively recruited psoriasis patients (N=115) underwent FDG PET/CT scans, and cardiometabolic profiling at baseline and one-year. Aortic VI was assessed as target-to-background ratio (TBR). Psoriasis severity was measured as Psoriasis Area Severity Index (PASI) score. The cohort was middle-aged, had a low cardiovascular risk by Framingham risk score and mild-to-moderate psoriasis with a median PASI score of 5.2 (interquartile range: 3-8.9). At follow-up, the total cohort had a median improvement in PASI score of 33% ($p < 0.001$) with use of topical therapy (60%), biological therapy (66%, mostly anti-TNF) and phototherapy (15%). Moreover, improvement in PASI score was associated with improvement in target-to-background ratio of 6% ($p < 0.001$). This association persisted beyond traditional risk factors ($\beta = 0.21$, $p = 0.03$) and was the strongest in those initiated on anti-TNF therapy ($\beta = 0.79$, $p = 0.029$). Improvement in psoriasis skin disease severity was associated with improvement in aortic vascular inflammation by 18-FDG PET/CT. These findings suggest that controlling remote target organ inflammation (e.g. the skin) may improve vascular diseases, however, randomized clinical trials are needed to confirm these findings.

Dynamic Epigenetic Status and Plasticity During CD4+T Cell Differentiation. Y. Ding, J. Song, K. Zhao; Laboratory of Epigenome Biology.

CD4+ helper T cells have critical functions in regulating immune responses by their ability to differentiate and develop into specialized subsets for various purposes. Our research is trying to investigate how plastic are the Th1 cells in their cell fate when facing the stimulation of Treg differentiation conditions. In our study model, Th1 like cells differentiated from naïve CD4 cells are able to convert to Treg cells under Treg stimulating conditions at certain time points in vitro. However, the plasticity of Th1 to Treg cells is highly time-dependent, and we discover at 48 hours CD4 T cells are still plastic while at 72 hours they lose plasticity and become more committed to their cell fate during the Th1 differentiation path. DNase-Seq and RNA-Seq data at different time points indicate the genome-wide chromatin accessibility and epigenetic differences associated with time. Integration of multiple data sets reveals several candidates Th1 regulators as key determinants of cellular plasticity, whose functions are under experimental validation. A deeper recognition of determinants that control CD4+ T cell lineage commitment versus flexibility/plasticity has obvious implications for disease pathogenesis and new therapeutic applications, to fight infections and to control autoimmune and allergic inflammatory disorders.

Does Supercoiling Locate DNA Lesions? A. Dittmore, K.C. Neuman; Laboratory of Single Molecule Biophysics.

DNA within the cell is maintained in a supercoiled state that is critical for genome packaging and the regulation of gene expression. We hypothesized that global DNA supercoiling could play a role in how local sequence defects on the base-pair level are sensed and discriminated from among millions of normal base pairs. To test this, we introduced base-pair defect regions of variable size (0-16 bp) at a known location within a 6 kb sequence using a cassette based single-strand nicking template generated by PCR. Supercoiling of individual DNA molecules using magnetic tweezers revealed that even a single mismatch or abasic site is sufficient to nucleate formation of a plectoneme—a looped structure in which two parts of the molecule intertwine. Presentation of the defect precisely at an extruded plectoneme tip potentially serves as a damage-sensing mechanism and facilitates binding of repair enzymes.

Repeat-Swap Homology Modeling of the Anion Exchanger (AE1) Reveals an Elevator-Like Antiport Mechanism. E. Ficici, J.D. Faraldo-Gómez, L.R. Forrest, M.L. Jennings; Theoretical and Molecular Biophysics Section.

Anion Exchanger 1 (AE1), or band 3, is a membrane transporter found in erythrocytes and the kidney collecting duct. As part of the process of carbon dioxide clearance from these tissues, AE1 exchanges the accumulated bicarbonate for chloride in the blood plasma. After years of extensive biochemical and functional studies, the structure of the AE1 C-terminal domain (A_{CTD}), which is the integral membrane domain catalyzing the anion exchange, has been finally solved at a resolution of 3.5 Å. The structure comprises two structural repeats of inverted transmembrane topology, organized into what has been referred as ‘core’ and ‘gate’ domains. The two repeats are, however, structurally asymmetric and the protein adopts an outward-facing conformation. Here, we gain insights into the nature of the alternating-access mechanism of this transporter, by constructing a model of the inward-facing state using the so-called repeat-swap homology modeling method. Comparison of the resulting model of the inward-facing state with the outward-facing crystal structure reveals that anion translocation takes place by way of an elevator-type mechanism in which the core domain moves vertically relative to the gate domain, which forms the dimerization interface. Taken together, the structures can account qualitatively for a wide range of biochemical and functional data, and suggest new avenues of experimentation.

Apolipoprotein A-I and Apolipoprotein E Differentially Modulate the Expression of Extracellular Matrix Proteins by IPF Lung Fibroblasts. D.M. Figueroa¹, S. Bui², L. Rodriguez², G.M. Grant², S.D. Nathan³, S.J. Levine¹; ¹Laboratory of Asthma and Lung Inflammation, NHLBI, ²Department of Biology, George Mason University, ³Advanced Lung Disease and Lung Transplant Clinic, Inova Fairfax Hospital.

Idiopathic Pulmonary Fibrosis (IPF) is a progressive interstitial lung disease with a median survival of 2 to 3 years. Both apolipoprotein A-I (apoA-I) and apolipoprotein E (apoE) have

protective effects in murine models of experimental pulmonary fibrosis. In addition, apoA-I levels are decreased in bronchoalveolar lavage fluid from IPF subjects. Collectively, this suggests that apoE and apoA-I may have protective functions in IPF. To assess whether apoA-I or apoE modify the expression of extracellular matrix (ECM) proteins [fibronectin (FN1) and type-I collagens, COL1A1 and COL1A2] and the myofibroblast protein, α -smooth muscle actin (α -SMA), by human lung fibroblasts. Pulmonary fibroblasts were isolated from the lungs of IPF subjects who underwent lung transplantation. Cultured fibroblasts ($n = 4$) were serum-starved overnight and treated with either human apoA-I or apoE3 for 24 hours and levels of ECM proteins and α -SMA were quantified by Western. Treatment with apoE (0.5 μ M) significantly suppressed protein levels of COL1A1 by 65% and COL1A2 by 38%, while treatment with apoA-I did not significantly decrease the type-I collagens. In contrast, apoA-I (5 μ M) significantly increased FN1 by 110%, while apoE did not. Lastly, neither apoA-I nor apoE induced significant increase in α -SMA expression. We demonstrate that apoA-I and apoE have differential effects on the constitutive expression of ECM proteins by IPF lung fibroblasts. While apoE significantly suppressed the expression of type-I collagens, apoA-I increased FN1, whereas there were minimal effects on α -SMA. This suggests that the differential effects of apoA-I and apoE on pathways regulating the expression of type I collagens and FN1 by lung fibroblasts may provide new insights into the mechanisms by which ECM deposition is regulated in IPF.

A Role for PPAR α in Sex Differences in Cardiac Hypertrophy. N. Fillmore, J. Harrington, S. Gao, Y. Yang, X. Zhang, P. Liu, A. Stoehr, D. Springer, J. Zhu, X. Wang, E. Murphy; Laboratory of Cardiac Physiology.

Heart failure remains a leading cause of death worldwide and treatment is complicated by sex differences in the development of this disease. While sex differences in cardiac hypertrophy are well documented, the mechanisms involved are poorly understood. The purpose of this study is to better understand the mechanisms that contribute to sex differences in cardiac hypertrophy. Male and female mice were treated with vehicle or Angiotensin II (AngII; 1.5 mg•kg⁻¹•day⁻¹) to induce cardiac hypertrophy and a systems biology analysis was performed on RNAseq data to identify pathways central to sex differences in cardiac hypertrophy. Cardiac hypertrophy was observed after 2 weeks of AngII and sex differences became apparent after 3 weeks. After 3 weeks of treatment ejection fraction (EF) in females was not different from control values (54% vs 56%). In males, however, EF dropped from 55% to 37%, which was significantly lower than EF in females after 3 weeks of treatment. RNA sequencing was performed on hearts and sex differences in mRNA expression at baseline and following hypertrophy were observed along with differences between baseline and hypertrophy within a sex. Sex differences in mRNA were substantial at baseline and reduced somewhat with hypertrophy, as the hypertrophic differences tended to overwhelm the sex differences. We selected genes that were

significant for the sex-disease interaction, and mapped them to the protein-protein interaction network constructed using STRING data. This identified a network centered on PPAR α . To examine the role of PPAR α in sex differences in cardiac hypertrophy, we treated male and female mice with a PPAR α inhibitor (GW6471; (4 mg•kg⁻¹•day⁻¹)) along with vehicle or AngII. The inhibitor blunted the development of hypertrophy in male hearts (+5% AngII+GW6471 vs +20% AngII), blocking sex differences in cardiac hypertrophy. These results suggest that PPAR α contributes to sex differences in cardiac hypertrophy.

Cellular Conformations of α -Synuclein Probed by Raman Spectroscopy. J.D. Flynn, S.M. Lacy, J.C. Lee; Laboratory of Protein Conformation and Dynamics.

α -Synuclein (α -syn), an intrinsically disordered protein implicated in Parkinson's disease (PD), aggregates and spontaneously forms β -sheet-rich amyloid fibrils *in vitro*. Clinically, Lewy bodies composed of α -syn fibrils are a pathological hallmark of PD, connecting amyloid structures to disease. However, the role of amyloid formation in cell death and the development of disease is ill-defined. In this work, we use Raman microspectroscopy to study the aggregation of α -syn and characterize the structure of amyloid fibrils *in vivo*. Because many biomolecular vibrations overlap in similar spectral ranges, Raman probes are needed that can discriminate peaks of amyloidogenic proteins of interest from those of endogenous cellular proteins. Overcoming that challenge, we have biosynthetically incorporated isotopic labels of ²H, ¹³C, and ¹⁵N to uniformly label the α -syn backbone and side-chains and site-specifically replaced methionine residues with terminal alkynes. The isotopic labels of ²H, ¹³C, and ¹⁵N shift Raman bands for the ¹³C-²H stretching and ¹³C=O amide-I stretching frequencies of α -syn, providing contrast to endogenous cellular signals. Furthermore, the small, homopropargylglycine (HPG) alkyne probes have a very strong Raman peak in the spectroscopically "quiet" cellular region near 2100 cm⁻¹, thus providing a unique, site-specific signature for α -syn in a cell. Using Raman microspectroscopy, amyloid formation of HPG- α -syn is monitored in real-time, using the amide-I peak to directly report on the transformation from disordered to β -sheet structure. For the first time, we demonstrate the observation of isotopic-shifts and alkyne Raman signatures for α -syn in cellular environments after passive feeding.

Reconstitution of Mammalian *In Vitro* Translation Using Endogenously Assembled mRNPs. S. Fritz, J.R. Hogg; Laboratory of Ribonucleoprotein Biochemistry.

Nonsense-mediated mRNA decay (NMD) is a eukaryotic mRNA quality-control pathway that degrades cellular transcripts undergoing premature translation termination as well as ~5-10% of apparently normal mRNAs. A central objective of the NMD field is to define how cells discriminate target transcripts from non-targets and to outline step-by-step features of the mechanistic process. A cell-free system in which purified messenger ribonucleoprotein complexes (mRNPs) can be introduced to translationally-active cytoplasmic extracts would

provide an environment in which precise targets, factors and/or steps could be tightly manipulated. Here we introduce a mammalian *in vitro* translation system in which tagged mRNAs are purified from mammalian cells in their native mRNP states and introduced to prepared mammalian cytoplasmic extracts. We show that purified mRNPs exhibit a greater-than-100-fold increase in translation efficiency over capped and polyadenylated *in vitro* transcribed RNAs. Removal of associated proteins significantly reduces the translation efficiency of purified mRNPs. Further, we show that endogenously assembled mRNPs and *in vitro* transcribed mRNAs have distinct K^+ and Mg^{2+} requirements for maximal translation efficiency. We propose this reconstituted mammalian *in vitro* translation system as a robust tool to study cellular translation-dependent processes like NMD.

A Long-Term Co-Culture with Supporting Cells of the Developing Heart Promotes Maturation of Induced Pluripotent Stem Cell-Derived Cardiomyocytes. I.H. Garcia-Pak¹, W. Li¹, H. Uosaki², E. Tampakakis², J. Zou³, Y. Lin³, C. Kwon², Y. Mukoyama¹; ¹Laboratory of Stem Cell and Neuro-Vascular Biology, NHLBI, ²Division of Cardiology, The Johns Hopkins University School of Medicine, ³iPSC Core Facility, NHLBI.

The successful derivation of cardiomyocytes from human induced pluripotent stem cells (iPSC) has opened up exciting possibilities for clinical applications such as tissue engineering, disease modeling, and drug toxicity testing. The limitation for such applications is that these cardiomyocytes are immature; they appear and behave like fetal cardiomyocytes. Studies in heart development clearly demonstrate that multiple cell types including endothelial cells, sympathetic neurons, and epicardium-derived fibroblasts and vascular smooth muscle cells associate with and provide signals to the developing cardiomyocytes. In this study, we aim to overcome this limitation using a co-culture system with iPSC-derived cardiomyocytes (iPSC-CMs) in order to mimic the complex cell-cell interactions in the heart development. We cultured iPSC-CMs, directly associated with epicardial cells and sympathetic ganglia from mouse embryos and human umbilical vein endothelial cells for 30 days. We found that the long-term co-cultured iPSC-CMs exhibit significant maturation in cardiomyocyte structure as exhibited in mitochondria shape, sarcomere organization, multinucleation, and gap junction distribution. Moreover, we found up-regulation of cardiac genes highly expressed in human adult cardiomyocytes. Among cellular components in this co-culture system, we focus on the role of sympathetic neurons in the cardiomyocyte maturation and are examining whether sympathetic activity influences cardiomyocyte structure and cardiac gene expression. These studies may benefit the field by providing a step forward toward mature cardiomyocyte application and therapies.

Arylsulfatase B Induce Increased Neurite Outgrowth in Hippocampal Neurons When Cocultured With Astrocytes. N. George, C. Mencio, P. Yu, Y. Katagiri, H.M. Geller; Developmental Neurobiology Section.

Sulfated glycosaminoglycans (GAGs) in the extracellular matrix are known to play an important role in axonal outgrowth and regeneration in neurodegenerative diseases and after central nervous system (CNS) injuries. Arylsulfatase B (ARSB) is a N-acetylgalactosamine 4-sulfatase present in endosomes and lysosomes of cells which removes the 4-sulfate from the non-reducing ends of dermatan sulfate and chondroitin sulfate. We have previously demonstrated that 4-sulfated GAGs are upregulated after neuronal injury and inhibit axonal outgrowth. Our study aims to investigate how ARSB treatment affects neurite outgrowth in both normal and injury *in vitro* models. Our studies showed that overexpressing ARSB in astrocytes results in increased neurite outgrowth of cocultured neurons. In contrast, silencing of ARSB expression in astrocytes using siRNA reduced the neurite length in coculture models. Pre-treatment of astrocytes through the addition of exogenous ARSB leads to increased neurite length of cocultured mouse hippocampal neurons, however this effect is only seen in the co-culture and disappears when neurons alone are cultured and treated. Our results show that ARSB treatment can alter astrocyte-neuron interactions and initiate changes that result in increased neurite growth. This may be due to ARSB modifying secreted GAGs or growth signals produced by astrocytes to promote neurite outgrowth or create a more permissive environment through alteration of the extracellular matrix. Further understanding of this enzyme and the role of GAGs and their sulfation in the growth of neurons may lead to novel strategies or therapeutic targets to aid neuronal regeneration in neurodegenerative diseases and after CNS injury.

House Dust Mite-Derived Proteases Induce Apolipoprotein E Secretion from Asthmatic Alveolar Macrophages via a ROS-dependent Pathway. E.M. Gordon, H. Xu, X. Yao, A.V. Barochia, M. Kaler, R. Cuento, S.J. Levine; Asthma and Lung Inflammation Section.

Apolipoproteins are key components of lipoprotein particles that mediate the transport of cholesterol and triglycerides into and out of cells and they are increasingly being recognized as players in lung diseases. We have previously reported that house dust mite (HDM)-challenged apolipoprotein E (apoE)-deficient mice have an increase in airway hyperreactivity and mucous cell metaplasia. Furthermore, administration of an apoE mimetic peptide attenuated HDM-induced airway disease, suggesting apoE has a protective function. ApoE is primarily expressed by alveolar macrophages (AMs) in the lung. Here we explored the molecular regulation of apoE secretion by AMs isolated from asthmatic and healthy subjects. Bronchoalveolar lavage fluid AMs were isolated from stable asthmatics (n = 12) and healthy subjects (n = 7). AMs were cultured *ex vivo* for 24 hours and apoE secretion was measured by ELISA. We showed that HDM, but not other pro-inflammatory mediators, such as type 1, type 2, and type 17 cytokines, as well as the TLR3 and TLR4 agonists, induced significant increases in apoE secretion by AMs from asthmatic subjects. This increase in apoE was suppressed by the serine protease inhibitor, AEBSF, and the cysteine protease inhibitor, E64.

Consistent with a role for HDM protease activity, antagonists of protease-activated receptor 2 (PAR2), but not PAR1, attenuated HDM-induced apoE secretion. We next explored whether the generation of reactive oxygen species (ROS) was necessary for HDM-induced apoE secretion by AMs. Inhibitors of ROS generation, apocynin and diphenyleneiodonium, both suppressed HDM-induced apoE secretion. We have identified that HDM-derived proteases activate PAR2, which contributes to HDM-induced apoE secretion from AMs by a ROS-dependent signaling pathway. We hypothesize that apoE production by AMs may serve a protective function in HDM-mediated allergic asthma.

The Adaptive Immune Microenvironment in the Bone Marrow of Healthy Adults and Relapsed/Refractory Acute Myeloid Leukemia Patients. M. Goswami, K. Lindblad, K. Oetjen, C. Hourigan; Myeloid Malignancies Section.

The bone marrow is a lymphoid organ rich in immune cells and it is becoming increasingly evident that lymphocytes infiltrating into the bone marrow are important for the adaptive immune system response. Since bone marrow is the primary site of disease in acute myeloid leukemia (AML), we are interested in characterizing the bone marrow tumor microenvironment in these patients, the relationship between adaptive immune cell subsets, and whether the nature of the immune infiltrate in the marrow is correlated with clinical outcomes. Previously, in a cohort of AML patients in remission, we showed persistent B-cell deficiencies but a grossly normal T-cell compartment in the peripheral blood following chemotherapy. In a separate study of relapsed/refractory AML (RR-AML) patients, we observed increased frequencies of PD-1+ CD8+ effector T-cells in the bone marrow. To examine these adaptive immune cell types in greater detail in both the blood and bone marrow of RR-AML and healthy donors (HD), we developed several 13-color flow cytometry panels enabling us to extensively examine phenotypic, exhaustion and activation markers on both T-cells and B-cells. We stained cryopreserved bone marrow mononuclear cells from 20 HD and 10 RR-AML patients recruited to the clinical trial NCT02527447. Our data suggests a loss of CD20+ B-cells across all differentiation stages, while total numbers of CD3+ T-cells are comparable to HD. However, we noted differences in the frequencies of activated and exhausted T-cells in RR-AML. Future work will now focus on deeper multivariate analyses of all cell subsets analyzed to determine differences between RR-AML and HD and to establish a baseline dataset of these cell types in HD that can be used as comparator across other cohorts of AML.

Macrophages from Patients with Arterial Calcification due to CD73 Deficiency Have Impaired Ability to Resolve an Inflammatory Response. A. Grubb, Y. Ma, D. Yang, G. Chen, N. Dmitrieva, E. Ferrante, M. Boehm; Laboratory of Cardiovascular and Regenerative Medicine.

Arterial calcification due to CD73 deficiency (ACDC) is a hereditary disease resulting from mutations in the *NT5E* gene encoding CD73, the major enzyme which converts adenosine-monophosphate (AMP) to adenosine. Patients develop severe

obstructive peripheral arterial disease due to significant medial calcification of the arteries along with extensive periarticular calcifications in the extremities. While monocytes and macrophages are key players in other forms of vascular disease such as atherosclerosis, little is known about their role within ACDC patient. The aim of this study was to investigate the role of CD73 in monocytes and macrophages and the cellular consequences of its deficiency. We hypothesized that due to CD73's prominent role in adenosine generation and adenosine's role in immune regulation, ACDC cells lacking CD73 would exhibit impaired resolution of an inflammatory response. Primary human monocytes from healthy controls and ACDC patients were isolated from whole blood and differentiated to macrophages. To simulate the resolution of an inflammatory response, cells were stimulated with LPS for 4 hours, washed, and media replaced with LPS free media. In healthy controls, CD73 mRNA is upregulated following removal of the inflammatory stimulus. Correspondingly, CD73 activity, which is minimal in resting macrophages, is upregulated during this post-wash period. Cytokine secretion after initial stimulation was similar between ACDC and control macrophages. After removal of the inflammatory stimulus, however, ACDC cells had sustained and increased secretion of pro-inflammatory cytokines such as IFN γ , IL1 β , and MIP1 β . These data suggest ACDC macrophages have an impaired ability to resolve an inflammatory response.

Eltrombopag Promotes DNA Repair in Human Hematopoietic Stem and Progenitor Cells: Implications for the Treatment of Fanconi Anemia. K.L. Guenther, R. Smith, A. Larochele; Regenerative Therapies for Inherited Blood Disorders.

Fanconi anemia (FA) is an inherited genomic instability syndrome characterized by faulty DNA repair. FA results from a mutation in one of the genes encoding proteins in the FA pathway, responsible for repairing DNA adducts and inter-strand crosslinks. Bone marrow failure (BMF) is the primary cause of morbidity and mortality in patients with FA. The only curative treatment option is HLA-matched hematopoietic stem and progenitor cell (HSPC) transplantation. However, donor availability, graft failure, and FA-specific transplant toxicities are significant hurdles towards a curative treatment of FA-associated BMF. Thrombopoietin (TPO) promotes DNA double strand break (DSB) repair in HSPCs by increasing DNA-PK dependent non-homologous end joining (NHEJ) repair efficiency. However, recombinant TPO is no longer used clinically. Eltrombopag is an FDA-approved, non-immunogenic TPO mimetic effective in the treatment of subjects with acquired BMF. We hypothesized that eltrombopag may also stimulate DNA repair activity in HSPCs. Because HSPC numbers are markedly reduced in FA, we created a model of FA HPSCs using CRISPR/Cas9-based knock down (KD) of the FANCA protein in human CD34+ cells obtained from healthy donors. These cells were pre-cultured with or without eltrombopag or TPO, subjected to γ -irradiation to induce DSB, and DNA repair activity was measured. We found that eltrombopag and TPO could similarly promote DNA-PK dependent

NHEJ DNA repair in FA HSPCs and significantly enhance their survival. These data provide support for further testing of eltrombopag as an alternate treatment option for patients with FA.

Zfr Coordinates Crosstalk Between RNA Decay and Transcription in Innate Immunity. N. Haque¹, R. Ouda², K. Ozato², J.R. Hogg¹; ¹Laboratory of Biochemistry, NHLBI, ²Division of Developmental Biology, NICHD.

Control of type-I interferon production is crucial to combat pathogen invasion while preventing deleterious hyperactivation of inflammatory responses. Pathways promoting rapid transcriptional induction of type-I interferons have been studied extensively, but the contribution of post-transcriptional regulatory mechanisms to innate immune signaling is poorly understood. Here, we show that the highly-conserved zinc finger RNA-binding protein (ZFR) plays a specialized role in repression of the type-I interferon response as part of its broader function as a regulator of alternative splicing.

We find that ZFR expression is under tight control during macrophage development: monocytes express a truncated form of the protein, while macrophages express a full-length isoform capable of modulating alternative splicing. Cells depleted for ZFR produces higher levels of IFN β in response to mimics of both viral and bacterial infection. These findings suggest that induction of ZFR in developing macrophages helps to guard against aberrant activation of the type-I interferon response. Explaining this finding, we show that ZFR represses type-I interferon signaling by promoting correct splicing of the histone variant macroH2A1/H2AFY. In the absence of ZFR, aberrant splicing leads to degradation of macroH2A1 mRNA by nonsense-mediated mRNA. When ZFR is present, macroH2A1 represses IFN β induction by directly binding the IFN β promoter. Together, our data reveal a network of mRNA processing and decay events that shapes the transcriptional response to infection.

This research was supported by the Intramural Research Program, NIH, NHLBI, NICHD.

Development Of “Ultra-High Speed” Western Blot Without Sacrifice of Sensitivity. S. Higashi, Y. Katagiri, H.M. Geller; Developmental Neurobiology Section.

On-surface bioassays (such as Western Blot (WB), microarray, ELISA, and tissue staining) have proven indispensable to biomedical research. Although WB and tissue staining are performed routinely on a daily basis, each iteration can take hours or even days to complete. The purpose of this study is to overcome this limitation in assay kinetics, using WB, without sacrificing sensitivity.

In most bioassays, detecting probes (antibodies) float in solution while their targets (antigens) are immobilized on the surface. Because of the high affinity of detecting probes, probes close to the surface bind to their targets quickly; however, it can take hours for more distant probes to diffuse to the surface and bind to their targets. This creates a depletion layer

with lower concentration of probes closest to the surface. Further, the retention of probes close to the surface can be seen due to rebinding before the probes can escape. To eliminate these effects, called “mass transport limitation”, a concept was proposed in which a depletion layer close to the target is disrupted by draining and re-applying repeatedly. We have applied this concept to WB by rotating a tube in a hybridization oven that contains the membrane and antibody. We have succeeded in completing the entire WB procedure (incubation with primary and secondary antibodies and image acquisition) in as short as 20 minutes without sacrifice of sensitivity through the use of an immunoreaction enhancing technology. Thus, this advanced “Ultra-High Speed” WB is highly beneficial to biomedical research.

Brownian Ratchet Mechanism for Faithful Segregation of Low-Copy-Number Plasmids. L. Hu¹, A. G. Vecchiarelli³, K. Mizuuchi², K. C. Neuman¹, J. Liu¹; ¹Laboratory of Molecular Biophysics, NHLBI, ²Laboratory of Molecular Biology, NIDDK, ³Department of Molecular, Cellular, and Developmental Biology, University of Michigan.

Bacterial plasmids are extrachromosomal DNA that provides selective advantages for bacterial survival. Plasmid partitioning can be remarkably robust. For high-copy-number plasmids, diffusion ensures that both daughter cells inherit plasmids after cell division. In contrast, most low-copy-number plasmids need to be actively partitioned by a conserved tripartite ParA-type system. ParA is an ATPase that binds to chromosomal DNA; ParB is the stimulator of the ParA ATPase and specifically binds to the plasmid at a centromere-like site, *parS*. ParB stimulation of the ParA ATPase releases ParA from the chromosome, after which it takes a long time to reset its DNA-binding affinity. We introduce a Brownian ratchet model that recapitulates the full range of actively segregated plasmid motilities observed *in vivo*. We demonstrate that plasmid motility is tuned as the replenishment rate of the ParA-depletion zone progressively increases relative to the cargo speed, evolving from diffusion to pole-to-pole oscillation, local excursions, and, finally, immobility. When the plasmid replicates, the daughters largely display motilities similar to that of their mother, except that when the single-focus progenitor is locally excursive, the daughter foci undergo directed segregation. We show that directed segregation maximizes the fidelity of plasmid partition.

Structure-Function Studies of ApoA-I Mimetic Peptides for ABCA1-dependent Cholesterol Efflux and HDL formation. R.M. Islam, M. Pourmousa, S. Gordon, D. Sviridov, R.W. Pastor, A.T. Remaley; Lipoprotein Metabolism Section.

We designed 4 peptides with a variable number of E, L, K and A residues and determined their ability to form HDL-like particle and promote ABCA1-dependent cholesterol efflux. To reflect a unique physical property, they were named: N=ELK-neutral (EKLKELLEKLEKLEKLEK), H=ELK-hydrophobic (EKLLELLKLEKLEKLEK), P=ELK-positive (EKLKALLEKLEKLEKLEK), Neg=ELK-negative (EELKEKLEELKEKLEELK). All peptides had greater than

40% helicity. However, H and Neg were mostly helical in TFF, a lipid mimicking, environment (62% and 50%, respectively). In both DMPC and a mixture of natural lipids vesicle solubilization assays, we observed following order: P>N>H>>Neg. N, H, P formed approximately 8, 8, and 18 nm size lipid particles, respectively when combined with DMPC, however, particles formed Neg were not detected. Cholesterol efflux studies showed following results: H>N>>P, whereas Neg peptide was inactive. All-atom MD simulation of N carried on containing POPC:cholest (200:20), 26 peptides, indicated a strong preference for a belt-like configuration. However, in a picket-fence configuration, N distorted to a belt-like pattern within 1 μ -sec. For Neg, both starting configurations were much less stable with dimers losing their connectivity and monomers migrating to the top and bottom of the disc, leaving large hydrophobic patches of acyl chains exposed. Cross-linking studies were consistent with the ability of H and N to form dimers to stabilize the HDL structure, and thereby, were also consistent with simulation. Together, we show that a net neutral charge, a relatively large hydrophobic moment (0.78), and a broad hydrophobic face (180 degrees) are optimum features for an apoA-I mimetic peptide to promote cholesterol efflux and to stabilize a nascent discoidal HDL structure.

Cholesterol-Enrichment of Cells Induces Unique Extracellular Cholesterol Microdomains. X. Jin¹, Y. Liu², L. Ad-dadi³, H.S. Kruth¹; ¹Laboratory of Experimental Atherosclerosis, NHLBI, ²NICHD, ³Weizmann Inst of Science, Rehovot, Israel.

We previously reported that cholesterol-enriched macrophages deposit cholesterol into the extracellular matrix and this process depends on ABCA1 and ABCG1. The extracellular cholesterol deposits can be mobilized by HDL, or ApoA-I, the latter dependent on ABCA1-mediated lipidation of ApoA-I. The objective of the current study was to determine the effects of other genes and inhibitors that affect cellular cholesterol trafficking on the deposition of extracellular cholesterol. We used a monoclonal antibody that labels cholesterol microdomains to detect the extracellular cholesterol deposits. Progesterone and U18666A previously were shown to induce accumulation of cholesterol within lysosomes, and we found that these agents also blocked macrophage deposition of extracellular cholesterol. Brefeldin A, an inhibitor of golgi and vesicular trafficking, inhibited extracellular cholesterol deposition. On the other hand, vacuolin, an agent that inhibits the fusion between autophagosomes and lysosomes and thereby induces cellular accumulation of autophagosomes, did not inhibit extracellular cholesterol deposition. To examine the effect of mutant genes known to affect cholesterol trafficking, we examined mutant cultured fibroblasts that were cholesterol-enriched by incubation with LDL plus the LXR agonist, T0901317. Like macrophages, normal cholesterol-enriched fibroblasts deposited extracellular cholesterol that was dependent on ABCA1, because ABCA1-deficient fibroblasts did not deposit extracellular cholesterol. While progesterone and U18666A inhibited fibroblast extracellular cholesterol deposition, surprisingly, fibroblasts deficient in NPC1 or NPC2, which also abnormally

accumulate cholesterol within lysosomes during cholesterol enrichment, nevertheless, deposited extracellular cholesterol similar to normal fibroblasts. That lysosomal hydrolysis of LDL cholesteryl ester is involved in extracellular cholesterol deposition was shown by substantially reduced extracellular cholesterol deposition by fibroblasts lacking acid cholesteryl ester hydrolase. Our findings indicate that a pathway not dependent on NPC1 or NPC2 mediates trafficking of cholesterol from lysosomes to the extracellular space.

Determinants of Vascular Inflammation by 18-Fluorodeoxyglucose PET/MRI: Findings from the Psoriasis, Atherosclerosis and Cardiometabolic Disease Initiative. M.T. Kabbany, A.K. Dey, A. Chaturvedi, J.P. Rivers, J.H. Chung, P. Shukla, A. Rana, J.A. Rodante, A.A. Joshi, J.B. Lerman, T.M. Abera, J.I. Silverman, Q. Ng, H.L. Teague, A. Dahiya, M.A. Ahlman, D.A. Bluemke, N.N. Mehta; Section of Inflammation and Cardiometabolic Diseases.

Inflammation is a risk factor for the initiation and progression of atherosclerosis. Psoriasis (PSO), a chronic inflammatory disease associated with increased cardiovascular risk, provides a clinical human model to study inflammatory atherogenesis. We aimed to assess the major determinants of vascular inflammation (VI) measured by 18FDG PET-MRI in a well-phenotyped PSO cohort. 124 consecutive patients with PSO underwent 18FDG PET-MRI scans. We used target-to-background ratio to quantify VI, 120 minutes' post FDG injection. Homeostatic model assessment of insulin resistance (HOMA-IR) was measured, along with cholesterol efflux capacity (CEC) and HDL particle concentration by NMR (Liposcience) fasting. Our cohort was middle aged (mean 49 \pm 13.3 years) with mild to moderate PSO, and low cardiovascular risk by Framingham risk score (FRS) (median 2, IQR 2-6). PSO was associated with increased VI (β =0.27, p <0.005), compared to healthy controls. VI was associated with HOMA-IR (β = 0.26, p <0.001), CEC (β = -0.12, p =0.04) and HDL particle concentration (β = -0.19, p =0.003) beyond traditional cardiovascular risk factors (age, gender, FRS and BMI). Among these, HOMA-IR provided maximum incremental value in predicting VI beyond traditional risk factors (χ^2 = 39.36, p <0.001). VI by 18FDG PET-MRI is associated with traditional cardiovascular risk factors and cardiometabolic parameters. Insulin resistance and CEC were most strongly associated with VI by 18FDG PET-MRI beyond traditional cardiovascular risk factors and BMI in PSO suggesting that cardiometabolic disease increases cardiovascular risk in PSO.

Facilitator Models of Weak Binding in Protein-Protein Interactions. S. Kale, M. Strickland, A. Peterkofsky, N. Tjandra, J. Liu; Theoretical Cellular Physics.

Pairwise interactions are intuitive to our understanding on protein-protein binding; however *in vivo* this is rarely true. Most intracellular proteins operate in a highly cooperative manner to perform tasks ranging from metabolic turnover to intricate signaling regulation. In some cases, one substrate needs to simultaneously interact with more than one binding partner to carry out faithful signal transductions. While one of these binding

partners is the determinant of such signal transduction, it shares very similar tertiary structure with the other but differs in functional role and abundance. Motivated by this observation, we explore the physical consequences of the mere steric presence of a non-specific ligand, the “competitor”, crowding the surface of a “substrate”. The specific interaction occurs between the substrate and the “target” ligand, which explores the same surface as well, albeit for its unique binding site. A simple lattice model incorporating these elements along with the natural rules of exclusion and hopping reveals the regimes for when recruitment (turnover) or residence (transition state stabilization) are favored. Exploration of the search dynamics of the two ligands along the substrate surface provides further insight.

Intentional Laceration of the Anterior Mitral Valve Leaflet to Prevent Left Ventricular Outflow Tract Obstruction (LAMPOON) during Transcatheter Mitral Valve Replacement: Pre-Clinical Findings. J.M. Khan, T. Rogers, W.H. Schenke, J.R. Mazal, M.Y. Chen, R.J. Lederman; Cardiovascular Intervention Program.

Left ventricular outflow tract (LVOT) obstruction is a life-threatening complication of transcatheter mitral valve replacement (TMVR), caused by septal displacement of the anterior mitral leaflet (AML). We developed a novel transcatheter transection of the AML. *In vivo* procedures in swine were guided by biplane X-ray fluoroscopy and intracardiac echocardiography. Retrograde transfemoral 6Fr guiding catheters were advanced to the LVOT and left atrium to straddle the AML. Radiofrequency current was concentrated at the tip of a 0.014” coronary guidewire using polymer jacket insulation to perforate the AML base from LVOT to left atrium. The guidewire was snared and externalized; the resulting guidewire loop further electrified and pulled, using a 5% dextrose flush to concentrate current at the leaflet, lacerating the AML. The procedure was performed successfully in eight pigs. Lacerations extended to $89 \pm 19\%$ of leaflet length and were located within 0.5 ± 0.4 mm of leaflet centerline. The chordae were preserved and retracted the leaflet away from the LVOT. LVOT narrowing after benchtop TMVR was significantly reduced with LAMPOON than without ($65\% \pm 10\%$ vs. $31 \pm 18\%$ of pre-implant diameter, $p < 0.01$). LAMPOON caused mean blood pressure to fall (54 ± 6 to 30 ± 4 mm Hg, $p < 0.01$), then remained steady until planned euthanasia. No collateral tissue injury was identified on necropsy. This technique mimicks surgical chord-sparing AML resection. Cautiously applied in patients ineligible for surgery, LAMPOON may prevent LVOT obstruction and enable TMVR.

Sequence-Specific Protection of mRNAs from Nonsense-Mediated Decay. A. Kishor, Z. Ge, J.R. Hogg; Laboratory of Ribonucleoprotein Biochemistry.

The nonsense-mediated mRNA decay (NMD) pathway degrades many apparently normal cellular transcripts in addition to its quality control function. Previous experiments in

various eukaryotes demonstrated that 3’UTR length is a conserved determinant of mRNA susceptibility to NMD. However, whole-genome studies of NMD target mRNAs indicate that a large number of potential NMD targets with long 3’UTRs are able to evade decay. In Rous sarcoma virus and some human mRNAs, this protection depends on RNA sequences that shield nearby termination codons from recognition by NMD.

Using RNA-based affinity purification and functional assays, we previously identified polypyrimidine tract binding protein 1 (PTBP1) as an anti-NMD factor. Through this mechanism, transcripts with long 3’UTRs and the PTBP1 recognition motif proximal to the termination codon bind PTBP1, reducing transcript association with UPF1. As a result, other NMD effector molecules are not recruited and the mRNA is protected from this form of decay. We have now identified a second protein, hnRNPL, that can also protect long 3’UTRs from recognition by NMD. Functional assays on transcripts with the hnRNPL binding motif, including measurements of transcript stability and steady state levels, demonstrate this anti-NMD effect. Additionally, using RNAseq, we find that hnRNPL binds and stabilizes a distinct population of human mRNAs from those protected by PTBP1. The existence of at least two such proteins suggests that cells have evolved multiple sequence-specific means to prevent UPF1 recognition of long 3’UTRs, which may be used to carry out distinct programs of gene expression.

Effects of alpha-Synuclein Uptake on Cellular Viability, Morphology, and Localization. S. Lacy, J. Flynn, J.C. Lee; Laboratory of Protein Conformation and Dynamics.

Alpha-synuclein is a 14kD protein that is strongly associated with Parkinson’s disease. This protein is a major component of Lewy Bodies, which are a distinctive feature of Parkinson’s. Alpha-synuclein exists as an intrinsically disordered protein and when it forms fibrils it has shown to be toxic to cells. Examining alpha-synuclein *in vitro* has given further insight into how this protein forms aggregates, but the mechanism of cell death is still unknown. Different constructs of alpha-synuclein can be labeled at the N and C termini with Tetramethylrhodamine, a relatively small fluorophore, which could decrease the chance of hindering the aggregation properties of alpha-synuclein. Characteristics of purified alpha-synuclein constructs can be distinguished using Circular Dichroism, Fourier Transform Infrared Spectroscopy, Transmission Electron Microscopy, and Aggregation studies of turbidity and ThT response over time. Different cell lines have varying levels of endogenous alpha-synuclein. By treating different cell lines with the different polymorphs of alpha-synuclein and examining the differing effects the fibrils have on the cell lines, a further understanding can be attained about endogenous levels of this protein contributing to the survival of the cells. Observable differences in fluorescence may also illuminate how the protein changes structurally when the fibrils internalize in the cell. By observing where these fibrils localize in cells, visualizing the morphological differences, and coupling to chemical viability

assays, we hope to gain a further understanding of the cell-killing mechanism.

Generation of Methionine Sulfoxide Reductase Quadruple Knockout Mice. L. Lai, C. Liu, R. Levine; Protein Function in Disease Section.

Methionine sulfoxide reductase (Msr) is an important antioxidant enzyme, but the mechanism by which it protects has not been elucidated nor have the *in vivo* substrates been identified. The mammalian Msr family has four members: MsrA, MsrB1, MsrB2, and MsrB3. Single knockouts of MsrA, MsrB1, and MsrB3 have been constructed, as well as a double knockout of MsrA and MsrB1. Except for deafness in the MsrB3 knockout, phenotypic changes are relatively subtle, perhaps due to redundancy of function among the Msr family members. The goal of this study is to generate a mouse strain with deletion of all four Msr proteins, providing a tool for further study of the function of the Msr family. Starting with the double knockout, MsrA^{-/-}MsrB1^{-/-}, we employed the CRISPR/Cas9 system to also knockout MsrB2 and MsrB3, thus generating the quadruple knockout. CRISPR targeting sites were selected within the first coding exon of the MsrB2 and MsrB3 genes. Together with Cas9 mRNA, sgRNAs were co-injected into zygotes collected from MsrA^{-/-}MsrB1^{-/-} mice. The embryos were transferred into pseudopregnant females, and pups carrying the mutant allele were identified by DNA sequencing. Deletion was confirmed by Western blotting of heart and liver. The quadruple knockout mouse is viable; growth and development appear normal. To test the response of the animal under oxidative stress, we treated them with a single dose of paraquat and monitored the survival rate. Surprisingly, about 60% of quadruple knockout mice survived after 7 days of the treatment while only 16% of the wildtype survived.

Novel Degenerative and Developmental Defects in a Zebrafish Model of Mucopolysaccharidosis Type IV. H. Li¹, W. Pei², S. Vergarajaregui^{1,3}, P.M. Zerfas⁴, N. Raben⁵, S.M. Burgess², R. Puertollano^{1*}; ¹Protein Trafficking and Organelle Biology, NHLBI, ²Translational and Functional Genomics Branch, NHGRI, ³Experimental Renal and Cardiovascular Research, Department of Nephropathology, Institute of Pathology, Friedrich-Alexander-Universität Erlangen-Nürnberg, Erlangen, Germany, ⁴Office of Research Services, Division of Veterinary Resources, NIH, ⁵Laboratory of Muscle Stem Cells and Gene Regulation, NIAMS.

Mucopolysaccharidosis type IV (MLIV) is a lysosomal storage disease characterized by neurologic and ophthalmologic abnormalities. There is currently no effective treatment. MLIV is caused by mutations in MCOLN1, a lysosomal cation channel from the transient receptor potential (TRP) family. In this study we used genome editing to knockout the two *mcoln1* genes present in *Danio rerio* (zebrafish). Our model successfully reproduced the retinal and neuromuscular defects observed in MLIV patients, indicating that this model is suitable for studying the disease pathogenesis. Importantly, our model revealed novel insights into the origins and progression of the MLIV

pathology, including the contribution of autophagosome accumulation to muscle dystrophy and the role of *mcoln1* in embryonic development, hair cell viability and cellular maintenance. The generation of a MLIV model in zebrafish is particularly relevant given the suitability of this organism for large-scale *in vivo* drug screening, thus providing unprecedented opportunities for therapeutic discovery.

Local Hypoxia Controls Nerve-Mediated Arterial Branching via HIF-Independent Pathways in Developing Skin. W. Li¹, K. Nakayama², Y.S. Mukoyama¹; ¹Laboratory of Stem Cell and Neuro-Vascular Biology, NHLBI, ²Oxygen Biology Laboratory, Medical Research Institute, Tokyo Medical and Dental University.

The vascular and nervous system share several anatomical characteristics and are often patterned similarly. In the developing skin, peripheral sensory nerves align with the pattern of arterial branching. At the molecular level, nerve-derived angiogenic signals such as CXCL12 and VEGF coordinate vascular branching pattern and arterial differentiation in the skin (Li et al. *Dev Cell* 2013). In this study, we seek to understand what specifies the correct timing of these angiogenic signals in the nerves. Consistent with the previous observation that *Cxcl12* and *Vegf-a* are hypoxia-induced genes, local hypoxia is detectable in/around the nerves prior to the establishment of the nerve-artery alignment in the skin and the oxygen-starved dorsal root ganglia (DRG) containing sensory neurons and glia enhance the expression of *Cxcl12* and *Vegf-a* in culture. Interestingly, hypoxia-inducible factors (HIFs) appear not to enhance the *Cxcl12* and *Vegf-a* expression in response to hypoxia in the DRG culture and *in vivo*. Rather, NF-kappaB (RelA) and cAMP-response Element-Binding Protein (CREB) are required for the *Cxcl12* and *Vegf-a* expression, respectively. In order to examine whether these signaling pathways control the nerve-vessel alignment and arterial differentiation in the skin, we are currently analyzing mutant mice carrying sensory nerve-specific inactivation of NF-kappaB (RelA) and CREB signaling pathways. These experiments will benefit the research about the regulation of vascular branching morphogenesis and patterning by non-HIF-regulated hypoxic responses.

High-Dimensional Immunophenotyping of the NK Cell Compartment in Acute Myeloid Leukemia. K. Lindblad, M. Goswami, K. Oetjen, C. Hourigan; Myeloid Malignancies Section.

Prognosis for those diagnosed with acute myeloid leukemia (AML) remains bleak with a five-year life expectancy of ~25% upon initial diagnosis. Evidence that AML is associated with an aberrant immunologic state suggests a potentially efficacious role for immunotherapeutic interventions. AML is associated with phenotypic and functional natural killer cell (NKC) aberrations that have been shown to be partially restored upon achieving remission. NKCs serve a vital role in recognizing and regulating malignant cells and they harbor the ability to recognize leukemic blasts, as demonstrated by the significant contribution of allogeneic NKCs to the powerful “graft-versus-leukemia” effect upon allogeneic hematopoietic

stem cell transplantation. This implies an underlying mechanism of innate immune evasion involving blast-induced loss of critical NKC activity. Our aim is to investigate the integrity of the NKC compartment within the tumor microenvironment of AML by high-dimensional flow cytometry. We developed and optimized a unique 13-color flow cytometry panel, enabling phenotypic compartmentalization of major NKC subsets and subsequent probing for CD335, CD314, CD158e1, CD226, PD-1, CD69, and CD159c expression. This panel was used to examine bone marrow mononuclear cells from 10 relapsed/refractory AML patients and a cohort of 20 age-matched healthy controls. These data provide further insight into aberrant immunological changes observed within the tumor microenvironment of AML. Further work geared at optimizing immunotherapeutic strategies to safely augment the intrinsic anti-tumor effects of NKCs in AML may lead to significant advancements in the treatment and overall survival of patients with this disease.

Origin, Distribution and Functions of Neural Tube Microglia in the Immunoprivileged Central Nervous System.

C. Liu, Y. Mukouyama; Laboratory of Stem Cell and Neurovascular Biology.

Pathogenesis of neurodegenerative diseases has been attributed to abnormal behavior of microglia, the resident innate immune cells in the central nervous system (CNS). Adult microglia emerge from progenitor cells during embryogenesis. Despite their embryonic origin, most studies are centered on adult microglia, and little is known about their developmental course as well as the contribution of the fetal programming of microglia in adult diseases. In this study, we have identified two populations of embryonic microglia with a gene signature similar to that is found in adult microglia. These embryonic microglia appear in the neural tube simultaneously at E10.5, yet exhibiting different cellular and spatial properties: the F4/80+ microglia within the neural tube, and the LYVE1+/F4/80+ microglia located at the interface of neural tube. This pattern of microglial distribution persists throughout fetal stages and adulthood. These cells are critical for neural tube development as genetic depletion of embryonic microglia results in neuronal and structural defects in the developing brain. Notably, the heterogeneous populations of embryonic microglia derive from a homogenous progenitor population in the yolk sac. This observation prompted us to explore what controls the unique patterning of embryonic microglia in the CNS tissues. Among the candidate genes from a comprehensive gene expression profiling of these embryonic microglia using RNA-seq analysis, we focused on neuronal progenitors-derived canonical Wnt signaling because Wnt receptors are differentially expressed between the two populations of microglia. We are currently examining what happens to the patterning of embryonic microglia distribution and neuronal development in the mutants lacking Wnt/ β -catenin signaling in microglia. Our work demonstrates the developmental characteristics and physiological significance of embryonic microglia. The clinical relevance of fetal microglia to adult CNS pathological conditions will be addressed in future studies.

Molecular and Physiological Impact of Regulated Mitochondrial Calcium Uptake. J.C. Liu, J. Liu, R.J. Parks, C. Liu, E. Murphy, T. Finkel; Laboratory of Molecular Biology.

Mitochondrial uptake of calcium plays important roles in cellular homeostasis, from the stimulation of ATP production to the triggering of necrosis. Hence, calcium entry through the mitochondrial calcium uniporter must be tightly regulated, yet the *in vivo* importance of this regulation is currently not well understood. The uniporter is comprised of multiple proteins, including the channel-forming protein MCU, the molecular scaffolding protein EMRE, and regulatory proteins in the MICU family. We have generated a mouse model of MICU1 deletion and confirmed that MICU1 acts as a gatekeeper of MCU, inhibiting MCU activity at low levels of extramitochondrial calcium and stimulating MCU when calcium levels rise. MICU1 deletion results in high perinatal lethality, and surviving MICU1^{-/-} mice exhibit ataxia and muscle weakness. These mice also show increased mitochondrial calcium, altered mitochondrial morphology, elevated lactate levels, and reduced ATP. To confirm the role of calcium overload in these phenotypes, we generated additional mice with a targeted deletion in EMRE, and found that the absence of one allele of EMRE rescued the high perinatal mortality resulting from MICU1 deletion. Furthermore, EMRE heterozygosity lowered mitochondrial calcium levels and significantly improved the biochemical, neurological, and myopathic features observed in MICU1^{-/-} mice. We have further characterized the phenotype of EMRE^{-/-} mice, including the effects of EMRE deletion on calcium uptake, calcium levels, body weight, and exercise capacity. These mouse models enable us to investigate the importance of mitochondrial calcium regulation on the mitochondrial, cellular, and organismal levels.

The Plasma Protein Profiling of Sickle Cell Diseases Patients by Tandem Mass Spectrometry Based Proteomic Analysis. D. Ma, A. Ikeda, Y. Yang, H. Ackerman; Sickle Cell Branch.

Proteomic analysis and biomarker identification in sickle cell disease has the potential to contribute to the understanding of pathological mechanism and the discovery of new treatment strategy. Given the tremendous complexity of the plasma proteome, we compared the data quality with and without 6 high abundant protein depletion followed by Surface-enhanced laser desorption/ionization time of flight mass spectrometry (SELDI-TOF MS) in a pilot study. The results showed that non-depleted samples showed higher number of detectable proteins (965 proteins) within a comparable shorter turnaround time. Further, we searched for protein profiling in 26 plasma specimens from subjects aged between 20 and 45 years without protein depletion. Among these samples, 14 samples were from sickle cell anemia patients during and post pain crisis, 6 samples were from sickle cell anemia patients at steady state and 6 samples were from health volunteers. As a group, patients with SCD demonstrated significantly lower haptoglobin levels than healthy control subjects, which was validated by

ELISA. The levels of proteins which are relevant to inflammation, coagulation and erythrocyte functions were also analyzed using different bioinformatics tools.

Functional Study of CCR5 in Human Macrophages using iPSC-Derived Myeloid *in vitro* Disease Model. Y. Ma, Y. Huang, F. Calcaterra, D. Mavilio, L.G. Biesecker, G. Chen, D. Yang, M. Boehm; Laboratory of Cardiovascular Regenerative Medicine.

C-C chemokine receptor 5 (CCR5) is a G-protein coupled receptor that binds several endogenous chemokines promoting immune cell trafficking and recruitment. Its natural ligands include MIP-1 α (CCL3) and 1 β (CCL4) and RANTES (CCL5). It is also an important co-receptor for M-tropic HIV entry, rendering immune cells susceptible to infection. A 32-base pair deletion in the CCR5 gene (CCR5 Δ 32) prevents receptor expression on the cell surface, making the cells resistant to HIV infection. While CCR5 is known to play an important role in inflammation, the mechanisms behind its actions, particularly in cytokine regulation, has yet to be understood. In this study, we generated myeloid lineage cells using iPSC colonies carrying CCR5 Δ 32 to study the functional response of CCR5. The characteristics of these cells were confirmed by the expression of myeloid markers using flow cytometry. A phagocytosis assay to investigate innate response of the iPSC-derived macrophages (iM Φ) showed similar phagocytic abilities to primary macrophages (M Φ). Luminex multiplex assay showed that the cytokine secretion of iM Φ was similar to that of M Φ . The function of CCR5 was examined by infecting both iM Φ and M Φ with HIV. iM Φ carrying the CCR5 Δ 32 mutation showed significant decrease in HIV infection compared to wild type iM Φ and M Φ . In RANTES stimulated cells, the MIP-1 β production was measured on both mRNA and secreted cytokine levels. No marked difference was observed in CCR5 Δ 32 group compared to wild type cells, possibly due to compensation by other members of the receptor family. In conclusion, iPSC-derived myeloid cells are comparable to those from peripheral blood and they can be used as a model for studying myeloid-related diseases and mutations. Further experiments must be completed to observe the mutation's effect on the production of CCR5 downstream targets, including identifying and blocking possible compensation receptors.

Illuminating Mitophagy in Living mt-Keima Mouse Tissues via Super-Resolution Microscopy. D. Malide, N. Sun, T. Finkel; Light Microscopy Core.

Alterations in mitophagy have been increasingly linked to aging and age-related diseases. There are, however, no convenient methods to analyze mitochondrial turnover and mitophagy *in vivo*. To this end we recently reported (Sun et al, Molecular Cell, 60, 2015) a transgenic mouse model in which we expressed a mitochondrial targeted form of the fluorescent reporter Keima (mt-Keima). Keima is a coral-derived protein that exhibits both pH-dependent excitation and resistance to lysosomal proteases. This reporter mouse containing the fluorescent reporter mitochondrial targeted mt-Keima allows for

the *in vivo* assessment of mitophagy in various tissues under normal conditions using confocal microscopy. Furthermore, on another scale of resolution, we demonstrated that mt-Keima is suitable for imaging via super-resolution STED microscopy allowing observation of biological phenomena never before seen. Fluorescence nanoscopy, or super-resolution microscopy has become an important tool for cell biologists with several methods achieving sub-100-nm resolution by taking advantage of reversible/irreversible photo-physical switching properties of fluorescent markers. Thus, using the mt-Keima mouse, we can assess at nanoscale resolution in living tissues including skeletal muscle, heart, liver, adipose tissue, and kidney, how tissues mitophagy is altered following changes in diet, oxygen availability, genetic perturbations, or aging. Dual and multi-color experiments showed 3D characterization of intracellular compartments: lysosomes, endoplasmic reticulum, nucleus, plasma membrane, lipid droplets. Moreover, we also achieved STED imaging using resonant-scanning fast-time acquisition. In conclusion, we demonstrated that mt-Keima mouse is a versatile tool for investigating mitophagy via fluorescence nanoscopy at 50-nm resolution.

Generation of a Mouse with a Methionine Sulfoxide Mimic in Place of Met77 in Calmodulin. M.C. Marimoutou, R.L. Levine, G. Kim; Laboratory of Biochemistry.

Calmodulin (CaM) is a ubiquitous signaling protein that upon binding calcium interacts with its intracellular targets, of which over 350 have been described. Methionine sulfoxide reductase A is a bifunctional enzyme capable of oxidizing Met in proteins to its sulfoxide (MetO) and of reducing MetO back to Met. When CaM was incubated with recombinant, myristoylated methionine sulfoxide reductase A under oxidase conditions, only one of the 9 Met residues was oxidized – Met77. When the incubation solution was changed to reductase conditions, the MetO77 in oxidized CaM was fully reduced back to Met. Thus, methionine sulfoxide reductase A can mediate the reversible covalent modification of Met77 in CaM. To assess whether this is a regulatory mechanism *in vivo*, we utilized CRISPR to mutate Met77 to Gln because Gln is a mimic of MetO. This was successful, with both copies of the CaM gene mutated (Met77Gln). The mutant mice are viable, and we are characterizing their growth, development, and phenotype.

Molecular Breakdown of DEER Data from Self-Learning Atomistic Simulations. F. Marinelli, G. Fiorin, J. Faraldo-Gómez; Theoretical Molecular Biophysics Section.

Double Electron-Electron Resonance (DEER) has become a landmark technique to investigate bio-molecular structure and dynamics. DEER allows obtaining the distance distributions between spin-labels attached to a biomolecule and in contrast to X-ray crystallography and NMR spectroscopy, DEER is neither limited by the need of crystallization nor by the size of the biomolecule. This notwithstanding, it is often not straightforward to interpret DEER data as it reflects a plethora of molecular conformations and rotameric states of the spin-labels. Several strategies to disentangle this variability have been put forward recently, either based on approximate

structural models or on atomistic simulations. Both kinds of approaches however rely on probability distributions that are inferred from the actual measured data and do not consider the experimental noise. Building upon the maximum entropy principle, we present an adaptive simulation framework to minimally bias an atomistic simulation to sample a conformational ensemble that reproduces the DEER data within the experimental uncertainty. We first test the performance of this approach for the spin-labeled T4 lysozyme. Then, we apply it to investigate the conformational dynamics of the apo VcSiaP binding protein, that undergoes an open to close conformational change upon substrate binding. The results indicate a wider opening of the VcSiaP apo state compared to both the X-ray structure and standard MD simulations, underlying that the proposed technique is a powerful tool to structurally characterize DEER experiments and to investigate the dynamics of biomolecules.

Multifaceted Role of Glycan Interactions on Clathrin-Independent Endocytosis of MHC1 and CD59. M.P. Mathew, J.G. Donaldson; Membrane Biology Section.

Altered glycosylation is a hallmark of cancer and while these changes have been viewed as passive by-products of cancer metabolism more recent results have shown that these glycans can serve important functional roles. The role that glycan interactions can play in clathrin-independent endocytosis (CIE) is an area of increasing interest because CIE is a form of endocytosis which, unlike clathrin mediated endocytosis (CME), does not have well defined canonical machinery. Thus, studying the role glycans can play in this setting could help elucidate some of the regulatory and molecular mechanisms that govern these trafficking pathways. In this study, we show that the perturbation of global cellular glycosylation patterns by metabolic flux modulation affects clathrin independent endocytosis. Interestingly, these changes in glycosylation appear to have cargo-specific effects. We then focused on the role of Galectin 3 a key component of the galectin lattice which is a major determinant of membrane characteristics. We found that knocking-down the expression of Galectin 3 led to a decrease in MHC1 uptake and an increase in CD59 uptake. Whereas, the inhibition of all glycan-galectin interactions by lactose treatment inhibits the uptake of both CIE cargo. These treatments did not affect the uptake of transferrin, a CME cargo protein, suggesting a CIE specific role for glycosylation. Our results suggest that glycans play a role in CIE that is quite nuanced, with each cargo affected in a specific manner. A better understanding of the role glycosylation plays in the context of CIE could open a window into how altered glycosylation can alter the progress of cancer via the CIE pathway.

Linking Lysosomal Activity to Parkinson's Disease. R.P. McGlinchey, N. Tayebi, E. Sidransky, J.C. Lee; Laboratory of Protein Conformation and Dynamics.

A cellular feature of Parkinson's disease (PD) is cytosolic accumulation and amyloid formation of α -synuclein (α -syn). Herein, we demonstrate using liquid chromatography mass

spectrometry that C-terminally truncated α -syn (Δ C-syn), identified from pathological α -syn aggregates is likely derived from incomplete α -syn degradation from lysosomal activity. These Δ C-syn truncations have previously been shown to accelerate amyloid formation. Specifically, the cysteine protease, asparagine endopeptidase (AEP) has been identified to truncate α -syn at C-terminal residues that match peptide fragments observed *in vivo*. Using purified lysosomes from young (2 month) and old mouse (17 month) brains, AEP activity assayed by a fluorogenic substrate is increased in aged mice. Both exogenously added and endogenously derived α -syn revealed accelerated degradation with the lysosomes from the 17-month old mouse. More recently, we have focused our efforts on assessing lysosomal activity using symptomatic PD mice with the genotype *SNCA^{A53T}/SNCA^{A53T}*. So far, these initial data suggest mouse brain lysosomal activity, specifically AEP activity, is increased during ageing and aggregation prone Δ C-syn fragments would be populated.

Consequences of Xyloside Treatment on Neuronal Cytoskeleton Assembly and Function. C. Mencio, S. Tilve, C. Agbaegbu, H. Katagiri, H. Geller; Developmental Neurobiology Group.

From neural development to regeneration, heparan sulfate (HS) and chondroitin sulfate proteoglycans (CSPGs) can play contradictory roles. Xylosides are small molecules which serve as a competitor for glycosaminoglycan (GAG) chain biosynthetic machinery. Xyloside treatment leads to the inhibition of endogenous PGs and the production of primed GAGs, or GAG chains built on the xyloside and as such lack a core protein. Primed GAGs are pushed out of the cell and can be found in the extracellular space. Much of the previous research has focused on high concentration treatment (≥ 1 mM) by xyloside. We have found that low concentration ($\leq 1\mu$ M) xyloside (LCX) treatment caused unexpected changes in cell behavior and morphology. LCX-treated neurons exhibit enlarged lamellipodia and growth cones. These were absent in cells treated with vehicle or 1mM xyloside. Other cytoskeletal elements show changes in expression and phosphorylation state after LCX treatment and an increase of high molecular weight CSPGs was also found in the cell lysate of neuronal cultures. Additionally, disruptions in cellular trafficking have been observed. *In vitro* visualization of lysosomes shows a lack of perinuclear localization in LCX-treated neurons as compared to vehicle treated neurons. Trafficking deficiencies may also explain increased CSPGs as changes in cytoskeleton may result in a disruption of vesicle transport within the cell and subsequent trafficking of proteins. This research serves as a first step to fully explore the potential of low concentration xyloside treatment as a research tool and better understand the role of proteoglycans in neural development and function.

Functional Implications of the RecQ Helicase - Topoisomerase III – SSB Complex: Insights from Single Molecule Measurements. M. Mills, Y. Seol, K.C. Neuman; Laboratory of Single Molecule Biophysics.

RecQ helicases are a family of DNA helicases that are critical for maintaining genome stability. In *E. coli*, RecQ is known to functionally interact with Topoisomerase III. The coupling of helicase activity and topoisomerase activity that results from this interaction is responsible for resolving DNA structures that arise from errors in recombination. Similar interactions have been demonstrated in homologous proteins in other organisms, including the human RecQ helicase BLM and Topo III α , and the yeast helicase SgsI and Topo III. There is also evidence that single-stranded DNA binding protein (SSB) interacts with RecQ and is a necessary component of this complex *in vivo*. We sought to explore the individual contributions of these proteins to topological changes in DNA and their effects on each other using single molecule experiments. To investigate the roles of RecQ, Topo III, and SSB, individually and together, we measured their effect on DNA hairpin unwinding and refolding using magnetic tweezers. Our results suggest that the three proteins directly interact with each other during DNA-processing and provide a framework for understanding the mechanism of the resolvase activity of the RecQ-TopoIII-SSB complex.

Micro Fabrication of Hard X-Ray Compound Refractive Lens Using Nanoprinting Process. M. Mirzaeimoghri, A. Morales, C. McCue, D. DeVoe, H. Wen; Imaging Physics Laboratory.

Focusing hard x-rays for microscopy has been a challenging task for a century. Compound refractive lens (CRL) technology represents one approach to addressing this challenge using series of lenses than can accumulate the small refraction of each lens. Different kinds of parabolic CRL fabrication process such as drilling holes inside the Aluminum block, inserting micro-bubbles in epoxy, planar lens, and other more complex technologies have been investigated. However, current limitations in the fabrication of 3D structures meant that they work for soft 8 keV x-rays with a focal length of 10 cm, limiting the magnification factor and the resolution to 10 μm .

We explored a novel and low cost fabrication process using a two-photon laser photopolymerization system to pattern epoxy-based CRLs by direct 3D nanoprinting. To fabricate the lenses, a droplet of IP-DIP resist was drop casted on the edge of the 700 μm thick fused Silica substrate. Then the micron scaled lenses were patterned on the resist using Nanoscribe Photonic Professional GT in DILL mode with high power laser, followed by a 15 min developing in the MPGA resist developer and 15 min post bake at 70°C. This Nano x-ray microscope consists of 905 μm long structure containing 16 blocks of half bubble concave lenses, where the bubble has 12 μm short radius and 24 μm long radius.

Experimental measurements were performed in a commercial micro-CT system and a custom benchtop system. The developed process has been shown to enable the formation of two-dimensional micron-scale CRL arrays with 19 mm focal length and ~100% focusing effect. We intend to use the lens arrays for tabletop x-ray microscopy of one micrometer resolution.

LDL-Receptor Related Protein-1 Attenuates House Dust Mite-Induced Airway Inflammation by Suppressing Dendritic Cell-Mediated Adaptive Immune Responses. A. Mishra¹, A. Saxena², E.M. Gordon¹, X. Yao¹, M. Kaler¹, R.A. Cuento¹, A.V. Barochia¹, P.K. Dagur², J.P. McCoy², K.J. Keeran³, K.R. Jeffries³, X. Qu⁴, Z. Yu⁴, S.J. Levine¹; ¹Laboratory of Asthma and Lung Inflammation, ²Flow Cytometry Core Facility, ³Animal Surgery and Resources Core Facility, ⁴Pathology Core Facility.

The LDL-receptor related protein 1 (LRP-1) is a scavenger receptor that regulates adaptive immunity and inflammation. LRP-1 is not known to modulate the pathogenesis of allergic asthma. To assess whether LRP-1 expression by dendritic cells (DCs) modulates adaptive immune responses in house dust mite (HDM)-induced airways disease. LRP-1 expression on peripheral blood DCs was quantified by flow cytometry. The role of LRP-1 in modulating HDM-induced airways disease was assessed in mice with a deletion of LRP-1 in CD11c⁺ dendritic cells (*Lrp1*^{fl/fl}; CD11c-Cre) and by the adoptive transfer of HDM-pulsed CD11b⁺ DCs from *Lrp1*^{fl/fl}; CD11c-Cre mice to wild-type mice. Human peripheral blood myeloid DC subsets from eosinophilic asthmatics have lower LRP-1 expression than cells from non-eosinophilic asthmatics. Similarly, LRP-1 expression by CD11b⁺ lung DCs was significantly reduced in HDM-challenged wild-type mice. HDM-challenged *LRP-1*^{fl/fl}; CD11c-Cre mice have a phenotype of increased eosinophilic airway inflammation, allergic sensitization, Th2 cytokine production, and mucous cell metaplasia. The adoptive transfer of HDM-pulsed LRP-1-deficient CD11b⁺ DCs into wild-type mice generated a similar phenotype of enhanced eosinophilic inflammation and allergic sensitization. Furthermore, CD11b⁺ DCs in the lungs of *Lrp1*^{fl/fl}; CD11c-Cre mice have an increased ability to take up HDM antigen, whereas bone marrow-derived DCs display enhanced antigen presentation capabilities. This identifies a novel role for LRP-1 as a negative regulator of DC-mediated adaptive immune responses in HDM-induced eosinophilic airway inflammation. Furthermore, the reduced LRP-1 expression by circulating myeloid DCs from eosinophilic asthmatics suggests a possible role for LRP-1 in modulating type 2-high asthma.

Fetal Mouse Heart Imaging Using Echocardiography. D. Mokshagundam^{1,2}, D. Donahue³, I. Garcia-Pak¹, B. Klaunberg³, Y. Mukoyama¹, L. Leatherbury^{1,2}; ¹Laboratory of Stem Cell and Neuro-Vascular Biology, NHLBI, ²Children's National Heart Institute, Children's National Health System, ³NIH Mouse Imaging Facility.

Human fetal echocardiography has revolutionized the detection and treatment of congenital heart disease and expanded our understanding of cardiac development. In studying the genetic basis of cardiac development, certain mutations confer a lethal phenotype for the embryo, such as *phox2b* mutants lacking sympathetic innervation in the heart. Newer generations of linear array animal ultrasound machines offer enhanced 2D and Doppler resolution allowing for possible in utero study of cardiac function and development prior to expiration of the

embryo. We herein established a fetal mouse heart imaging using fetal echocardiography. We examined C57BL/6 pregnant females with an expected litter size of 6-8. Using a Visualsonics Vevo 2100 with a 30MHz and 40MHz linear array probe both free hand and with a fixed arm, we identified the dam's bladder and then each individual embryo. We were successfully able to measure embryo heart size, heart rate, and cardiac function. The mice and embryos survived multiple applications of this process allowing for day-to-day measurements in the same mouse. We visualized and made measurements on embryos as young as 12.5dpc. Our established protocol shows promise in studying cardiac phenotypes including congenital heart malformations and functional deficits at sequential stages of fetal mouse development.

alpha-Synuclein Crosslinked by Pyrrole Linkages Derived from Dopamine. S. Monti, J.W. Werner-Allen, A. Bax, R.L. Levine; Protein Function in Disease.

α -synuclein has been implicated in Parkinson's disease both by mutations linked to familial Parkinson's disease and its prevalence in the Lewy body aggregates that are the hallmark of the disease. Parkinson's disease is characterized by the loss of dopaminergic neurons leading to a chronic and progressive motor disorder. Although Parkinson's disease was described over a hundred years ago and has been associated with redox imbalance and oxidative stress, little has been confirmed about the cause of the majority of Parkinson's disease cases. One hypothesis, driven in part by the specific loss of dopaminergic neurons, suggests that dysregulation of dopamine metabolism leads to an overabundance of the dopamine metabolite, 3,4-dihydroxyphenylacetylaldehyde (DOPAL), which is known to be toxic to the cell. The mechanism of DOPAL toxicity and its contribution to Lewy body formation remain to be elucidated. Previously it was demonstrated that incubation with DOPAL leads to α -synuclein oligomerization, and that DOPAL reacts with the lysine residues of α -synuclein to form di-catechol pyrrole lysine (DCPL) adducts containing a central pyrrole ring. Our recent work establishes that these DCPL adducts can dimerize through pyrrole-pyrrole linkages. Liquid chromatography-mass spectrometry analysis of α -synuclein samples oligomerized by DOPAL reveals masses consistent with α -synuclein dimers linked by DCPL adducts. These results suggest that oxidative stress in dopaminergic neurons leading to increased levels of DOPAL could cause α -synuclein oligomerization mediated by DCPL adduct interactions.

iPS-Cardiomyocytes Transfer to Treat Heart Failure from Ischemic Cardiomyopathy – Non-Human Primate Model. K. Navarengom, E.A. Ferrante, G. Chen, J. Hawkins, S. Hong, J. Chan, Y. Lin, J. Zou, C. Dunbar, M. Boehm; Laboratory of Cardiovascular Regenerative Medicine.

Centers for Disease Control estimate that about 5.7 million adults in the US have heart failure (HF) and more than 550,000 new cases are diagnosed every year. The definitive treatment of end-stage HF remains orthotopic heart transplantation (OHT). The mortality rate while waiting for OHT is high (35% in 4 months) due to shortage of donor hearts. Our team

is developing a novel therapeutic strategy to improve cardiac function using autologous, induced pluripotent derived cardiomyocytes (iPS-CM) to treat HF. The advantage of autologous cell injection is that it bypasses the need for immunosuppression. In a preclinical non-human primate study, we developed a complex surgery protocol to induce myocardial infarction and inject iPS-CM in rhesus monkeys. We have programmed human truncated CD19 (h Δ CD19) and Sodium-iodide symporter (NIS) using the CRISPR/Cas9 system to track rhesus iPS-CM ex vivo (histology) and in vivo (Positron Emission Tomography imaging), respectively. Histological evaluation of the heart showed the area of infarct and the presence of CD19+ iPS-CMs in completed studies. PET imaging of NIS iPS-CM in a teratoma mouse model could visualize iPS-CM before the teratoma could be felt by touch. We also tested a remote telemetry system to monitor abnormal cardiac rhythms before and after iPS-CM injection. Our first set of survival surgeries with iPS-CM injection are ongoing. An improvement in cardiac function and reduction in area of damage are expected, similar to studies by other investigators using allogenic cell transfer protocols. Future studies will help in designing clinical protocols for treatment of HF in humans.

The Effects of Fasting and Refeeding on Regulating NLRP3 Inflammasome Activation in Asthmatic Subjects.

A. Nguyen, K. Han, J. Li, M. Kwarteng-Siaw, J. Traba, M. Sack; Laboratory of Mitochondrial Biology and Metabolism.

Asthma is an NLRP3-inflammasome-linked disease. We have shown that fasting (24 hours) blunts and refeeding (3 hours after a meal) activates the NLRP3 inflammasome in peripheral blood mononuclear cells (PBMCs) from healthy volunteers and that the serum extracted at the fasted and refeed time points can recapitulate components of this effect in THP-1 macrophage cells. At the same time a clinical study has shown that intermittent fasting reduces asthma exacerbations. Our pilot study aimed to evaluate whether fasting and refeeding regulate the NLRP3 inflammasome in mild to moderate asthmatic subjects exposed to a 24-hour fasting and 2.5-hour refeeding protocol. We hypothesized a 24-hour fast could suppress the NLRP3 inflammasome and improve bronchial airflow in medically stable asthmatic subjects. PBMCs and serum from subjects' blood were extracted for analysis and for cell culture studies. Preliminary data in the first 12 study participants have been analyzed. Interestingly, the non-steroid (NS) treated (n=5) asthmatic subjects showed a 34% increase in refeeding activation of the NLRP3 inflammasome as measured by IL-1 β release as was found in the healthy volunteers. However, steroid-treated asthmatic subjects (n=7) did not show an induction of the inflammasome with refeeding. The refeed serum from the NS-treated asthmatic subjects recapitulated aspects of immune activation by increasing inflammation transcript levels in THP-1 cells and by inducing IL-33 in lung epithelial cells. Our preliminary data suggest that: (i) inhaled steroids have systemic effects and disrupt the immune modulatory effects of fasting and refeeding and (ii) refeeding can evoke inflammatory pathway in NS-treated asthmatic subjects. In the future, we aim to (i)

confirm whether serum from fasted versus fed asthmatic subject attenuates *in-vitro* inflammation in cultured airway epithelial cells and (ii) analyze circulating factors that may mediate nutrient-level dependent inflammasome programming.

Altered Extracellular Matrix Metabolism as a Potential Link to the Pathophysiology of Vascular Abnormalities in Autosomal Dominant Hyper-IgE Syndrome. D. Nguyen¹, N.I. Dmitrieva¹, B.A. Kozel², A.F. Freeman³, M. Boehm¹; ¹Laboratory of Cardiovascular Regenerative Medicine, NHLBI; ²Laboratory of Vascular and Matrix Genetics, NHLBI; ³Laboratory of Clinical Infectious Diseases, NIAID.

Autosomal dominant hyper-IgE syndrome (AD-HIES) is a primary immunodeficiency caused by mutations in the signal transducer and activator of transcription 3 (STAT3), leading to recurrent infections, elevated level of IgE, poor post-operative recovery, and skeletal and connective tissue abnormalities. Current therapies are limited to prophylactic antibiotics and post-infection management. About 70% of AD-HIES patients present with either tortuous or dilated vessels. Complications of these vascular abnormalities result in myocardial infarction and subarachnoid hemorrhage, and are major causes of mortality in patients. The mechanism of how STAT3 deficiency manifests into these phenotypes remains unknown. RNA-seq analysis of global gene expression in patients' skin fibroblasts identified decreased expression of components of extracellular matrix remodeling pathway, including matrix metalloproteinases (MMPs) and laminin. Thus, this study aims to identify specific extracellular-matrix (ECM) protein(s) that undergo altered metabolism to provide clues to the vascular abnormalities seen in patients. We stained post-mortem coronary arteries from 5 AD-HIES and 6 control individuals using chromogen immunohistochemistry (IHC) to detect ECM protein expression. IHC intensities were quantified by yellow channel extraction using an automated computer image analysis CMYK color model. Consistent with the decreased expression of MMPs, the analysis indicates increased accumulation of MMPs substrates: elastin, collagen I, and collagen IV in patient coronary walls. Additionally, decreased protein expression of basement membrane component, laminin, suggests a possible cause for vessel dilation. Results from this study reveal altered extracellular matrix metabolism as the potential explanation for vascular abnormalities in AD-HIES and provide a target for clinical treatment.

High Sensitivity Detection of Mutations Implicated in Chronic Lymphocytic Leukemia Drug Resistance. C. Nichols, C. Underbayev, S. Herman, A. Wiestner; Hematology Branch.

Chronic lymphocytic leukemia (CLL) affects primarily older adults and involves uncontrolled monoclonal expansion of B cells in the blood and lymphoid organs. While anti-CD20 therapies like Rituximab and Ofatumumab have greatly improved clinical prognosis for many CLL patients, the problem of relapsed and refractory disease progression remains a challenge. The presence of *NOTCH1* mutation has been shown to associate with lower mean progression free survival, overall

survival, and higher risk of Richter's transformation; all markers of poor prognosis.

Mutations in *NOTCH1* occur in roughly 11% of CLL cases at diagnosis, generally comprised of a highly recurrent c.7541-7542delCT two base pair frameshift deletion in exon 34. This deletion causes truncation of the C-terminal PEST domain, yielding a stable form of the Notch intracellular domain (NICD) that propagates constitutive Notch signaling. Moreover, *NOTCH1* mutation has been correlated with low CD20 levels caused by down regulation of MS4A1 transcript levels, the mRNA encoding CD20 protein.

We aim to investigate *NOTCH1* mutation in Ofatumumab-treated CLL patients using highly sensitive droplet digital PCR (ddPCR) to better understand this aberration as a potential driver mutation of anti-CD20 therapy resistance.

Single-Cell RNA Sequencing Analysis of Bone Marrow Populations. K.A. Oetjen, C.S. Hourigan; Myeloid Malignancy Section.

The bone marrow contains the entire spectrum of immature and maturing blood cells, which are responsible for the production of all circulating blood cells and many immune responses. To deeply characterize the transcriptional profiles for this immensely complicated cellular environment, we performed single-cell RNA sequencing of bone marrow aspirates. We recruited 20 healthy volunteers, comprised of 10 men and 10 women with a wide range of ages from 24 to 84 years old (median 51 years old). For two donors, the procedure was repeated to obtain a second sample, 2 months or 5 months later, to further characterize variability in cell populations over brief periods of time. Droplet-based single-cell RNA sequencing was performed using the 10X Genomics Chromium Single Cell 3' version 2 kit. This platform uses a barcoded primer gel bead encapsulated with a single cell inside an oil emulsion droplet during reverse transcription to tag cDNA transcripts with a cellular barcode and a unique molecular index. In our preliminary data, this approach identified expected cell populations within the bone marrow, such as immature progenitor cells, and revealed gene expression changes during maturation of red blood cells, monocytes and B cells. Furthermore, this approach identified the transcriptional profiles of T cells, NK cells and dendritic cells within the bone marrow environment. We anticipate this rich dataset will become a valuable resource for research groups studying normal blood cell development and immunologic responses, as well as diseases including bone marrow failure syndromes and leukemia.

Role of Ca²⁺/Calmodulin-Dependent Protein Kinase II (CaMKII) in Modulating Calcium Uptake in Mitochondria. M. Oldham, G. Amanakis, R. Parks, E. Murphy; Laboratory of Cardiac Physiology.

Cardiovascular disease is the major cause of death in the US; therefore, a better understanding of the mechanisms regulating cell death in ischemia and reperfusion injury are important. Mitochondrial calcium has proven to play a crucial role in the normal functioning of many processes, including the regulation of cardiac biochemical pathways and mediating

ischemia-reperfusion injury. The uptake of calcium into the mitochondrial matrix is regulated by the mitochondrial calcium uniporter (MCU). This protein is located within the inner mitochondrial membrane and when over stimulated causes the opening of mitochondrial permeability transition pore (mPTP). Increased mitochondrial calcium activates mPTP which initiates cell death. Ca²⁺ Calmodulin Dependent Kinase II (CaMKII) has also been shown to regulate cell death. This kinase enzyme has proven to have increased activity during ischemia reperfusion injury and myocardial infarction. Marked inhibition of CaMKII has further shown to reduce myocardial cell death (Nature 2012). The goal of this study is to test several hypotheses by which CaMKII might alter mitochondrial cell death pathways. One hypothesis is that CaMKII phosphorylates MCU and alters uptake of calcium. To test this hypothesis, I will be using wild type mouse embryonic fibroblast (WT MEFs) to test changes in calcium uptake with and without KN93 (competitive inhibitor of CaMKII). It is expected that KN93 would have no effect on MCU knockout (MCU- KO) MEFs since this line does not take up calcium.

Membrane Binding and Fluidity Sensing by α -, β -, and γ -Synuclein. E.I. O’Leary, Z. Jiang, J.C. Lee; Laboratory of Protein Conformation and Dynamics.

α -Synuclein (α -Syn) is a neuronal protein associated with Parkinson’s disease that has an N-terminal lipid-binding motif and a disordered C-terminal tail. It has been demonstrated that α -syn can bind and remodel membranes composed of zwitterionic and anionic phospholipids; however, there has been little consideration for lipid phase in binding preference. We provide evidence through circular dichroism (CD) and steady-state fluorescence experiments that α -syn binds preferentially to the gel phase of zwitterionic small unilamellar vesicles (SUVs) composed of 1-palmitoyl-2-oleoyl-*sn*-glycero-3-phosphocholine (POPC) or 1,2-dipalmitoyl-*sn*-glycero-3-phosphocholine (DPPC). For DPPC, α -syn transitions from an α -helical to a disordered conformation at the lipid’s melting temperature (T_m) of 41 °C, which was independently verified using differential scanning calorimetry. Contrastingly, in the presence of anionic SUVs composed of 1,2-dipalmitoyl-*sn*-glycero-3-phospho-(1'-*rac*-glycerol) (DPPG), α -syn favors the fluid phase. To understand which regions of α -syn are essential for binding and fluidity sensing, we used two homologs, β -syn and γ -syn, which have been independently linked to diseases such as dementia with Lewy bodies and breast carcinomas, respectively. While their sequences are highly conserved in the N-terminus, β -syn lacks 11 residues (73–83) in the central region and γ -syn has a truncated C-terminus compared to α -syn. Interestingly, both β -syn and γ -syn have similar fluidity sensing capabilities as α -syn, but γ -syn binds weaker to vesicles compared to both α -syn and β -syn. These results suggest that the C-terminus may play a larger role in modulating α -syn–lipid interactions than previously assumed, and offer new insights into the mechanism of α -syn lipid binding and fluidity sensing.

Evaluation of Early Biomarkers Associated with Graft Rejection in Patients with Sickle Cell Disease. P.

Olkhanud¹, F. Seifuddin², M. Pirooznia², C. Pittman¹, A. Biantotto³, R. Pfeiffer⁴, C. Fitzhugh¹; ¹Laboratory of Early Sickle Mortality Prevention, NHLBI, ²Bioinformatics and Computational Biology Core Facility, NHLBI, ³Center for Human Immunology, Autoimmunity, and Inflammation, NHLBI, ⁴Biostatistics Branch, NCI.

Hematopoietic stem cell transplantation (HSCT) is the only curative option for patients with sickle cell disease (SCD). However, currently no validated biomarkers exist to predict allograft rejection. We therefore sought to identify plasma biomarkers associated with allograft tolerance and rejection in HSCT. A total of 21 adult patients with SCD who underwent non-myeloablative haploidentical peripheral blood stem cell transplantation were analyzed. Patients were conditioned with alemtuzumab, 400cGy total body irradiation, post-transplant cyclophosphamide doses ranging from 0-100mg/kg, and sirolimus. We measured 48 cytokine concentrations from plasma samples prospectively collected pre-transplant and at serial time points post-transplant (PT) at days 30, 60, 100 and 180. Florescent bead-based immunoassay (Luminex) was used to measure cytokine levels.

We observed that the most significant differences in cytokine levels between successfully engrafted (mixed chimerism at PT-Day 180) and rejected groups after Bonferroni correction was at PT-day 60 ($p < 0.001$, Fisher’s exact test) which corresponded with clinical findings of rejection. Increased levels of IL-4, IL-10, IL-9, IL-1RA, MIP-1 α , FGF, G-CSF, GM-CSF, VEGF, and TNF α at PT-Day 60 predicted transplant outcome with receiver operating curve AUC 0.85>, $p < 0.05$. Random forest variable importance measure identified that MIP-1 α was strongly associated with successful engraftment.

Our results suggest that these cytokines can be used as predictive biomarkers for allograft rejection and are useful diagnostic biomarkers for graft tolerance. Further studies are indicated to validate our findings.

A *Drosophila melanogaster* Screen Reveals Novel Functions For Microcephaly Genes. R.S. O’Neill, N.M. Rusan; Laboratory of Molecular Machines and Tissue Architecture.

Primary microcephaly and microcephaly with primordial dwarfism (MPD) are genetic disorders characterized by reduced cortex (and body size in MPD). Many primary microcephaly and MPD genes have functions relating to centrosomes, kinetochores, and DNA damage repair (DDR). In most cases, a mechanistic understanding of how microcephaly phenotypes arise is not directly established; rather, cell culture phenotypes are often used to infer a general underlying cause, such as reduced cell proliferation or increased apoptosis. We are screening mutant and RNAi lines of primary microcephaly and MPD gene orthologs in *Drosophila melanogaster* to uncover gene functions related to neural development. *nopo* is the ortholog of the MPD gene *TRAIIP*. *nopo* and *TRAIIP* encode E3 ubiquitin ligases which have a function in activating DDR pathways. We found that *nopo* mutants have a specific defect in the mushroom body (MB), which is a brain region critical for memory formation; *nopo* mutant MB lobes are thin, fused, and are occasionally missing or have misguided axons. *Spc105r* is the

ortholog of the human microcephaly gene *KNL1*. *Spc105r* and *KNL1* encode critical kinetochore-associated proteins. We found that knockdown of *Spc105r* in neural stem cells completely disrupts organization of the central brain, but not the optic lobes; knockdown in post-mitotic neurons is even more severe, suggesting a novel non-mitotic role for *Spc105r* in neurons. As we continue to screen for and characterize microcephaly and MPD mutant and knockdown phenotypes in *D. melanogaster*, we are likely to uncover previously undiscovered functions that also contribute to these disorders.

CypD-Mediated Regulation of the Permeability Transition Pore is Altered in Mice Lacking the Mitochondrial Calcium Uniporter. R.J. Parks¹, S. Menazza¹, A.M. Aponte², T. Finkel³, E. Murphy¹; ¹Systems Biology Center, ²Proteomic Core Facility, ³Center for Molecular Medicine.

Knockout (KO) of the mitochondrial Ca²⁺ uniporter (MCU) abrogates rapid mitochondrial Ca²⁺ uptake and permeability transition pore (PTP) opening. However, hearts from global MCU-KO mice were not protected from ischemic injury. Furthermore, MCU-KO hearts were resistant to protection by cyclosporin A (CsA), a cyclophilin D (CypD)-dependent pore desensitizer. This study investigates the hypothesis that the lack of protection in MCU-KO may be explained by alterations in PTP opening due to compensatory changes in CypD signaling. To investigate whether pore opening can occur in MCU-KO, Ca²⁺ uptake and swelling were measured in isolated mitochondria in the presence of the Ca²⁺ ionophore ETH129 to permit Ca²⁺ entry into the matrix. With ETH129, MCU-KO mitochondria took up Ca²⁺ and underwent pore opening similar to WT. To investigate the Ca²⁺ sensitivity of PTP in MCU-KO, basal Ca²⁺ was set to the same level in mitochondria from KO and WT prior to measuring Ca²⁺ uptake. MCU-KO underwent PTP opening before WT, suggesting that PTP Ca²⁺-sensitivity is altered in the absence of MCU. To determine whether CypD-mediated regulation of PTP may be different following global MCU deletion, experiments were performed to examine the interaction between CypD and the proposed PTP component ATP synthase. WT and MCU KO cardiac mitochondria were incubated with an immunocapture antibody to pulldown ATP synthase. Interestingly, results suggest that there was more CypD associated with ATP synthase in MCU KO in comparison to WT (n=7, P=0.047). As phosphorylation of CypD has been proposed to enhance PTP opening, immunoprecipitation experiments were performed using an antibody for phosphorylated proteins. MCU KO mitochondria had an increase in the amount of phosphorylated CypD (n=9, P=0.027). These results suggest that absence of MCU may alter PTP opening such that less Ca²⁺ is required to trigger PTP, which may be due to compensatory changes in CypD-mediated pore regulation.

Genetic Modifiers of Cardiovascular Phenotype in Elastin-Mediated Disease. P. Parrish, M. Lugo, B. Kozel; Laboratory of Vascular and Matrix Genetics.

Elastin (*ELN*) is an extracellular matrix protein that allows tissues including the skin, lungs, and blood vessels to stretch

and recoil. Elastin insufficiency is often associated with pathologic cardiovascular outcomes such as vascular smooth muscle cell hyperproliferation that produces stiff, narrow blood vessels. This blood vessel stenosis is a hallmark of the genetic disease Williams Syndrome (WS), which affects about 1 in 8,000 individuals worldwide. In WS, elastin insufficiency is caused by a microdeletion of 26-28 genes (including *ELN*) at the 7q11.23 locus. Common large-vessel defects in WS include supravalvular aortic stenosis, which involves thickening of the ascending aortic arch above the aortic valve, and pulmonary artery stenosis, in which the main pulmonary artery and its branches exhibit narrowing. However, although 20-30% of WS patients have severe vascular disease requiring surgical intervention, a similar proportion of patients have limited to no abnormalities of their aorta or pulmonary arteries. Therefore, our laboratory uses a variety of genetic techniques including CMA and whole-exome sequencing to identify both copy number and single-nucleotide variants that could modify the severity of large-vessel stenosis in WS patients. We have taken an extreme-phenotype approach to burden testing in WS patient genetic data to identify variants both inside and outside the WS region that could affect cardiovascular disease severity in this population. An improved understanding of genes and pathways associated with cardiovascular pathology will help in drug targeting and development and ultimately decrease morbidity and mortality due to large-vessel stenosis in the WS population.

Modifying Chondroitin Sulfate Proteoglycans Enhances Retinal Ganglion Cell Axon Regeneration in the Mouse Optic Nerve. C.S. Pearson, K.R. Martin, H.M. Geller; Developmental Neurobiology Section.

Retinal ganglion cell (RGC) axon regeneration can be induced by inflammation and genetic manipulation, but regrowth to central targets is limited in part due to the inhibitory extracellular environment of the optic pathway. We characterized the expression of chondroitin sulfate proteoglycans (CSPGs) after optic nerve crush (ONC) in mice. CSPGs were assessed by immunohistochemistry 1, 3, 7, 14, and 21 days post crush (dpc) using antibodies against CSPGs and markers for astrocytes (GFAP) and microglia (Iba1) (n=3 per group). Elevation of CSPGs was observed at from 3d until 21d post crush. Reactive astrocytes withdrew from the lesion, creating a GFAP-negative zone filled with Iba1-positive microglia and macrophages. Next, to assess the effects of CSPGs on RGC axon regeneration, mice received ONC, and at 3 dpc were administered an intravitreal injection of zymosan and a 1 mm³ gelfoam scaffold soaked in either chondroitinase ABC (ChABC) or a control buffer directly to the injured optic nerve (n=8 mice per condition). GAP-43 was used to visualize regenerating RGC axons in cryosections obtained 14 dpc. Axon regeneration was quantified by counting GAP-43+ axons crossing various distance benchmarks (0.5 to 1.5 mm) distal to the lesion and calculating the total regenerating axons per nerve. The results showed that zymosan effectively stimulates RGC axon regeneration, and delivery of ChABC increased the number and distance of regenerating axons. In conclusion, CSPG expression increased after mouse optic nerve crush, and

levels remained high for 3 weeks. This suggests that CSPGs at the lesion site inhibit growing axons and that modifying the extracellular environment may improve intrinsic regenerative therapies.

Oxidative Phosphorylation Complex Interactions in Intact Mitochondria. B.M. Rabbitts, F. Liu, P. Lössl, A.J. Heck, R.S. Balaban; Laboratory of Cardiac Energetics, NHLBI and Bijvoet Center for Biomolecular Research, University of Utrecht, The Netherlands.

Supercomplex formation, between the multisubunit protein complexes responsible for mitochondrial oxidative phosphorylation, is a concept with important potential implications for energy and redox regulation, and a high rate of debate in current literature. However, empirical evidence to test this theory remains limited. We used recently established crosslinking mass spectrometry methods to examine intact mitochondria from mouse heart, and discovered a highly interactive network between all pairs of oxphos complexes: we identified 122 unique intercomplex crosslinked lysine sites. This suggests that all five oxphos complexes exist in close spatial proximity in intact mitochondria. The specificity of the crosslinks is demonstrated by a perturbation: 80% of these sites were sensitive to electrostatic disruption conditions, which we show to eliminate the supercomplexes as measured by conventional gel methods. 22 of our sites (7 of which were disruption-sensitive) were between the three complexes that comprise the recent high resolution cryoEM structure (complexes I, III, and IV) and may be useful for refining models of this supercomplex, including evidence for alternate positions of complex IV and alternate conformations between complexes I-III. In addition to intercomplex crosslinks, oxphos complexes were also interconnected with cytochrome c and chaperones/assembly factors. This result is part of a database of 3,322 unique crosslinks, covering 47% of the preparation's proteome; the most comprehensive visualization of the mitochondrial "interactome" to date. Our crosslinks have 98% agreement with consensus crystal structures, provide accurate sub-mitochondrial resolution, and suggest the mitochondrial localization of several novel proteins. The data were obtained by materials and methods that are all publicly available, using less than a milligram of protein input material, allowing researchers to map the mitochondrial interactome in health and disease with unprecedented depth.

Real-Time Flow MRI to Monitor Exercise Stress. R. Ramasawmy¹, D. Herzka, J.M. Khan¹, T. Rogers¹, R.J. Lederman¹, M.S. Hansen², A.E. Campbell-Washburn²; ¹Cardiovascular Intervention Program, ²Laboratory of Imaging Technologies.

Interventional cardiovascular MRI exams have shown an increased diagnostic strength through the combined use of functional MRI quantification of cardiac output combined with simultaneous catheter measurements of cardiovascular pressures. Cardiovascular dysfunction is often more apparent during physiological provocations such as exercise, nitric oxide and dobutamine; diagnosis can be inferred from the acute reaction and peak function. Thus, a real-time measure of cardiac

output in response to exercise stress will offer further confidence in the diagnostic decision, as the online assessment of acute and peak function during such provocations. This research proposes using an under-sampled and efficient image acquisition methods to yield measurements of blood flow using phase-contrast MRI. Real-time flow MRI was designed from an eight-shot spiral trajectory with a 4-fold under-sampling, to produce an assessment of blood flow every 40 ms, and this was applied to three healthy volunteers exercised within the MRI scanner using a compatible ergometer. *Real-time flow MRI was within a 12.2% agreement to a reference clinical flow sequence.* A significant increase ($p < 0.001$, Kruskal-Wallis) in cardiac output between rest (5.36 ± 0.82 L/min, *mean \pm std*), medium intensity (8.08 ± 2.38 L/min), and higher intensity exercise (9.74 ± 0.57 L/min) was detected using real-time flow MRI. Real-time flow MRI was successful in capturing beat-to-beat cardiac function, and will be applied within the cardiovascular interventional program.

A Novel CD19/CD3 Bispecific Antibody Induces Potent Response Against Chronic Lymphocytic Leukemia. H. Robinson¹, J. Qi², S. Baskar¹, C. Rader², A. Wiestner¹; ¹Hematology Branch, NHLBI; ²The Scripps Research Institute, Jupiter, FL.

Although treatment of chronic lymphocytic leukemia (CLL) has been advanced by use of targeted therapies such as tyrosine kinase inhibitors and monoclonal antibodies, there remains a need for adjunct treatments capable of inducing deeper initial response, response in the setting of resistance to first-line agents, and/or CLL cure. Bispecific antibodies (biAbs) can be used to target endogenous T cells against tumor cells via the formation of cytolytic synapses. Blinatumomab, an anti-CD19/CD3 biAb designed in the 54.1 kDa BiTE format, is approved for treatment of Philadelphia chromosome-negative relapsed/refractory B-cell acute lymphoblastic leukemia, and has potential for use in other lymphoid malignancies. However, due to its short half-life of 2.1 hours, blinatumomab requires continuous intravenous dosing for efficacy. We have developed a novel anti-CD19/CD3 biAb in the 100 kDa single chain-Fv Fc format (CD19/CD3-scFv-Fc). With a half-life approximately 100-fold longer than blinatumomab, CD19/CD3-scFv-Fc may be suitable for weekly dosing, which would provide a significant logistical advantage in the clinic. In ex vivo experiments, CD19/CD3-scFv-Fc and blinatumomab induced comparable, potent killing of CLL cells. This response was associated with expansion of autologous CD4⁺ and CD8⁺ T cells, as well as increases in T cell granzyme B and IFN- γ expression. In a NOD/scid/ γ c(null) (NSG) CLL xenograft mouse model, CD19/CD3-scFv-Fc convincingly eliminated CLL cells with both once- and twice-weekly dosing. However, blinatumomab failed to induce a response when dosed on the same schedule. This data supports promise of CD19/CD3-scFv-Fc as a novel immunotherapy for use in CLL and other lymphoid malignancies.

Development of a Targeted RNA-seq Assay for the Detection of Minimal Residual Disease in Acute Myeloid Leukemia. G.W. Roloff, L.W. Dillon, H.Y. Wong, C.S. Hourigan; Myeloid Malignancies Section.

Although most patients with acute myeloid leukemia (AML) achieve an initial complete remission with standard chemotherapy, relapse frequently occurs and progressive disease remains the most common cause of death. The presence of persistent leukemic burden after treatment is referred to as minimal residual disease (MRD). It is well recognized that detectable MRD after induction therapy or at the time of stem cell transplantation predicts for adverse outcomes. Clinical complete remission is defined using a light microscope to assess bone marrow morphology, which has a low sensitivity for detecting residual disease. Therefore, the development of new techniques with greater sensitivity and specificity for measuring MRD and predicting patient outcomes is imperative. To help overcome this limitation, we are developing a multi-gene, targeted RNA-sequencing-based panel for the sensitive detection and quantitation of MRD-associated genetic signatures spanning multiple AML subtypes. The targeted RNA-seq panel utilizes gene-specific primers and unique molecular indices to specifically detect and measure known AML-associated genetic signatures, including known insertions and translocations. Targeted RNA-seq libraries were successfully generated from both a DNA standard template and RNA from AML cell lines harboring the targeted mutations and preliminary analysis confirms that the targeted regions can be detected simultaneously. Ongoing work seeks to further define the assay's limit of detection and ability to track MRD in patient samples at longitudinal time points.

VEGFA Concentration *In-Vitro* Modulates Hemogenic Endothelium Differentiation and Downstream Hematopoietic Stem and Progenitor Cell Identity. J.P. Ruiz, C. Porcher, A. Larochelle; Laboratory of Regenerative Therapies for Inherited Blood Disorders.

Hematopoietic Stem Cells (HSCs) reconstitute and maintain a functional blood system for the lifespan of an individual. The development of induced pluripotent stem cell (iPSC) and CRISPR-Cas9 gene-editing technologies opened the possibility for generating iPSCs from patients, correcting genetic defects, and differentiating disease-free iPSCs into transplantable, autologous HSCs. Though most blood cell types have been derived from iPSCs, differentiating engrafting HSCs remains a challenge. During development, HSCs arise from a specialized subset of endothelium known as hemogenic endothelium (HE) through an endothelial to hematopoietic transition in the dorsal aorta. Recent studies have demonstrated the importance of the arterial niche for HSC development from HE. However, this niche is not recapitulated in current pluripotent stem cell differentiation protocols. We hypothesized that increasing concentrations of vascular endothelial growth factor A (VEGFA) during *in-vitro* differentiation would induce arterial specification and facilitate the emergence of functional HSCs. Our data shows that a brief 24 hour induction with 10x concentrations of VEGFA compared to control cultures at the

stage of endothelial progenitor specification leads to a delay in activation of the hematopoietic program in favor of an arterial one. This delay is also Notch-independent. Burst treatment with high VEGFA concentrations leads to a > 5-fold increase in the total numbers of Type II pre-HSCs and immunophenotypically-defined adult HSCs (SLAM LSK) after six days in culture. Studies are ongoing to investigate engraftment and multi-lineage differentiation potential.

Equilibration of the Chemical Potential Between Lipid Leaflets During Molecular Dynamics Simulation. F. Samarjeet, T. Woolf, B.R. Brooks; Laboratory of Computational Biology.

Periodic boundary conditions (PBC) are used in molecular dynamics simulations to avoid problems due to boundary effects caused by the finite size of the simulated system. The normal PBC employed in molecular dynamics simulations, called P1 PBC, ensures that atoms that leave one face of the box appear on the opposite face. This scheme, however, creates a problem during simulation of lipid bilayers as it does not allow switching of lipids between the leaflets. In this work, we introduce P21 space group [denoted by $(-x, y+1/2, -z)$ symmetry operation] in CHARMM in a massively parallel domain decomposition (DOMDEC) implementation. This allows lipids exiting a leaflet to re-enter the opposite leaflet through an orthogonal face, thus equilibrating the chemical potential between the layers. This method gives a better corroboration of simulation results with those from the experiments.

Soluble APP Functions as a Vascular Niche Signal That Controls Adult Neural Stem Cell Number. Y. Sato, Y. Uchida, Y. Mukoyama; Laboratory of Stem Cell and Neurovascular Biology.

Adult neural stem cells (NSCs) are retained in subventricular zone (SVZ) of lateral ventricle, where a specialized niche maintains neurogenesis throughout life. Accumulating evidence suggests that vascular niche signals regulate NSC quiescence and growth. To uncover soluble vascular signals, we used an established NSC culture (neurosphere culture) from adult mouse SVZ cells and tested whether brain microvascular endothelium-derived conditioned medium (bEND3-CM) influence NSC behavior. These experiments demonstrated that the bEND3-CM significantly increased the number of neurospheres but reduced the size of individual neurospheres, suggesting that the bEND3-CM enhance neurosphere-forming potential but suppress NSC growth. Liquid chromatography-mass spectrometry analysis of the bEND3-CM revealed 29 proteins, among which we focused on soluble amyloid precursor protein (sAPP). Like the bEND3-CM, sAPP potentiated the neurosphere-forming activity but suppressed NSC growth. The observation that sAPP decreased proliferating cells but appeared not to affect cell death in Sox2⁺ NSCs suggests that sAPP serves as a negative regulator for NSC growth. Further *in vivo* studies demonstrated that endothelial deletion of *App* causes a significant increase in the number of BrdU⁺ label-retaining NSCs in the SVZ, while NSC/astrocyte deletion of

App has no detectable effect on the NSC number. Taken together, our results strongly suggest that endothelial APP serves as a vascular niche signal that negatively regulates NSC growth to control the NSC number in the SVZ.

Uncovering Molecular Mechanisms of Microcephaly. T. Schoborg, L. Smith, C. Fagerstrom, N.M. Rusan; Laboratory of Molecular Machines & Tissue Architecture.

Autosomal recessive primary microcephaly (MCPH) is a neurodevelopmental disorder characterized by reduced brain size and life span. While the clinical aspects of the disorder are well characterized, the molecular mechanism remains poorly understood. The currently accepted hypothesis favors cell division defects induced by mitotic spindle errors as the cause of the disorder, as mistakes in chromosome segregation can lead to abnormal differentiation and apoptosis. Either of these scenarios can reduce neuron/glia numbers, which in turn results in a smaller brain. The most commonly mutated gene in human MCPH patients, *Abnormal Spindle-Like, Microcephaly Associated (ASPM)* is known to be important for proper centrosome and mitotic spindle function during mitosis. However, our recent analysis of the *Drosophila melanogaster* ortholog, *Abnormal Spindle (Asp)*, showed that mitotic spindle & cell division defects are not the primary cause of MCPH in *Asp* mutant animals, suggesting the current model needs to be revised. To do so, we are establishing a set of criteria that defines MCPH using novel imaging methods such as microcomputed tomography (micro-CT) and optical sectioning of intact adult heads and brains, coupled with sophisticated image segmentation and registration algorithms. Our data has revealed that a null mutation of *Asp* specifically disrupts proper development of the adult optic lobes but not other brain regions. Surprisingly, our structure-function analysis of the protein suggest *Asp* may have a novel role in the interphase nucleus of mature neurons that might be important for its role in specifying proper optic lobe development and proper brain size.

Parkin Targets NOD2 to Regulate Astrocyte ER Stress and Inflammation. K. Singh, M.N. Sack; Laboratory of Mitochondrial Biology in Cardiometabolic Syndromes.

Loss of dopaminergic neurons in the substantia nigra region of the brain causes Parkinson's disease (PD). Degenerative PD usually presents in patients >60 years of age. However, genetic disorders such as mutations in the *PARK2* gene can give rise to early-onset PD (EOPD) in patients <50 years. *PARK2* encodes an E3 ubiquitin ligase Parkin that translocate to mitochondria in response to mitochondrial stressors to maintain mitochondrial fidelity. However, the role of Parkin in extra-mitochondrial compartments are underexplored. In the brain, we found that Parkin was highly enriched in astrocytes and hypothesized that Parkin regulates astrocyte biology to optimize neuronal health. Primary astrocytes isolated from Parkin knockout (KO) mice displayed: exaggerated ER (endoplasmic reticulum) stress, ER-stress induced inflammation, stress signaling, and decreased brain derived neurotrophic factor (BDNF) secretion. In parallel, dopaminergic SHSY5Y cells exhibited higher cell death when co-cultured with Parkin KO

compared to wildtype astrocytes. Since Parkin deficiency impacted ER stress and inflammation signaling in astrocytes, we explored whether Parkin regulates NOD1 and/or NOD2, which are cytosolic receptors and concurrently function as mediators of ER stress and inflammation. We found that Parkin specifically interacted with and modulated NOD2 levels. Consistently, Parkin KO astrocytes, and mice striatum, and cortex have increased NOD2 protein expression when exposed to ER stress. Additionally, Parkin overexpression ameliorated inflammation in THP1 cells expressing NOD2. NOD2 shRNA knockdown suppressed exaggerated inflammation defects in Parkin KO astrocytes. These data suggest a potential novel Parkin function in modulating NOD2 as a regulatory node in astrocytic control of neuronal homeostasis.

A Novel HIV-1 Inhibitor Blocks Ubiquitin Recognition by Tsg101. M. Strickland, L. S. Ehrlich, S. Watanabe, M. Khan, M-P. Strub, M. D. Powell, J. Leis, C. Carter, N. Tjandra; Laboratory of Molecular Biophysics.

Proton pump inhibitors are traditionally used to treat acid reflux. Recently, high-throughput small-molecule screening also identified these compounds as potent inhibitors of HIV-1, the causative agent of AIDS. The inhibitors cause viral particles to become tethered to the surface of an infected cell, preventing their release to infect other cells. Tsg101, the human protein that was the target of the ligand screening, is known to be hijacked by HIV-1 Gag, and would normally recruit the cellular machinery that pinches off and releases the budding HIV-1 particle. In order to develop improved versions of the drugs tailored to the treatment of HIV-1, and to further understand the mechanism of inhibition, we determined the high-resolution NMR structure of Tsg101 with one of the inhibitors identified in the screen. Unexpectedly, the compound did not bind Tsg101 near to the binding site of HIV-1 Gag; instead, tenatoprazole formed a covalent interaction with a cysteine residue near to the ubiquitin recognition site of Tsg101. The fact that the drug targeted virus particle release is interesting, since the interaction did not interfere with the binding of Gag, but instead lowered the ubiquitin-Tsg101 binding affinity, indicating a central role of the latter in HIV-1 particle production. In summary, the knowledge gained has revealed a new target for the inhibition of HIV-1 particle production, namely ubiquitin-Tsg101 interaction. Moreover, the high-resolution structure of the Tsg101-tenatoprazole complex has provided us with the necessary tools to improve the binding characteristics of this novel class of HIV-1 inhibitors.

In-vivo Trafficking of Adoptively Transferred NK Cells Using ⁸⁹Zirconium Cell Labelling and PET/CT. K. Stringar¹, J.K. Davidson-Moncada¹, N. Sato², R. Reger¹, C. Dunbar¹, P. Choyke², R.W. Childs¹; ¹Laboratory of Transplantation Immunotherapy, NHLBI, ²Molecular Imaging Clinic, NCI.

Natural killer cells directly kill tumor cells without requiring antigen recognition and are therefore an attractive prospect for cell therapy. Recently our data suggest sub-optimal homing of these NK cells to tumor sites. Current methods to track NK cells in-vivo are limited. We developed a method of labeling

NK cells with ^{89}Zr -oxine (^{89}Zr), which enables us to see cell distribution with PET/CT after adoptive NK cell transfer in rhesus macaques (RM). NK cells expanded with human recombinant IL-2 and irradiated LCL feeder cells for 14-21 days were incubated with ^{89}Zr at room temperature. NK cells retained ^{89}Zr and could be visualized and localized by PET/CT for up to 7 days. Importantly, in vitro, ^{89}Zr did not affect human or RM NK phenotype or cytotoxic function and did not transfer to other cells. Our results show NK cells tracking initially to lung, then by 4 hours, to liver and spleen where they remain for several days (fig 1). With this model, we can track NK cells in vivo for up to a week with a very low dose of radioactivity and no adverse effects on NK cell viability or function. ^{89}Zr -oxine labelling could be used as a method to assess the validity of new strategies aimed at improving NK cell homing to the bone marrow where many hematological malignancies reside. Importantly, our data suggest this model could also be safely used in humans to optimize the capacity of adoptively infused NK cells to home to tumors.

Non-Nuclear Estrogen Receptor Alpha Activation in Endothelium Reduces Cardiac Ischemia-Reperfusion Injury in Mice. J. Sun, S. Menazza, E. Murphy; Cardiac Physiology Section.

Steroid hormone receptors, such as estrogen receptors (ER) function as ligand-regulated transcription factors. However, recent data indicate that estrogen also elicits effects through binding to estrogen receptors (ER- α , ER- β and GPER) at the plasma membrane and initiating signaling. In this study, ovariectomized C57BL/6J mice were treated with estradiol (6 $\mu\text{g}/\text{day}$) or estrogen-dendrimer conjugate (EDC, a membrane delimited ER modulator) for two weeks. Ischemia-reperfusion injury was evaluated in Langendorff perfused hearts. Similar to estradiol-treated hearts, EDC treatment significantly decreased infarct size and improved post-ischemic functional recovery. EDC treatment also resulted in an increase in protein S-nitrosylation (SNO), consistent with previous studies showing a SNO role in cardioprotection. In further support of a role for SNO, inhibition of nitric oxide synthase but not soluble guanylyl cyclase blocked EDC-mediated protection. ICI_{182,780} (antagonist of classic ER but agonist of GPER) significantly blocked the EDC-mediated cardioprotection, suggesting EDC-induced protection is mediated by classic ER. Cardiac- or endothelial-specific (cs- or es-) ER α knockout (KO) mice were generated to test tissue-specific ER α involved in EDC protection. In cs-ER α KO mice, EDC treatment still significantly decreased infarct size and improved functional recovery similar to that found in wildtype, while protection was lost in es-ER α KO mice, suggesting an important role for endothelial ER α . In contrast to wildtype hearts, EDC treatment did not increase SNO in es-ER α KO mice. ER α but not ER β was found significantly decreased in cs-ER α KO mice, while opposite results were found in es-ER α KO mice. Thus, loss of EDC-induced protection and SNO increase in es-ER α KO mice could also be due to significant down-regulation of cardiac ER β /SNO signaling. In conclusion, these results demon-

strated a role of activation of membrane delimited ER in cardioprotection, suggesting that EDC-like compounds could be used clinically to provide cardiovascular benefit without the classical steroid hormone side effects, such as stimulation of uterine and breast cancer.

Mutations in Non-Muscle Myosin 2A Causing MYH9-Related Disease Disrupt Sertoli Cell Junctions and Germ Cell Polarity Resulting in Infertility. D.C. Sung, B.D. MacTaggart, C. Lerma, Y. Zhang, S. Kawamoto, M.A. Conti, X. Ma, R.S. Adelstein; Laboratory of Molecular Cardiology.

Mutations in non-muscle myosin 2A (NM2A) encompass a wide spectrum of anomalies collectively known as MYH9-Related Disease (MYH9-RD) that includes cataracts, hearing loss, glomerulosclerosis, and macrothrombocytopenia. We previously created mouse models of the three most frequent NM2A mutations found in humans: R702C, D1424N, and E1841K. While homozygous R702C and D1424N mutations are embryonic lethal, we found homozygous mutant E1841K mice to be viable, but male, and not female, mice were infertile. Here, we report that these mice have reduced testes size associated with disruptions in Sertoli cell junctions, resulting in a compromised blood-testis barrier and spermiogenesis defects. These adhesion defects cause premature germ cell loss in the epididymis and further result in misorientation of spermatids due to loss of Par proteins at the Sertoli-germ cell interface. Together, these results identify a previously unreported consequence of NM2A mutations in models of MYH9-RD and provide further insight into the role of NM2A in Sertoli cell function during postnatal testes development.

Biochemical Characterization of the *Drosophila* Methionine Sulfoxide Reductase A. S. Tarafdar, G. Kim, N.M. Rusan, R.L. Levine; Laboratory of Biochemistry.

Methionine sulfoxide reductase A (MsrA) stereospecifically catalyzes the reduction of S-methionine sulfoxide to methionine and is important in defense against oxidative stress. Recently, we reported that mammalian methionine sulfoxide reductase A stereospecifically and selectively oxidizes Met77 in calcium-bound calmodulin and can fully reduce it as well. The control mechanism that prevents futile cycling is hypothesized to be through interaction with a postulated regulatory protein. Thus, cyclic oxidation and reduction of methionines in proteins by MsrA could function as a redox-based mechanism of cellular regulation. Our aim in this study was to elucidate the physiological significance of methionine sulfoxide reductase A mediated reversible oxidation of calmodulin Met77 in *Drosophila*. However, we found that *Drosophila* MsrA, unlike its mammalian counterpart, is not a methionine oxidase. This led us to explore the mechanistic details of the enzyme. Using a double alkylation approach with HPLC-mass spectrometric sequencing, we found that the active site cysteine residue in *Drosophila* MsrA becomes locked in a disulfide bond with the terminal cysteine residue of the protein and thus cannot mediate oxidation. A mutant *Drosophila* MsrA lacking the two C-terminal cysteine residues also lacked oxidase activity, despite not being able to form a disulfide bond with the active site cysteine. We

are now determining the solution structure of the *Drosophila* MsrA to understand the structural basis for its difference in catalytic capability from the mammalian enzyme.

Low Density Granulocytes Associate with Non-Calcified Coronary Plaque and Endothelial Cell Damage in Psoriasis. H.L. Teague, J.I. Silverman, A. Dey, A. Joshi, E. Stansky, M.M. Purmalek, Y. Baumer, P.K. Dagur, C.L. Harrington, T. Aridi, G. Sanda, A.V. Sorokin, D.A. Bluemke, M. Chen, M.P. Playford, J.P. McCoy Jr, M.J. Kaplan, N.N. Mehta; Section of Inflammation and Cardiometabolic Diseases.

Chronic inflammation is increasingly recognized as a fundamental component of early cardiovascular disease (CVD). We utilized psoriasis, a skin disease associated with increased susceptibility to CVD, as a model of chronic inflammation, to investigate the association between a unique neutrophil subset, low-density granulocytes (LDGs), and early development of CVD. We used *in vivo* imaging by coronary computed tomography angiography and immunophenotyping via flow cytometry to determine the association between LDG frequency and coronary burden in psoriasis. We then assessed the cytotoxic effects of LDGs compared to normal-density granulocytes (NDG) *in vitro* when co-cultured with human aortic endothelial cells (HAoEC). We determined circulating LDG and NDG frequencies are elevated in psoriasis compared to healthy volunteers, however, only LDGs are associated with psoriasis severity and coronary burden. Additionally, we determined psoriatic LDGs spontaneously form neutrophil extracellular traps and induce HAoEC apoptosis in a NET-dependent manner compared to their NDG counterparts. Our results identify a novel association of cardiovascular damage with the LDG subtype, gleaned insight into the causative role of LDGs in atherosclerotic plaque development and inflammatory atherosclerosis.

Passive Spiritual Health Locus of Control is Associated with Lower Physical Activity Levels in an Urban, Faith-based Community. S. Thomas, A.T. Brooks, G.R. Wallen, C. Ayers, V. Mitchell, T. Powell-Wiley; Social Determinants of Cardiovascular Risk and Obesity.

There is some evidence of Spiritual health locus of control (SLOC) being associated with health behaviors in African-American communities. Less is known about the relationship between SLOC, physical activity (PA) behaviors, and the use of wearable mobile health (mHealth) PA-monitoring technology. This analysis was conducted using data from a community-based participatory research (CBPR) study designed to evaluate psychosocial and environmental factors associated with cardiovascular health in a predominantly African-American church population in at-risk Washington, D.C. communities (NCT#01927783). Participants (n=99, 78% female, 99% African American) also received a mHealth PA monitor and were instructed to wirelessly upload PA data weekly to church-based data collection hubs. SLOC was captured using a 13-item validated and scored scale. Associations between PA and mHealth usage and SLOC scores were evaluated by Spearman correlation coefficients (r_s). Among participants (age: 58 ± 11.0

years; BMI: 33 ± 7 kg/m²), median score for active and passive SLOC was 46 (interquartile range [IQR]=41-51) and 3 (IQR=2-5) points respectively. Increasing passive SLOC was associated with less leisure-time vigorous PA in minutes/week ($r_s = -0.30$, $p = 0.04$), more hours watching TV/week ($r_s = 0.26$, $p = 0.01$), and annual household income under \$60,000 ($r_s = 0.34$, $p = 0.001$). There was no association between mHealth device usage and passive SLOC ($r_s = -0.08$, $p = 0.43$). In contrast, active SLOC was not associated with PA, sedentary time, or mHealth device usage ($p > 0.05$ for all). Among faith-based communities in at-risk Washington, D.C. areas, those with passive SLOC may be less likely to engage in leisure-time PA. These findings highlight the potential for SLOC to identify a target population for a CBPR-designed PA intervention in this community.

Peculiar Cell Phenotypes Caused by Plasticity Related Gene 3/5 Due to RhoA/Rac1 Imbalance. S. Tilve, C. Mencia, N. George, C. Agbaegbu Iweka, C. Pearson, Y. Katagiri, H.M.Geller; Developmental Neurobiology Section.

PRG-3 is a six-transmembrane protein that belongs to a protein family called plasticity-related gene (PRG-1 to -5), which is a novel brain-specific subclass of the lipid phosphate phosphatase superfamily. PRG1/2 have prominent roles in synapse formation and axonal pathfinding. We found that PRG-3 overexpression in the mouse neuroblastoma cell line (N2A) results in two peculiar phenotypes - long elastic fibrous structures that are left as a trail resulting from breaking plasma membrane and excess filopodia formation. These changes are caused by cytoskeletal re-arrangement brought about by PRGs. The cytoskeleton is governed by activation of molecular switches which are members of the Rho-GTPase protein family. We hypothesized that the PRG effect on cytoskeleton was due to a shift in the activity balance of RhoA/Rac1 GTPases, increasing Rho A and decreasing Rac1 levels. Focal adhesions (FA) grip the substrate for lamellipodium to protrude forward during motility. Their turnover is highly dependent on Rho activation. Overexpression of PRG3/5 decreased turnover of paxillin (FA protein) as observed by TIRF microscopy. To study substrate attachment further, we used Interference Reflection Microscopy and saw an increased attachment with PRG 3/5. PRG3/5 cells had reduced actin turnover and slower migrating speed. The PRG-induced phenotype of long fibres and filopodia was abolished by introducing active Rac1 and dominant negative RhoA. In summary, our data indicate that PRG3/5 decreases active Rac1 levels that lead to breaking of Rac1-dependent lamellipodia causing elastic trailing fibres. An increase in Rho A levels lead to stronger focal adhesions and increased formin generated filopodia.

Differences in Protein Hydration Dynamics in Cryo-EM and X-Ray Structural Models. F. Tofoleanu¹, F. C. Pickard¹, L. Earl², S. Subramaniam², B. R. Brooks¹; ¹Laboratory of Computational Biology, NHLBI, ²Laboratory of Cell Biology, NCI.

Water plays a critical role in many biological phenomena, such as correctly folding a protein, performing its biological function and mediating oligomerization or ligand binding. Recently, cryo-electron microscopy (cryo-EM) advanced a 2.2-Å

resolution structure for β -galactosidase that identified water densities. By using molecular dynamics simulations, we compare the kinetics of the corresponding water molecules and of the water contained in the X-ray structure of the native protein. We also analyze the behavior of the conserved water molecules across all known X-ray structures for β -galactosidase. During the simulations, cryo-EM-placed water maintains its proximity to the protein better than the X-ray-placed water. Unlike X-ray, cryo-EM placed the water molecules in solvent-sheltered regions, with low accessible solvent area irregardless of the residue type. Water molecules preserved in both structures are located near residues with low mobility. Our study shows that cryo-EM is able to place a large fraction of the conserved water, which plays a crucial part in stabilizing protein structure and flexibility.

Prolonged Fasting Suppresses Mitochondrial NLRP3 Inflammasome Assembly and Execution via SIRT3 Mediated Activation of Superoxide Dismutase 2. J. Traba, S.S. Geiger, M. Kwarteng-Siaw, K. Han, O.H. Ra, R.M. Siegel, D. Gius, M.N. Sack; Laboratory of Mitochondrial Biology in Cardiometabolic Syndromes.

We previously performed a study with volunteers showing that twenty-four hours of fasting blunt the NLRP3 inflammasome, an innate immune surveillance complex involved in the activation of inflammatory cytokines. Sirtuin 3 (SIRT3), a mitochondrial lysine deacetylase involved in mitochondrial homeostasis, is a likely candidate to mediate this effect by controlling reactive oxygen species (ROS), known inducers of NLRP3 activation. To characterize the molecular mechanism of the fasting effect we evaluated the inflammasome in wildtype and SIRT3 knockout mice after nutrient deprivation. Consistent with the human data, fasting blunted inflammation in peritoneal macrophages obtained from wildtype mice but not in those from SIRT3 KO mice. In SIRT3 KO primary bone marrow-derived macrophages or in SIRT3 knockdown J774A.1 murine macrophages, NLRP3 induction promoted excessive cytosolic extrusion of mitochondrial DNA, in parallel with increased levels of mitochondrial ROS and reduced superoxide dismutase 2 (SOD2) activity. Interestingly, the negative regulation of SIRT3 on NLRP3 was not due to transcriptional control or priming of canonical inflammasome components, but was rather via SIRT3 deacetylation-mediated post-translational control of mitochondrial SOD2. In parallel, siRNA knockdown of SIRT3 or SOD2 in human THP-1 cells increased NLRP3 supercomplex formation and activation. Conversely, the overexpression of wildtype or a constitutively active SOD2 mutant blunted inflammasome assembly and activation, whereas the overexpression of an inactive mutant did not. Finally, the in-vivo administration of lipopolysaccharide produced increased liver injury and induction of cytokine levels in SIRT3 KO mice. These data support the emerging concept that enhancing mitochondrial resilience against damage-associated molecular patterns may play a pivotal role in preventing inflammation and that the anti-inflammatory effect of fasting mimetic diets may be mediated, in part, through SIRT3-directed blunting of the NLRP3 inflammasome.

NCF1 Mutation Improves Vascular Stiffness in Elastin Haploinsufficiency Through its Effect on Blood Pressure.

A. Troia, R. Knutsen, J. Danback, B. Kozel; Laboratory of Vascular and Matrix Genetics.

Williams Syndrome (WS) deletions that involve decreased copy number of the gene NCF1 have been found to have improved vascular disease. NCF1 is a component of Nox1 and Nox2 NADPH oxidase complexes; both of which have been implicated in hypertension and vascular stiffness. We are conducting an animal study using an elastin deficient mouse model to study the Nox effect and understand how oxidative stress alters vascular disease severity in WS. To analyze the Nox effect on elastin insufficiency we used an elastin deficient mouse model (*Eln^{-/-}*) and crossed it to NCF1^{+/-}, Nox1^{-/-}, Nox2^{-/-} or Rag1^{-/-} mice. We performed oxidative stress analysis with DHE staining, evaluated biomechanical changes using histology, and assessed vascular physiology. Analysis of the DHE data showed a lower level fluorescence in the *Eln* WT versus the *Eln^{+/-}*, suggesting higher oxidative stress in the elastin-deficient vessel. Analysis of the blood pressure data revealed significant *eln*-interaction effect of systolic blood pressure between all cohorts, with blood pressure being lower in the *Eln^{+/-}* Nox pathway mutants than in the *Eln^{+/-}* alone. The compliance data for each *Eln* cross group showed no biomechanical differences in the large vessels. The vessel structure of the *Eln^{+/-}*, NCF1^{+/-} showed no significant change to lamellar number between NCF1 genotypes. These results demonstrate that Nox reduction improves hypertension in *Eln^{+/-}*, however, not through large vessel biomechanical changes. Understanding how Nox reduction influence vascular disease with a focus on resistance vessels will be addressed in future studies.

Cell-Free DNA as a Biomarker in Sickle Cell Disease: Method Optimization and Analysis.

L. Tumburu, S. Yang, Y. Wakabayashi, N. Igbineweka, M. Pirooznia, I. Tunc, Y. Li, J. Zhu, S.L. Thein; Sickle Cell Branch.

Cell-free DNA (cfDNA) with a fragment size of ~167 bp are present at low concentrations in plasma and other bodily fluids in healthy humans, primarily originating from the hematopoietic lineage. In contrast, it has been hypothesized that in disease, a considerable proportion of cfDNA is derived from other tissues. Thus, understanding the biological properties of cfDNA is essential for its efficient use as a clinical biomarker in SCD. To address this, we performed i) standardization of cfDNA extraction and quantitation, ii) optimization of cfDNA library preparation, and iii) next generation sequencing (NGS) of libraries prepared from cfDNA and bi-sulfite treated cfDNA. We compared the efficiency of cfDNA extraction between the automated QIA-symphony and manual QIAamp extraction systems (Qiagen). To monitor the extraction efficiency, we used an in-house spike-in control involving fragments of green fluorescent protein (GFP) relevant to the size of cfDNA (165 and 320 bp). We used endogenous (reference) genes (*GAPDH*, *TERT*, *ALU*) for cfDNA quantitation. We compared double-stranded DNA library preparation methods between ThruPLEX Plasma-seq (Rubicon Genomics) and Accel-NGS 2S DNA Library (Swift Biosciences) kits. Sequencing of

cfDNA libraries were performed on the Illumina HiSeq platform. While the automated (QIAasympphony) extraction gave consistent yield, manual (QIAamp) extraction yielded higher cfDNA. Spike-in with GFP fragments followed by quantification confirmed the efficiency of cfDNA extraction to be ~15%. Preliminary results of quantitation assays showed *GAPDH* and *TERT* can be used to accurately estimate the cfDNA yield. Remaining quantitation assays as well as analysis of sequenced data are currently underway, to further understand the biological properties (size distribution and tissue of origin) of cfDNA in SCD.

Development of an Optimized Toolkit for High-Efficiency Lentiviral Genetic Modification of Human Natural Killer Cells. G. Waller, D. Allan, D. Chinnasamy, M. Chakraborty, M. Hochman, R. Reger, R. Childs; Laboratory of Transplantation Immunotherapy.

Infusion of large numbers of natural killer (NK) cells, expanded *in vitro*, represents a promising immunotherapeutic intervention in cancer. To augment the function and homing of NK cells with expression of particular genes, we are optimizing the process of lentiviral transduction of primary human NK cells. Stimulation of NK cells with IL-2 alone for 2-4 days was found to be necessary and sufficient to achieve high transduction efficiency, while the addition of other cytokines had negligible or transient effects. Identical off-the-shelf lentiviral constructs with 8 different promoter sequences driving expression of *EGFP* were examined, and the PGK, EFS, and SV40 promoters consistently facilitated transduction efficiencies in the range of 25-60% with minimal loss of expression over two weeks of culture in our clinical grade feeder-based *in vitro* expansion protocol. Transduced and expanded primary NK cells did not show functional deficiencies in degranulation, IFN γ , or TNF α production. To permit identification, tracking, and isolation suitable for scalable use under GMP, constructs expressing both the gene of interest and a truncated CD34 marker are being examined, both as 2A-fusions and expressed from independent promoters. These strategies aim to produce large number (>10¹⁰) of uniformly modified NK cells suitable for infusion in our clinical NK cell treatment protocol.

GCN5L1 Modulates Cross-Talk Between Mitochondria and Cell Signaling to Regulate FoxO1 Stability and Gluconeogenesis. L. Wang, I. Scott, L. Zhu, K. Wu, K. Han, Y. Chen, M. Gucek, M.N. Sack; Laboratory of Mitochondrial Biology and Metabolism.

The mitochondrial enriched GCN5-like 1 (GCN5L1) protein has previously been shown to modulate mitochondrial protein acetylation, and genetic depletion of GCN5L1 initiated mitochondrial deacetylation-dependent activation of mitochondrial biogenesis and endosomal-lysosomal nuclear regulatory programs. To further characterize GCN5L1 and its role in retrograde signaling we generated GCN5L1 liver-specific knockout (LKO) mice. The basal metabolic phenotyping showed reduced fasting glucose levels and blunted hepatic glucose production in response to pyruvate in the absence of

changes in systemic glucose tolerance. To interrogate this phenotype targeted gene expression studies of glucose synthetic pathways were assayed in WT and LKO hepatocytes. LKO hepatocytes showed diminished *PEPCK* and *G6Pase* transcript levels with reduced glucose production. Levels of FoxO1, a critical transactivator of *PEPCK* and *G6Pase* expression, was diminished with evidence of proteasome-dependent FoxO1 degradation. Mitochondrial reactive oxygen species mediated activation of ERK-1/2 phosphorylation of FoxO1 similarly modulated FoxO1 stability. ERK inhibition reduced FoxO1 degradation and restored gluconeogenic enzyme expression and glucose production in LKO hepatocytes. Finally, reconstitution with mitochondrial-targeted GCN5L1 blunted mitochondrial ROS, ERK activation and restored FoxO1 levels, gluconeogenic enzyme expression and hepatocyte glucose production. These findings support that mitochondrial GCN5L1 levels modulate the post-translational control of FoxO1, the regulation of gluconeogenesis and supports an additional role of mitochondrial GCN5L1 in retrograde control of metabolic pathways via ROS mediated ERK activation. Exploring the mechanisms underpinning mitochondrial GCN5L1 mediated ROS signaling should expand our understanding of the role of mitochondria in gluconeogenesis control.

Developmental Regulation of Mitochondrial Biogenesis During *Drosophila* Oogenesis. Z.H. Wang, H. Xu; Laboratory of Molecular Genetics.

In animals, the mitochondrial genome is inherited from mother. Females can lower the loads of severe mitochondrial DNA (mtDNA) mutations input into their offspring, a mechanism called purifying selection. Previously, we reported that purifying selection in *Drosophila* is achieved by selective replication of functional mtDNA in mitochondria with normal electron transport chain (ETC) activities during early oogenesis. However, it is unclear how ETC activities or mitochondrial fitness are regulated developmentally. Here, we show that ETC activities and the expression of some of nuclear encoded mitochondrial proteins are low in anterior gerarium, but significantly increased in posterior region, consistent to mtDNA replication. To examine what developmental pathways regulate this spatial pattern, we performed a candidate RNAi screen in *Drosophila* female germ cells (GC) and found that loss of insulin/TORC signaling pathway depletes both ETC activities and mtDNA replication. Surprisingly, dMyc, but not dPGC-1, overexpression (OE) can rescue ETC activities upon loss of insulin pathway. In addition, both levels of insulin pathway activity, marked by phospho-Akt, and dMyc protein are highly induced in posterior of gerarium and dMyc is post-transcriptionally regulated by insulin pathway, suggesting that dMyc is downstream of insulin signaling in regulating mitobiogenesis. Intriguingly, ectopic dMyc OE in anterior gerarium can sufficiently induce mitobiogenesis. At posterior gerarium, follicle cells (FC) envelope germ cells. We conducted a candidate RNAi screen in FCs and found that wingless signaling in FCs regulates the insulin pathway-dMyc-mitobiogenesis axis in GCs. In addition, OE of Insulin peptide in wingless pathway

depleted FCs restores the insulin pathway-dMyc-mitobiogenesis axis in GCs, suggesting that FCs can non-autonomously alter physiology in GCs. Collectively, this study reveals a developmentally regulated mitobiogenesis during *Drosophila* oogenesis that may contribute to purifying selection.

Smooth Muscle Cell Proliferation in Fetal ELN Heterozygous versus Control Mice, Suggests Mechanism Underlying William Syndrome Cardiac Disease. A. Watson, M. Levin, B. Kozel; Laboratory of Cardiac Physiology.

Williams syndrome is now recognized as a clinical manifestation of elastin deficiency, with a mutation sequenced in chromosome 7q11.23. Elastin, an extracellular matrix protein, is the major component of elastic fibers responsible for the elastic and rheologic properties of arteries. Normal deposition of elastin is a critical event in vessel development. The mouse model has been successfully used as a correlate of the elastin deficient genotype found in Williams patients. With the use of this mouse model we investigated the effects of elastin deficiency on embryonic development. The BrdU alternative Click-iT EdU was used to perform a proliferation assay and assist in discovering the phenotypes associated with embryonic elastin deficiency. As we continue to study the effects on majority of the murine embryonic time points, embryonic day 13 (E13) has thus provided some valuable data. The data provided from E13 has shown greater smooth muscle cell (SMC) proliferation in the ELN^{+/−} aorta in comparison to controls. Though, many cardiovascular diseases have been characterized by defective lamellae and excess SMC's, the mechanism linking these pathological features is currently unknown. We hypothesize that with the continuation of this study we will discover the peak of SMC proliferation within the cardiovascular network, allowing us to identify the mechanism causing the hyperproliferation.

A Membrane Trafficking Screen to Identify Clathrin-Independent Endocytosis Machinery. J. Wayt, D. Dutta, J.G. Donaldson; Membrane Biology Section.

Endocytosis is an important event that cells utilize to internalize cell surface proteins and fluid into the cell. There are two main forms of endocytosis: clathrin-mediated endocytosis (CME) and clathrin-independent endocytosis (CIE), amongst which CME is the most studied. While CME is important for the internalization of many surface proteins, bulk trafficking of fluid occurs primarily in a clathrin-independent manner. Our lab has focused on Arf6 associated CIE, although other pathways exist, and has identified an endosomal sorting system in HeLa cells that sorts CIE cargo proteins after being endocytosed from the cell surface. While we have established the trafficking itinerary of classical CIE cargoes like MHCI, CD59, CD147 and CD98, little is known about the entry mechanisms and the proteins that regulate the initial steps of endocytosis for these proteins. To identify proteins essential for the internalization of the GPI-anchor protein CD59 and the cell surface protein MHCI in HeLa cells, we designed an siRNA screen utilizing the Dharmacon™ Membrane Trafficking library, which contains siRNA targeting 140 established membrane

trafficking genes. Target genes were individually knocked down and cells were allowed to internalize primary antibodies against the CIE cargo proteins of interest. Following internalization, the proteins were visualized by immunofluorescence, the amount of internalized protein was determined and positive and negative hits were scored. Interestingly, there was little overlap among the list of proteins identified as important for internalization of these two cargoes, suggesting that regulation of CD59 and MHCI internalization occurs via two different mechanisms. Among these candidates was the kinase ROCK2, which was identified as preferentially inhibiting CD59 internalization, a result which was further confirmed using small molecule inhibitors. Elucidating the role of ROCK2 in the internalization of CD59 will be the focus of future studies.

Personalized Deep Detection of Measurable Residual Disease in Acute Myeloid Leukemia. H.Y. Wong, M.P. Mulé, Q.G. Liu, C.S. Hourigan; Myeloid Malignancies Section.

Acute Myeloid Leukemia (AML) is the most common acute blood cancer in adults and accounts for ~1.3% of all cancer cases in the United States. Despite AML's rarity, it is a rapid and fatal disease with an average 5-year survival rate of only ~25%. While many patients initially attain complete remission (CR) after intensive induction chemotherapy, the majority go on to relapse and ultimately die from the disease. The most likely explanation for this phenomenon is that CR is defined using 1956 criteria, which utilizes the low sensitivity technique of counting bone marrow blasts by light microscopy. The use of modern molecular tools, such as targeted next generation sequencing (NGS) and droplet digital PCR (ddPCR), may better detect residual disease responsible for relapse. Furthermore, the mutational genetic landscape of AML is diverse, which requires us to investigate patients individually. Here, we demonstrate personalized deep detection of MRD in one AML patient. Mutations in DNMT3A, KIT, and FLT3 were discovered by bulk NGS and single-cell NGS revealed the presence of two divergent clones, where DNMT3A is the founder mutation and KIT and FLT3 mutations are mutually exclusive. To track the response of these clones to therapy, we developed ddPCR assays which revealed that chemotherapy and subsequent targeted therapy effectively suppressed the KIT clone while the FLT3 clone persisted and eventually resulted in relapse. In conclusion, we demonstrated the ability to deeply detect MRD in AML, which sheds light on the prognosis and treatment of AML.

GCN5L1 Interacts with RanBP2 to Mediate Lysosome Positioning. K. Wu, L. Wang, M.N. Sack; Laboratory of Mitochondrial Biology and Metabolism.

Lysosomes are membrane-bound organelles whose main function is the engulfment of and degradation of intracellular biomacromolecules. A key step of this process is the spatial distribution of lysosomes to appropriate intracellular locations to facilitate their interaction with transport vesicles, endosomes and intracellular organelles. We identified that GCN5L1, a subunit of the biogenesis of lysosome-related or-

ganelles complex-1, is involved in controlling lysosome positioning. The genetic knockout of GCN5L1 resulted in the abnormal pericentriolar accumulation of lysosomes, accompanied by with reduced proteolysis of canonical lysosomal cargo due to impaired delivery of internalized proteins and hydrolase precursors from late endosomes to lysosomes. In consequence of attenuated lysosomal trafficking toxic autophagic intermediates accumulated. To explore the underpinning mechanism, we employed a proximity-based labeling technique, BioID, to determine novel GCN5L1 interacting proteins. RAN binding protein 2 (RanBP2) was identified as an interacting protein. Interestingly, GCN5L1 depletion increased RanBP2 levels and RANBP2 silencing phenocopied aberrant pericentriolar lysosome accumulation of GCN5L1 deficiency suggesting a narrow range of RANBP2 for appropriate lysosomal mobility. Further interaction studies found that RanBP2 associated with microtubules and that the modulation of GCN5L1 and RANBP levels modulate α -tubulin acetylation. Given that α -tubulin acetylation modulates microtubule stability, which is essential for organelles transport. This interaction between GCN5L1 and RanBP2 may play critical roles in lysosome-mobility and function.

Distinct Focal Adhesion Morphologies Emerge from Interplay Between Retrograde Actin Flux and Stress Fiber.

Z. Wu, J. Liu; Laboratory of Molecular Biophysics.

Focal adhesion (FA) is an anchorage of the cell that transduces traction force on substrate for migration. FA is a dynamic structure that develops from its nascent stage into diverse morphologies. While many essential players are individually well characterized, it is unclear how these components work together in FA growth. We establish a theoretical model that bridges this gap, suggesting that the FA morphology reflects the spatiotemporal coordination between retrograde actin flux and stress fiber during FA growth. Specifically, actin flux-mediated drifting underlies proximal FA growth that sets the stage for stress fiber formation. The resulting stress fiber stabilizes the growing FA via actomyosin contraction, and blocks the local actin flux. This negative feedback orchestrates the diverse FA morphologies, including FAs with coherent domains of different shapes and ones splitting into finger-like domains. The model thus sheds light on the underlying mechanism of FA growth.

Origin of Pericytes in Developing Skin and Brain Vasculature. T. Yamazaki¹, A. Nalbandian¹, Y. Uchida¹, W. Li¹, T.D. Arnold², Y. Mukoyama¹; ¹Laboratory of Stem Cell and Neuro-Vascular Biology, NHLBI, ²Department of Pediatrics, Physiology, and Program in Neuroscience, University of California, San Francisco.

Interactions between endothelial cells and mural cells (pericytes and vascular smooth muscle cells), the cellular components in blood vessels, are essential for the regulation of vascular networks and maintenance of vascular integrity. Despite the significance of pericytes in the vascular function, the origin of pericytes in the developing vasculature of ectodermal tissues such as skin and brain has been elusive. Here we show that

tissue-localized myeloid progenitors differentiate into pericytes in the developing skin and brain vasculature. To determine their developmental origin, we conducted a series of *in vivo* fate-mapping experiments using different cell type-specific *Cre* lines and carried out high-resolution whole-mount immunohistochemical analysis. These experiments indicated that pericytes have heterogeneous origins and tissue myeloid progenitors generate a subset of pericytes in the skin and brain. The observation that *PU.1* mutants lacking myeloid cells have defective pericyte development suggests the requirement of the tissue-myeloid progenitors for the pericyte development *in vivo*. Furthermore, FACS-isolated F4/80⁺ myeloid progenitors from embryonic skin give rise to pericytes in culture. Interestingly, transforming growth factor- β (TGF- β) signaling is required for pericyte differentiation from tissue myeloid progenitors in culture, and hematopoietic specific deletion of type2 TGF- β receptor (*Tgfb2*) results in deficient pericyte development. We are currently investigating whether such embryonic myeloid-derived pericytes are preserved in the adult.

Mitochondria Maintain Intestinal Stem Cell Homeostasis via ROS and FOXO Pathways. F. Zhang, H. Xu; Laboratory of Molecular Genetics.

Compared to adult somatic cells that emphasize on oxidative phosphorylation (OXPHOS)-based aerobic energy production, stem cells often rely heavily on anaerobic glycolysis. The mitochondrial activation, which switches the glycolysis - OXPHOS metabolism, is believed to play key roles in stem cell differentiation. Mitochondrial inactivation has also been considered as an efficient way to facilitate the somatic cell-pluripotent stem cell reprogramming by reversing this metabolic transition. However, whether mitochondria are always necessary for stem cell differentiation and the cellular signaling orchestrating the metabolic shift is largely unknown. The link between mitochondrial activity and stem cell differentiation remains to be explored. We took advantage of genetic tools for mtDNA in *Drosophila* to disrupt mitochondrial function in the intestinal stem cells (ISCs). We generated ISCs carrying homoplasmic lethal mtDNA mutation and monitored behaviors of these stem cells and the progenitor cells, enteroblasts (EBs), derived from them. We found that ISCs carrying dysfunctional mitochondria divided much slower to nearly quiescent. Very few progenitors derived from these stem cells failed to differentiate into enterocytes (ECs) or enteroendocrine cells (EEs). Further studies reveal that mitochondrial ROS plays key role in ISC differentiation, especially EEs fate determination. While FOXO pathway negatively regulates ISCs to ECs differentiation. Our results demonstrate that mitochondrial activity is essential for stem cells proliferation and differentiation, also suggested that the maintenance of ISC homeostasis is achieved by the complex coordination of mitochondrial ROS and FOXO pathways.

Selective Protein Synthesis on the Mitochondrial Surface Drives the mtDNA Selection. Y. Zhang, H. Xu; Laboratory of Molecular Genetics.

Strong purifying selections limiting the transmission of harmful mtDNA mutations have been demonstrated in the female germlines of metazoans. During early *Drosophila* oogenesis, mtDNA replication depends on mitochondrial activity, which may allow selective proliferation of healthy organelle and restrict the transmission of deleterious mtDNA mutations. Nonetheless, the molecular mechanism underlying mtDNA selective inheritance remains elusive. We recently uncovered that the MDI-Larp complex on the mitochondrial surface promotes the local protein synthesis and mtDNA replication in ovary. Here we show that MDI-Larp boosts protein synthesis on the healthy mitochondria selectively and is essential for mtDNA selective inheritance. We found that *de novo* synthesis of nuclear encoded mitochondrial proteins is greatly decreased in a temperature sensitive lethal mutant, *mt:ColT³⁰⁰¹* ovary at restrictive temperature. On the other hand, the overexpression of Tom20-Larp that constitutively localized on mitochondrial outer membrane partially restored the local protein synthesis and mtDNA replication in *mt:ColT³⁰⁰¹* background. Additionally, mtDNA selection was greatly compromised in both *mdi* mutant ovary that lack the local protein synthesis and ovaries overexpressing Tom20-Larp that boosts protein synthesis promiscuously. These observations prove that the selective protein synthesis drives mtDNA replication and mtDNA selection subsequently. We also found PINK1 accumulated in *mt:ColT³⁰⁰¹* ovary and phosphorylated Larp. Moreover, the selective mtDNA inheritance was impaired in *PINK1* mutant ovary. Furthermore, the decreased mtDNA selection in Tom20-Larp overexpression ovary was restored when PINK1 was overexpressed together. Our results suggest that PINK1 accumulation in defective mitochondria inhibits MDI/Larp's activity and suppresses the local protein synthesis. This regulation allows selectively propagation of healthy mitochondria carrying wild type genome and thereby limits the transmission of deleterious mtDNA mutations.

The Role of Non-Muscle Myosin 2A and 2B in Contact Guidance. A. Zhovmer¹, E. Tabdanov², H. Miao³, H. Wen³, L. Kam⁴, P. P. Provenanzo², X. Ma¹, R. S. Adelstein¹; ¹Laboratory of Molecular Cardiology, NHLBI, ²Laboratory for Engineering in Oncology, University of Minnesota, ³Imaging Physics Laboratory, NHLBI, ⁴Microscale Biocomplexity Laboratory, Columbia University.

The phenomenon of contact guidance in vivo is responsible for both proper positioning and migration of cells inside the growing embryo or during maintenance of adult tissues. As non-muscle myosin 2A and 2B proteins were shown to be crucial for embryonic development and cell migration we addressed their roles in contact guidance using a micropatterning technique that allowed precise control of the cellular topographical environment in order to dissect out possible non-redundant functions of these isoforms. We found that the 2A and 2B isoforms indeed play distinct roles in contact guidance.

The role of 2B isoform is diminishing of pattern-enforced cellular polarization and migration. However, if polymerization of actin or 2B activity is perturbed, 2A becomes responsible for the topographically-induced polarization of the cell during contact guidance. Moreover, 2A and 2B isoforms differentially modulate the dynamics of focal adhesions, where 2B is required for separation of viscous and elastic components, namely focal adhesions and actin bundles, in stress fibers.

Registered Attendants

Gregory Adams Jr
Laboratory of Cell and Tissue
Morphodynamics
gregory.adams2@nih.gov

Robert Adelstein
Laboratory of Molecular
Cardiology
robert.adelstein@nih.gov

Joel Adu-Brimpong
Social Determinants of
Cardiovascular Risk and Obesity
joel.adu-brimpong@nih.gov

Chinyere Agbaegbu Iweka
Developmental Neurobiology
Section
chinyere.agbaegbu@nih.gov

Chaarushi Ahuja
Social Determinants of
Cardiovascular Risk and Obesity
chaarushi.ahuj@nih.gov

Christopher Alexander
Laboratory of Cell Biology
chris.alexander@nih.gov

Aisha Aljanahi
Hematopoietic Stem Cell and
Gene Therapy
aljanahiaa@nih.gov

David Allan
Laboratory of Transplantation
Immunotherapy
david.allan@nih.gov

Luigi Alvarado
Molecular Hematopoiesis Section
luigi.alvarado@gmail.com

George Amanakis
Laboratory of Cardiac Physiology
george.amanakis@nih.gov

Stasia Anderson
Animal MRI Core
andersos1@nhlbi.nih.gov

Alessio Andreoni
Optical Spectroscopy Section
alessio.andreoni@nih.gov

Nikolaos Angelis
Sickle Cell Program
nikos.angelis@nih.gov

Jodian Brown
Theoretical Molecular Biophysics
Section
jodian.brown@nih.gov

Michelle Baird
Laboratory of Cell and Tissue
Morphodynamics
michelle.baird@nih.gov

Thomas Baird
Laboratory of Ribonucleoprotein
Biochemistry
tom.baird@nih.gov

Koyeli Banerjee
Laboratory of Structural
Biophysics
koyeli.banerjee@nih.gov

Emilia Alina Barbu
Sickle Cell Branch
emilia.barbu@nih.gov

Sivasubramanian Baskar
Laboratory of Lymphoid
Malignancies
baskars@nih.gov

Yvonne Baumer
Section of Inflammation and
Cardiometabolic Diseases
yvonne.baumer@nih.gov

Christopher Bleck
Electron Microscopy Core
christopher.bleck@nih.gov

Lisa Bossert
Office of Scientific Director
lisa.bossert@nih.gov

Lynda Bradley
Laboratory of Single Molecule
Biophysics
lynda.bradley@nih.gov

Owen Brady
Laboratory of Computational
Biology
brb@nih.gov

Steven Brooks
Sickle Cell Branch
steven.brooks2@nih.gov

Xiangning Bu
Translational Research Section
xiangning.bu@nih.gov

Mala Chakraborty
Hematopoietic Stem Cell and
Gene Therapy
chakrabm@mail.nih.gov

Long Chen
Laboratory of Transplantation
Immunotherapy
long.chen@nih.gov

Zhe Chen
Laboratory of Molecular
Genetics
long.chen@nih.gov

Elena Cherkasova
Laboratory of Transplantation
Immunotherapy
cherkasovae@mail.nih.gov

Chung-Lin Chou
Epithelial Systems Biology
Laboratory
chouj@nhlbi.nih.gov

Jonathan Chung
Section of Inflammation and
Cardiometabolic Diseases
jonathan.chung@nih.gov

Christian Combs
Light Microscopy Core
combsc@nih.gov

Denise Crooks
Office of Technology Transfer and
Development
crooksd@nhlbi.nih.gov

Joas Da Silva
Pulmonary Clinical Medicine
Section
joas.dasilva@nih.gov

Eman Dadashian
Laboratory of Lymphoid
Malignancies
edadashian@gmail.com

Thaddeus Davenport
Laboratory of Molecular & Cellular
Imaging
thaddeus.davenport@nih.gov

Michael Davis
Office of Technology Transfer and
Development
michael.davis4@nih.gov

Enrique De La Cruz
Keynote Speaker
enrique.delacruz@yale.edu

Amit Dey
Section of Inflammation and
Cardiometabolic Diseases
amit.dey@nih.gov

Laura Dillon
Myleoid Malignancies Section
laura.dillon2@nih.gov

Natalia Dmitrieva
Laboratory of Cardiovascular
Regenerative Medicine
dmitrien@nhlbi.nih.gov

Yi Ding
Systems Biology Core
yi.ding2@nih.gov

Andrew Dittmore
Laboratory of Single Molecule
Biophysics
andrew.dittmore@nih.gov

Julie Donaldson
Laboratory of Cell Biology
julie.donaldson@nih.gov

Dipannita Dutta
Laboratory of Cell Biology
dipannita.dutta@nih.gov

Hiroko Endo
Translational Research Section
endohiro@mail.nih.gov

Carey Fagerstrom
Laboratory of Molecular Machines
and Tissue Architecture
carey.fagerstrom@nih.gov

Xing Fan
Hematopoietic Stem Cell and
Gene Therapy
xing.fan@nih.gov

Claudia Fernandes De Brito
Laboratory of Molecular
Physiology
claudia.debrito@nih.gov

Elisa Ferrante
Laboratory of Cardiovascular
Regenerative Medicine
elisa.ferrante@nih.gov

Emel Ficici
Theoretical Molecular Biophysics
Section
ficicie@nih.gov

Debbie Figueroa
Asthma and Lung Inflammation
Section
debbie.figueroa@nih.gov

Natasha Fillmore
Laboratory of Cardiac Physiology
natasha.fillmore@nih.gov

Courtney Fitzhugh
Sickle Cell Branch
fitzhughc@nhlbi.nih.gov

Rhonda Flores
Lipoprotein Metabolism Section
rhonda.flores@nih.gov

Hillary Flowers
Office of the Scientific Director
hillary.flowers@nih.gov

Jessica Flynn
Laboratory of Molecular
Biophysics
jessica.donehue@nih.gov

Lita Freeman
Lipoprotein Metabolism Section
litaf@mail.nih.gov

Sarah Fritz
Laboratory of Ribonucleoprotein
Biochemistry
sarah.fritz@nih.gov

Brian Galletta
Laboratory of Molecular Machines
and Tissue Architecture
brian.galletta@nih.gov

Iris Garcia-Pak
Laboratory of Stem Cell & Neuro-
Vascular Biology
iris.pak@nih.gov

Herbert Geller
Developmental Neurobiology
Section
gellerh@nhlbi.nih.gov

Nancy Geller
Office of Biostatistics Research
gellern@nhlbi.nih.gov

Naijil George
Developmental Neurobiology
Section
naijil.george@nih.gov

Brian Glancy
Laboratory of Muscle Energetics
glancybp@nhlbi.nih.gov

Elizabeth Gordon
Laboratory of Asthma and Lung
Inflammation
elizabeth.gordon@nih.gov

Meghali Goswami
Myleoid Malignancies Section
meg.goswami@nih.gov

Thirupugal Govindarajan
Laboratory of Molecular
Cardiology
thirupugal@nih.gov

Alex Grubb
Laboratory of Cardiovascular
Regenerative Medicine
grubbaf@nih.gov

Kacey Guenther
Hematopoietic Stem Cell and
Gene Therapy
kacey.guenther@nih.gov

Pinar Gurel
Laboratory of Macromolecular
Interactions
pinar.gurel@nih.gov

John Hammer
Laboratory of Cell Biology
hammerj@nhlbi.nih.gov

Kyungreem Han
Laboratory of Computational
Biology
kyungreem.han@nih.gov

Nazmul Haque
Laboratory of Biochemistry
nazmul.haque@nih.gov

James 'Buster' Hawkins
Animal Surgery and Resources
Core
hawkinsj@nih.gov

Sara Heissler
Laboratory of Molecular
Physiology
sarah.heissler@nih.gov

Sarah Herman
Laboratory of Lymphoid
Malignancies
sarah.herman@nih.gov

Sayuri Higashi
Developmental Neurobiology
Section
sayuri.higashi@nih.gov

Bobby Hogg
Laboratory of Ribonucleoprotein
Biochemistry
j.hogg@nih.gov

Amy Hong
Laboratory of Molecular
Physiology
ahong@nhlbi.nih.gov

Longhua Hu
Theoretical Cellular Physics
longhua.hu@nih.gov

Yinan Hua
Cell Biology Section
yinan.hua@nih.gov

Paul Hwang
Laboratory of Cardiovascular and
Cancer Genetics
hwangp@mail.nih.gov

Rovira Ilsa
NHLBI Safety Committee
rovirai@nih.gov

Rafique Islam
Lipoprotein Metabolism Section
rafique.islam@nih.gov

Ji Yong Jang
Laboratory of Molecular Biology
jiyong.jang@nih.gov

Xueting Jin
Laboratory of Experimental
Atherosclerosis
tina.jin@nih.gov

Christopher Jones
Laboratory of Ribonucleoprotein
Biochemistry
christopher.jones2@nih.gov

Hyun Jun Jung
Laboratory of Kidney &
Electrolyte Metabolism
hyunjun.jung@nih.gov

Mohammad Kabbany
Section of Inflammation and
Cardiometabolic Diseases
mohammadtarek.kabbany@nih.gov

Or Kalchiem-Dekel
Laboratory of Asthma and Lung
Inflammation
o.kalchiem-dekel@um.edu

Seyit Kale
Theoretical Cellular Physics
seyit.kale@nih.gov

Ju-Gyeong Kang
Laboratory of Cardiovascular
Cancer Genetics
kangju@mail.nih.gov

Jiro Kato
Translational Research Section
katoj@nhlbi.nih.gov

Sachiyo Kawamoto
Laboratory of Molecular
Cardiology
kawamots@mail.nih.gov

Leslie Kennedy
Systems Biology Core
leslie.kennedy@nih.gov

Camron Keshavarz
Electron Microscopy Core
camron.keshavarz@nih.gov

Jaffar Khan
Cardiovascular Intervention
Program
jaffar.khan@nih.gov

Dami Kim
Office of Education
dami.kim@nih.gov

George Kim
Protein Function in Disease
Section
king@nhlbi.nih.gov

Aparna Kishor
Laboratory of Ribonucleoprotein
Biochemistry
aparna.kishor@nih.gov

Howard Kruth
Laboratory of Experimental
Atherosclerosis
kruthh@nhlbi.nih.gov

Shannon Lacy
Laboratory of Protein
Conformation and Dynamics
shannon.lacy@nih.gov

Catherine Lai
Myeloid Malignancies Section
catherine.lai@nih.gov

Lo Lai
Protein Function in Disease
Section
lo.lai@nih.gov

Linda Leatherbury
Laboratory of Developmental
Systems Biology
lleather@cnmc.org

Jackie Lee
Office of Education
jackie.lee@nih.gov

Jennifer Lee
Laboratory of Protein
Conformation and Dynamics
leej4@mail.nih.gov

Rod Levine
Laboratory of Biochemistry
rlevine@nih.gov

Stewart Levine
Asthma and Lung Inflammation
Section
levines@nhlbi.nih.gov

Huiqing Li
Cell Biology Section
huiqing.li@nih.gov

Wenling Li
Laboratory of Stem Cell & Neuro-
Vascular Biology
liw3@mail.nih.gov

Jie Li
Laboratory of Cardiovascular &
Cancer Genetics
lij19@mail.nih.gov

Yuesheng Li
DNA Sequencing &
Computational Biology Core
yuesheng.li@nih.gov

Jung Mi Lim
Protein Function in Disease
Section
jungmi.lim@nih.gov

Katherine Lindblad
Myeloid Malignancies Section
katherine.lindblad@nih.gov

Chang Liu
Laboratory of Stem Cell & Neuro-
Vascular Biology
chang.liu@nih.gov

Chengyu Liu
Transgenic Core
liuc2@mail.nih.gov

Julia Liu
Laboratory of Molecular Biology
julia.liu@nih.gov

Poching Liu
DNA Sequencing &
Computational Biology Core
pcliu@mail.nih.gov

Rong Liu
Laboratory of Molecular
Physiology
rong.liu@nih.gov

Dongying Ma
Sickle Cell Branch
mad2@nhlbi.nih.gov

Xuefei Ma
Laboratory of Molecular
Cardiology
max@nhlbi.nih.gov

Yuchi Ma
Laboratory of Cardiovascular
Regenerative Medicine
yuchi.ma2@nih.gov

Daniela Malide
Light Microscopy Core
dmalide@nih.gov

Fabrizio Marinelli
Laboratory of Structural
Biophysics
fabrizio.marinelli@nih.gov

Mery Marimoutou
Laboratory of Biochemistry
mery.marimoutou@nih.gov

Jose Martina
Laboratory of Cell Biology
jmartina@nhlbi.nih.gov

Mohit Mathew
Cell Biology Section
mohit.mathew@nih.gov

Ryan McGlinchey
Laboratory of Molecular
Biophysics
mcglincheyr@mail.nih.gov

Nehal Mehta
Section of Inflammation and
Cardiometabolic Disease
nehal.mehta@nih.gov

Caitlin Mencio
Developmental Neurobiology
Section
menciocp@nhlbi.nih.gov

Laurel Mendelsohn
Sickle Cell Branch
mendelsohnl@mail.nih.gov

Maria Mills
Laboratory of Single Molecule
Biophysics
millskm@nhlbi.nih.gov

Mona Mirzaeimoghri
Laboratory of Imaging Physics
mona.mirzaeimoghri@nih.gov

Amarjit Mishra
Asthma and Lung Inflammation
Section
amarjit.mishra@nih.gov

Deepa Mokshagundam
Laboratory of Stem Cell & Neuro-
Vascular Biology
dmokshagun@childrensnational.org

Sarah Monti
Protein Function in Disease
Section
sarah.monti@nih.gov

Joel Moss
Translational Research Section
mossj@nhlbi.nih.gov

Yosuke Mukoyama
Laboratory of Stem Cell & Neuro-
Vascular Biology
mukoyamay@mail.nih.gov

Elizabeth Murphy
Laboratory of Cardiac Physiology
murphy1@mail.nih.gov

Keron Navarengom
Laboratory of Cardiovascular
Regenerative Medicine
navarengomkb@nih.gov

Keir Neuman
Laboratory of Molecular
Biophysics
kcneuman@gmail.com

An Nguyen
Laboratory of Mitochondrial
Biology in Cardiometabolic
Syndromes
an.nguyen2@nih.gov

Dai Nguyen
Laboratory of Cardiovascular
Regenerative Medicine
dai.nguyen@nih.gov

Cydney Nichols
Laboratory of Lymphoid
Malignancies
cydney.nichols@nih.gov

Sayantane Niyogi
Cell Biology Section
sayantane@niyogi@nih.gov

Karolyn Oetjen
Myeloid Malignancies Section
karolyn.oetjen@nih.gov

Mahogany Oldham
Laboratory of Cardiac Physiology
mahogany.oldham@nih.gov

Emma O'Leary
Laboratory of Protein
Conformation and Dynamics
emma.o'leary@nih.gov

Vaslatiy Olga
Imaging Probe Development
Center
vaslatiyo@mail.nih.gov

Purevdorj Olkhanud
Laboratory of Sickle Mortality
Prevention
purevdorj.olkhanud@nih.gov

Ryan O'Neill
Laboratory of Molecular Machines
and Tissue Architecture
oenillrs@nih.gov

Ji-Hoon Park
Laboratory of Cardiovascular &
Cancer Genetics
ji-hoon.park@nih.gov

Randi Parks
Laboratory of Cardia Physiology
randi.parks@nih.gov

Phoebe Parrish
Laboratory of Vascular and Matrix
Genetics
phoebe.parrish@nih.gov

Craig Pearson
Developmental Neurobiology
Section
craig.pearson@nih.gov

Grzegorz Piszczek
Biophysics Core
piszczeg@nhlbi.nih.gov

Mohsen Pourmoussa
Laboratory of Computational
Biology
pourmoussa@nih.gov

Tiffany Powell-Wiley
Social Determinants of
Cardiovascular Risk and Obesity
tiffany.powell@nih.gov

Beverley Rabbitts
Laboratory of Cardiac Energetics
beverley.dancy@nih.gov

Rajiv Ramasawmy
Cardiovascular Intervention
Program
rajiv.ramaasawmy@nih.gov

Soumya Ranganathan
Laboratory of Ribonucleoprotein
Biochemistry
soumya.ranganathan@nih.gov

Min Ren
Laboratory of Molecular
Immunology
min.ren@nih.gov

Matthew Restivo
Laboratory of Imaging Technology
mcr4u@virginia.edu

Joshua Rivers
Section of Inflammation and
Cardiometabolic Disease
joshua.rivers@nih.gov

Hannah Robinson
Laboratory of Lymphoid
Malignancies
hannah.robinson@nih.gov

Gregory Roloff
Myeloid Malignancies Section
gregory.roloff@nih.gov

Xiangbo Ruan
Biochemical Physiology Section
xiangbo.ruan@nih.gov

Juan Pablo Ruiz
Hematopoietic Stem Cell and
Gene Therapy
juanpablo.ruiz@nih.gov

FNU Samarjeet
Laboratory of Computational
Biology
samar.samarjeet@nih.gov

Marianita Santiana
Laboratory of Host-Pathogen
Dynamics
marianita.santiana@nih.gov

Dalton Saunders
Laboratory of Molecular
Cardiology
saundersd@nhlbi.nih.gov

Ankit Saxena
Flow Cytometry Core
ankit.saxena@nih.gov

Todd Schoborg
Laboratory of Molecular Machines
and Tissue Architecture
todd.schoborg@nih.gov

James Sellers
Laboratory of Molecular
Physiology
sellersj@nhlbi.nih.gov

Fayaz Seifuddin
Bioinformatics Core
fayaz.seifuddin@nih.gov

Yazmin Serrano Negrón
Laboratory of Systems Genetics
yazmin.serranonegron@nih.gov

Ahmad Shaikh
Sickle Cell Branch
ahmad.shaikh@nih.gov

James Shepherdson
Laboratory of Obesity & Metabolic
Disease
james.shepherdson@nih.gov

Yu Shi
Laboratory of Obesity & Metabolic
Diseases
yu.shi@nih.gov

Emily Siegel
Laboratory of Molecular Genetics
emily.siegel@nih.gov

Komudi Singh
Laboratory of Mitochondrial
Biology in Cardiometabolic
Syndromes
komudi.singh@nih.gov

Colleen Skau
Laboratory of Cell and Tissue
Morphodynamics
colleen.skau@nih.gov

Agila Somasundaram
Laboratory of Molecular & Cellular
Imaging
agila.somasundaram@nih.gov

Sarah Speed
Laboratory of Molecular Machines
and Tissue Architecture
sarah.speed@nih.gov

Danielle Springer
Office of Scientific Director
ds628k@nih.gov

Erin Stempinski
Electro Microscopy Core
erin.stempinski@nih.gov

Madeleine Strickland
Laboratory of Structural
Biophysics
maddy.davison@nih.gov

Nuo Sun
Laboratory of Molecular Biology
nuo.sun@nih.gov

Junhui Sun
Laboratory of Cardiac Physiology
sun1@mail.nih.gov

Derek Sung
Laboratory of Molecular
Cardiology
derek.sung@nih.gov

Denis Sviridov
Lipoprotein Metabolism Section
sviridovd@mail.nih.gov

Vinay Shankar Swaminathan
Laboratory of Cell and Tissue
Morphodynamics
swaminathanv@mail.nih.gov

Kate Stringaris
Laboratory of Transplantation
Immunotherapy
kate.stringaris@nih.gov

Yasuharu Takagi
Laboratory of Molecular
Physiology
takagi@nih.gov

Jessica Tang
Laboratory of Molecular Genetics
jessica.tang@nih.gov

Jingrong Tang
Lipoprotein Metabolism Section
tangi@mail.nih.gov

Sreya Tarafdar
Protein Function in Disease
Section
sreya.tarafdar@nih.gov

Heather Teague
Inflammation and Cardiovascular
Intervention
heather.teague@nih.gov

Swee Lay Thein
Sickle Cell Branch
sweelay.thein@nih.gov

Hawa Racine Thiam
Cell Biology Section
hawa.racinethiam@nih.gov

Samantha Thomas
Social Determinants of
Cardiovascular Risk and Obesity
samantha.thomas@nih.gov

Sharada Tilve
Developmental Neurobiology
Section
sharada.tilve@nih.gov

Florentina Tofoleanu
Laboratory of Computational
Biology
florentina.tofoleanu@nih.gov

Javier Traba Dominguez
Laboratory of Mitochondrial
Biology in Cardiometabolic
Syndromes
javier.trabadominguez@nih.gov

Angela Troia
Laboratory of Vascular and Matrix
Genetics
angela.troia@nih.gov

Laxminath Tumburu
Sickle Cell Branch
lax.tumburu@nih.gov

Chingiz Underbayev
Laboratory of Lymphoid
Malignancies
chingiz.underbayev@nih.gov

Martha Vaughan
Laboratory of Metabolic
Regulation
vaughanm@nhlbi.nih.gov

Sharon Veenbergen
Laboratory of Molecular
Immunology
sharon.veenbergen2@nih.gov

Sebastian Vogel
Sickle Cell Branch
sebastian.vogel@nih.gov

Giacomo Waller
Laboratory of Transplantation
Immunotherapy
giacomo.waller@nih.gov

Pingyuan Wang
Laboratory of Cardiovascular &
Cancer Genetics
wangp4@mail.nih.gov

Xunde Wang
Sickle Cell Branch
xwang@mail.nih.gov

Zong-Heng Wang
Laboratory of Molecular Genetics
zong-heng.wang@nih.gov

Lingdi Wang
Laboratory of Mitochondrial
Biology in Cardiometabolic
Syndromes
lingdi.wang@nih.gov

Kizuku Watanabe
Translational Research Section
kizuku.watanabe@nih.gov

Anderson Watson
Laboratory of Cardiac Physiology
anderson.watson@nih.gov

Jessica Wayt
Membrane Biology Section
jessica.wayt@nih.gov

Tingyi Wei
Laboratory of Molecular
Cardiology
tingyi.wei@nih.gov

Rose Willett
Cell Biology Section
rose.willett@nih.gov

Hong Yuen Wong
Myeloid Malignancies Section
hongyuen.wong@nih.gov

Chuanfeng Wu
Molecular Hematopoiesis Section
wuc3@mail.nih.gov

Jing Wu
Laboratory of Mitochondrial
Biology in Cardiometabolic
Syndromes
jing.wu@nih.gov

Kaiyuan Wu
Laboratory of Mitochondrial
Biology in Cardiometabolic
Syndromes
kaiyuan.wu@nih.gov

Zhanghan Wu
Laboratory of Molecular
Biophysics
zhanghan.wu@nih.gov

Jianhua Xiong
Laboratory of Molecular Biology
jianhua.xiong@nih.gov

Haitao Xu
Laboratory of Asthma and Lung
Inflammation
haitao.xu@nih.gov

Xihui Xu
Laboratory of Obesity & Aging
Research
xihui.xu@nih.gov

Xin Xu
Sickle Cell Branch
xin.xu2@nih.gov

Idalia Yabe
Hematopoietic Stem Cell and
Gene Therapy
idalia.yabe@nih.gov

Yaake Yaffe
Laboratory of Host-Pathogen
Dynamics
yaake.yaffe@nih.gov

Tomoko Yamazaki
Laboratory of Stem Cell & Neuro-
Vascular Biology
tomoko.yamazaki@nih.gov

Zu-Xi Yu
Pathology Core
yuz@nhlbi.nih.gov

Sato Yuya
Laboratory of Stem Cell & Neuro-
Vascular Biology
yuya.sato@nih.gov

Fan Zhang
Laboratory of Molecular Genetics
zhangfan@mail.nih.gov

Li Zhang
Laboratory of Translational
Research
li.zhang3@nih.gov

Yi Zhang
Laboratory of Molecular Genetics
yi.zhang4@nih.gov

Yingfan Zhang
Laboratory of Muscle Energetics
zhangy4@mail.nih.gov

Alexander Zhovmer
Laboratory of Molecular
Cardiology
zhovmera@nih.gov

Xuefeng Zhu
Laboratory of Molecular Biology
xuefeng.zhu@nih.gov

Jie Zhuang
Laboratory of Cardiovascular &
Cancer Genetics
jie.zhuang@nih.gov